Pore-water advection and organic matter mineralization in North Sea shelf sands

Dissertation zur Erlangung des Doktorgrades
der Naturwissenschaften

Dem Fachbereich Biologie / Chemie
der Universität Bremen vorgelegt von

Felix Janssen

Bremen im Februar 2004

Die vorliegende Arbeit wurde in der Zeit von Juli 1999 bis Februar 2004 am Max-Planck-Institut für marine Mikrobiologie in Bremen angefertigt.

Gutachter

Prof. Dr. Bo Barker Jørgensen (Erstgutachter)
Prof. Dr. Venugopalan Ittekkot (Zweitgutachter)

Prüfer

Prof. Dr. Dieter Wolf-Gladrow
Dr. Ursula Witte

Weitere Mitglieder des Prüfungsausschusses

Priv. Doz. Dr. Matthias Zabel
Stud. rer. nat. Patricia Wecker

Datum des Promotionskolloquiums: 2. April 2004

Acknowledgements

I would like to thank Prof. Bo Barker Jørgensen for accepting me as a PhD student and for supporting this work.

I am most grateful to my mentor Dr. Ursula Witte, who greatly supported me in numerous ways during the entire PhD project. Often it was her ability to separate important from irrelevant things that helped a lot whenever things got complicated, e.g. during cruise preparation, last minute technical developments, and manuscript writing…

Dr. Markus Hüttel is thanked very much for a lot of help and for sharing his great experience in the field of sandy sediments from the initial thesis planning all the way to critical manuscript reading.

I'd further like to thank Prof. B. B. Jørgensen and Prof. V. Ittekkot for examination of the thesis. Together with Prof. D. Wolf-Gladrow, Dr. U. Witte, Dr. PD. M. Zabel, and P. Wecker they are also acknowledged for participating as committee members in the thesis defense.

Prof. R. Reuter and K.-D. Lorquay (University of Oldenburg), Dr. A. Bartholomae (Senckenberg Marine Station Wilhelmshaven), and Dr. W. Armonies (AWI Wadden Sea Station Sylt) are acknowledged for providing deck space during their cruises with FS HEINCKE, UTHOERN, and SENCKENBERG which allowed for field testing of the newly constructed devices.

Dr. K. Motamedi and Dr. S. Dick (Federal Maritime and Hydrographic Agency of Germany) are thanked for providing grain size and current model data.

Special thanks go all the technicians that contributed to the construction of the new devices: Volker Meyer, Paul Färber, Harald Osmers, Georg Herz, Alfred Kutsche, Olaf Eckhoff, Jens Langreder, Axel Nordhausen, Stefan Meyer, Florian Nowottny, Rydi Rimek, Axel Cremer, Thomas Kumbier, and Eric Labahn. Without their skills and dedication this work would have never been possible. Dr. O. Pfannkuche, Wolfgang Queisser, and Axel Cremer (Geomar, Kiel) have also been very helpful in providing various equipment as well as technical assistance.

I am indebted to the following people for their help and technical assistance in the laboratory: Gabi Schüssler, Susanne Menger, Martina Alisch, Kirsten Neumann, Cäcilia Wigand, Gabi Eickert, Anja Eggers, Ines Schröder, Fanni Aspetsberger, Abdul M. Alraei, and Christoph Deutscher.

Many thanks go to the captains and crews of RV HEINCKE, UTHOERN, SENCKENBERG, and GENETIKA for their great support during the cruises. Solveig Bühring, Sandra Ehrenhauß, Anja Kamp, Manfred Schlösser, Abdul M. Alraei, Martina Keller, and Holger Woyt are gratefully acknowledged for all their help during cruise preparation as well as on board.

My colleagues in the Flux and Microsensor Group and in the Biogeochemistry Department are thanked for their warmth which made the (pretty long) period of my PhD a very pleasant time. My long time office members, Christine Beardsley, Anne Portwich, Rebecca Ludwig, Dörte Altmann, and Uschi Werner are thanked very much for a lot of help and discussion, and for keeping me in a good mood (how did you do that?). Björn Grunwald, as well as Lubos Polerecky and Arzhang Khalili helped a lot with mathematics and gave me a slight idea of all the things I missed at school. Elimar Precht, Hans Røy, Solveig Bühring, Sandra Ehrenhauß, and Perran Cook are gratefully acknowledged for their friendship, for fruitful discussions that largely improved this thesis, and for their help in the finalizing stage.

Most of all, I am deeply indebted to my family, Antje, Emil, and Ole for their love and support also in times when PhD work and family life seemed a bit contradictory… My grandmothers are thanked very much for supporting me both financially and with their strong belief that I would finish the thesis some day.

Finally the Max-Planck-Society is acknowledged for providing funding of the work.

Table of contents

Thesis introduction

The continental shelf

Characterization of the physical environment

The continental shelf represents the link between the continents and the open oceans. It occupies the uppermost part of the ocean margins that further include the continental slope and rise. The shelf extends from the shore to the shelf-break where the gentle slope of the shelf (typically 0.1°) changes to the typical sloping of the continental slope area (~ 4°) (Wollast 2003). The depth where the shelf break is found typically ranges between 100 and 150 m with a global mean of 130 m but can be up to 400 m deep in polar regions. The width of the shelf varies between 1 and 1500 km with an average of ~ 80 km. Narrow shelves are generally associated with tectonically active ocean margins as they are common in the Pacific Ocean while broad shelves prevail at passive margins typically found in the Atlantic Ocean. In some places the shelf extends deep into the continents forming shelf seas such as the Hudson Bay, the Baltic Sea, or the Persian Gulf. In total the shelf covers an area of 27.1 million km^2 which represents 7.5 % of the world ocean (Menard and Smith 1966).

Shelf sediments. Within the Quaternary (i.e., the last 1.8 million years) long glacial periods and short interglacials led to substantial sea level fluctuations. At the last glacial maximum, 21.000 years before present, the sea level was approximately 125 m lower than today and the vast majority of the shelf was part of the terrestrial environment (Fleming et al. 1998). At that time, large quantities of terrigenous sediments were transported towards the coast by water and ice and deposited in today's shelf area. Upon the last sea level rise, the fine-grained fraction of these deposits was largely eluted and transported off the shelf to the upper slope, leaving behind coarse, well sorted sandy deposits (Milliman et al. 1972; Milliman and Summerhayes 1975). Since the present sea level was reached approximately 7000 years ago (Lambeck and Chapell 2001), these coarse deposits remained mostly unchanged as the time was much too short to reach sedimentary equilibrium with the present hydrodynamic conditions. Around two thirds of the present sea floor in shelf areas are still covered by these non-accumulating coarse deposits referred to as "relict sands" (Emery 1968) (fig. 1). Recent input of river-transported fine-grained material leaves the sandy areas on the shelf largely unburied as

deposition typically takes place in distinct mud belts close to the river mouths (McCave 1972).

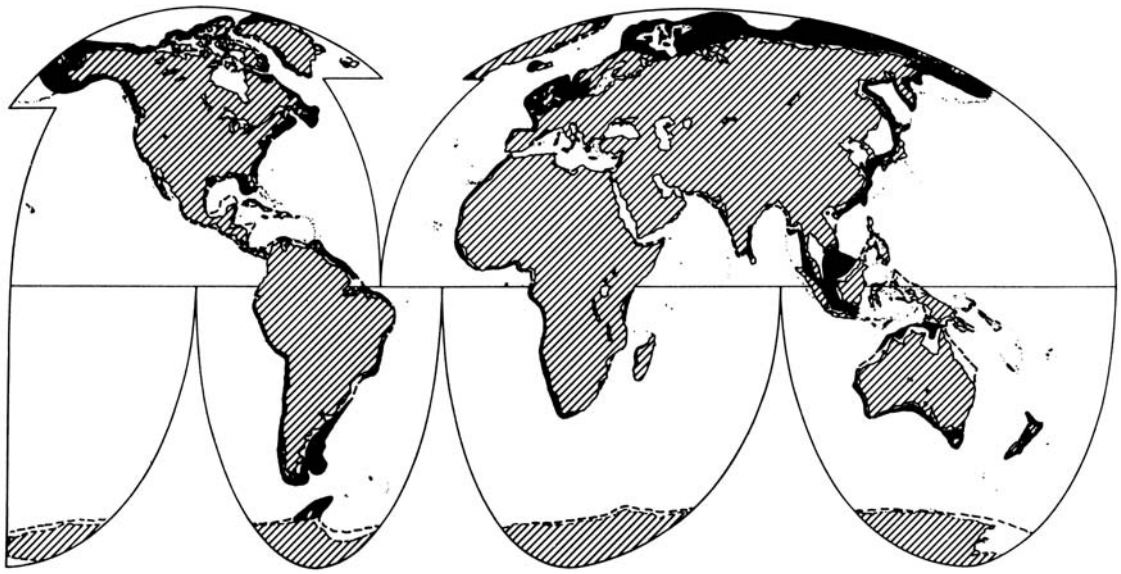

Fig. 1. Generalized distribution pattern of relict sediments (black areas) on continental shelves of the world. Most of the white areas on the shelves receive abundant supplies of modern sediments from glaciers, rivers, or calcareous organisms. From Emery (1968).

Hydrodynamics. The large scale circulation pattern in shelf areas is mainly driven by wind- and density-driven currents (McCave 2003). Density currents develop due to horizontal and vertical density gradients that originate from fresh water input by river discharge. Wind-induced currents generally induce across-shelf circulation patterns with a combined landward surface- and seaward near-bed flow or vice versa, depending on the main current direction and the hemisphere (Nittrouer and Wright 1994). The current velocities associated with wind- and density-driven currents are relatively low and rarely induce sufficient bottom shear to erode and transport the sediment (McCave 2003).

Strongest hydrodynamic forcing is found in the inner shelf due to a combination of waves and tides (Nittrouer and Wright 1994). At water depths lower than half the wave length, surface gravity waves generate oscillatory currents at the sea floor (Denny

1988). These currents frequently result in sediment transport at the inner shelf seafloor as peak current velocities are highest in shallow waters (Kawamata 1998; Sternberg and Larsen 1976). Only during storm events long period storm surges can create resuspending oscillatory currents down to depths of up to 200 m, i.e. at the entire continental shelf seafloor.

Tidal currents are also most intense in coastal areas as tidal forcing usually grows towards the shore and tidal ranges tend to be highest in shallow waters (Bearman 1989; Chamley 1990). In areas where tidal currents are strong (e.g., Southern North Sea, English channel, Bay of Fundy, George's Bank) they can also result in intense sediment transport (McCave 2003).

The outer shelf region close to the shelf-break is less affected by tides and waves, but nevertheless receives significant hydrodynamic forcing. Here, wind-driven up- and downwelling, intersection of fronts with the seabed, cascading of dense water across the shelf-break, and slope currents are the main processes (McCave 2003). Furthermore, major oceanic currents can enter shelf systems at special sites (e.g., the gulf stream at the shelf off Cape Hatteras or the Agulhas current off southeast Africa) (McCave 2003).

Production and fate of organic matter in shelf areas

Compared to the ocean as a whole continental shelf waters are characterized by high primary productivity (fig. 2) that often increases by up to an order of magnitude from the open ocean towards the coast (Galloway et al. 1996). Approximately 75 % of the primary production in coastal waters is assigned to diatoms (Tréguer et al. 1995). In mid and high latitudes, shelf water productivity typically differs strongly between seasons with highest rates during diatom-dominated spring blooms. These often provide the bulk of the annual primary production (Conley and Johnstone 1995). Productivity also depicts a significant spatial variability and is most intense in upwelling regions and in regions that receive strong river discharge (De Haas et al. 2002).

Compilations of the existing data from diverse shelf areas resulted in an estimated mean primary production of 200 - 230 g C m^{-2} yr^{-1} or 6 - 8 billion tons of carbon per year for the entire continental shelf (Wollast 2003). This implies that, despite its small

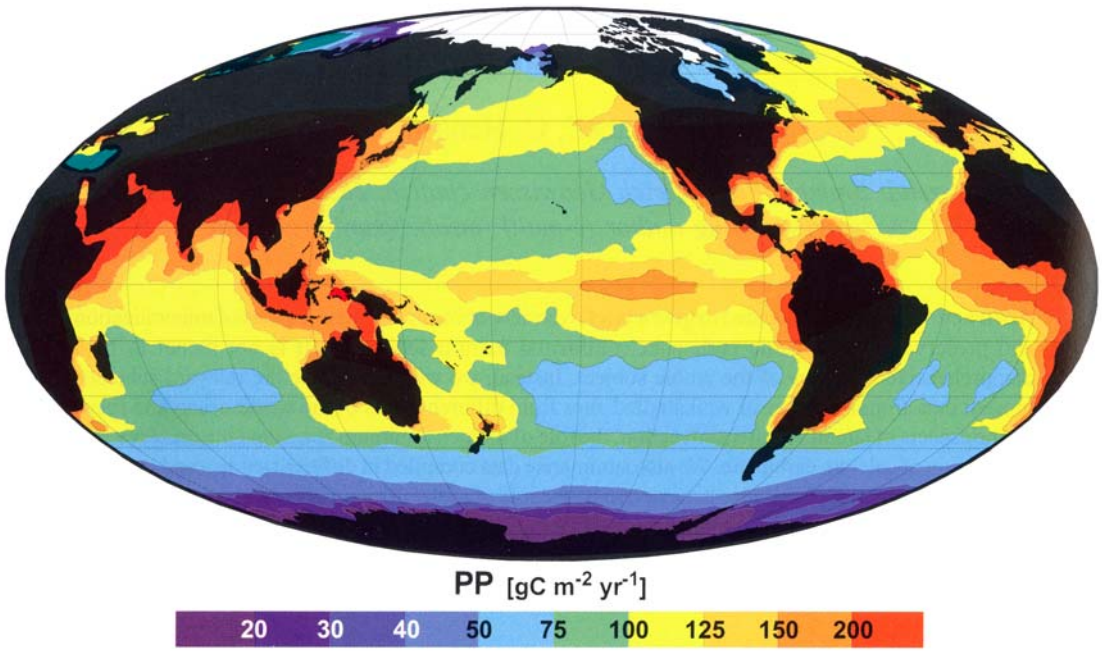

Fig. 2. Global mean annual primary production in g C m^{-2} yr^{-1}. From Zabel and Hensen (2003) after Antoine et al. (1996). © American Geophysical Union.

size, the shelf contributes approximately 25 % to the global marine primary production. In addition to the pelagic production, benthic microalgae may play a significantly role in areas where the seafloor is located within the euphotic zone. Especially at coarse-grained sites benthic primary production may take place at high rates (Cahoon et al. 1999). In the South Atlantic Bight, for example, the uppermost sediment layer was found to contain several times more chlorophyll than the entire overlying water and the average benthic primary production rate was estimated to be 126 g C m^{-2} yr^{-1}, which is > 25 % of the pelagic primary production in that area (Jahnke et al. 2000; Nelson et al. 1999). On a global scale the net benthic primary production is expected to provide 0.5 billion tons of carbon per year (Cahoon 1999).

The basis of the high productivity in shelf areas is the high nutrient availability due to the transfer of nutrient-rich deep oceanic waters across the shelf break (Galloway et al. 1996; Walsh 1991; Wollast 2003). A minor contribution is assigned to riverine input (Meybeck 1993; Wollast 2003), but anthropogenic input of nutrients may be considerable in some areas (Brockmann et al. 1990; Richardson 1996; Smetacek et al.

1991). As hydrodynamic forces are strong, the nutrients are kept within the upper mixed layer which also favors a high productivity.

While the high productivity of coastal waters is widely accepted, the fate of the produced organic matter is still under discussion (see De Haas et al. (2002) and Wollast (2003) for recent reviews). Only a relatively small fraction of the primary production is expected to be consumed through zooplankton grazing as the food web in shelf waters is comparatively small (Wollast 1998). Hence, a large fraction of the primary production (~ 30 %) is believed to end up directly as detrital organic carbon.

Possible pathways of the produced organic matter are mineralization in shelf waters and sediments, burial on the shelf, and export across the shelf-break. Considering the amount of the organic matter produced, the fate of this production is important with respect to the global carbon cycle. If significant burial takes place, the shelf would act as a CO_2 sink while a substantial export of organic matter would correspond to a transfer of CO_2 from the atmosphere to deeper waters, a process referred to as the "biological pump" (Wollast 1991).

Berner (1982) suggested that up to 87 % of the entire global organic matter burial takes place in shelf areas. From the present knowledge of transport and deposition of organic matter in shelf areas this seems highly unlikely, as most areas of the continental shelves do not show any organic matter accumulation (De Haas et al. 2002). Only locally, high rates of organic matter supply and appropriate hydrological and sedimentological conditions may allow for accumulation and burial of significant amounts of organic matter (e.g. in river estuaries like on the Amazon shelf or in upwelling areas like in the western Arabian Sea).

A substantial export of organic matter from shelf areas was hypothesized in the early 1980's (Malone et al. 1983; Walsh et al. 1981). The observation of a decoupling of primary production and consumption in the water column seemed to indicate that organic matter would be lost from the system before it could be degraded by heterotrophs. In periods of peaking primary production, especially during the spring bloom, up to 90 % of the produced organics were expected to escape from the shelf and to be deposited on the continental slope. The observation of depocenters on the upper continental slope supported this view and lead to the conclusion that export from the

shelf represents a major route for the transfer of CO_2 from the atmosphere to the deep ocean (Walsh et al. 1985). In order to test the hypothesis of a substantial export of shelf primary production, several studies were carried out within the SEEP projects on the eastern North American shelf. Budgets of organic carbon, however, detected neither a substantial organic matter export to the adjacent slope nor large discrepancies between production and consumption on the shelf itself (Anderson et al. 1994; Rowe et al. 1986; Rowe et al. 1988). This was confirmed by a recent review of sediment trap data which suggested that only 12 % of the continental shelf primary production is exported (Liu et al. 2002). In a recent attempt to integrate the available data on sedimentation, transport, and turnover of organic matter from several shelf areas De Haas et al. (2002) concluded that less than 5 % of the available organic matter escapes the shelf while > 95 % is mineralized in the water column and in the sediments.

If burial and export of organic matter are both relatively unimportant and pelagic heterotrophs are incapable to efficiently consume the primary products, then organic matter mineralization has to take place in the shelf sediments. Most of the shelf is covered with sands. These sediments are mostly poor in organic matter as organic carbon content generally scales inversely with grain size (Bergamaschi et al. 1997; Keil et al. 1994b; Li and Amos 1999). Due to this apparent lack of organic matter to fuel sediment metabolic activity, sands were traditionally considered as biogeochemical deserts (Boudreau et al. 2001; Shum and Sundby 1996; Webb and Theodor 1968). As bacteria abundances in sands are also generally low (Böttcher et al. 2000; DeFlaun and Mayer 1983; Llobet-Brossa et al. 1998), it seems that the contribution of sands to mineralization is limited both by the scarcity of organic matter and by the lack of microorganisms to degrade it.

Such a view, however, does not differentiate between standing stock and turnover of organic matter which is obviously rather simplistic. Another strong argument for a distinction of mineralization and sediment carbon content is the fact that typically most of the organic matter found in sediments is refractory and not available to the sediment heterotrophs. More than 90 % of the organic matter content of shelf sediments is generally adsorbed to the mineral surface of the sediment grains (Keil et al. 1994b; Mayer 1994) which largely excludes microbial degradation (Keil et al. 1994a). As the

organic matter content is thus probably of minor importance this indicates that the extent to which a shelf sediment may contribute to organic matter mineralization will largely depend not on the standing stock but on the actual rates of supply with labile organic matter.

The contribution of different sediment types to the mineralization of organic matter was investigated by Rowe et al. (1988) in the mentioned organic carbon budget for the New England shelf. They compared mineralization rates and standing stock of biota and organic debris in a silty and a sandy shelf area and found that, irrespective of the differences in organic carbon content and bacteria standing stock (being 11 and 3 times higher in the silt) the mineralization activity of both sediments equally corresponded to 25 % of the pelagic primary production. This indicates that the sandy sediment, despite its lack of large pools of organic matter and microbiota, nevertheless significantly contributes to organic matter mineralization in that area.

This raises the question how sandy shelf sediments may get access to the particulate organic matter that is produced in shelf waters. While the shallow water depth in shelf areas principally facilitates the supply of organic particles to the sediment, sedimentation rates of low-density organic matter are expected to be low in the presence of strong hydrodynamic forces as they prevail in sandy areas (Wollast 1991). Gravitational settling will be further reduced as turbulences tend to break up organic aggregates that may have formed and which would settle relatively fast (Eisma and Kalf 1987; Milligan and Hill 1998).

Strong evidence for a supply of shelf sands with labile organic matter was provided by Bacon et al. (1994) for the Mid Atlantic Bight shelf. The area is dominated by coarse and organically poor sandy deposits with comparatively low bacterial abundances (Rusch et al. 2003). Bacon and co-workers based their investigation on a budget of ^{210}Pb that enters the water body from the atmosphere and adheres to the organic matter that is produced in the water column. If the organic matter is decayed in the sediment the radionuclide is scavenged by the organic coatings of the sediment grains which allows to trace the former presence and mineralization of organic matter (Moore et al. 1988). Balancing deposition, decay, resuspension rates, and the sedimentary ^{210}Pb inventory, Bacon et al. (1994) concluded, that almost all the particulate organic material that is

produced in the water column at high rates (250 g C m^{-2} yr^{-1}), arrives in the sediments. Subsequently, the organic particles undergo several cycles of resuspension and trapping in the sediments during which they are gradually mineralized. The export off the shelf is then restricted to refractory matter and to an amount corresponding to less than 25 % of the primary production. The results of Bacon et al. (1994) indicate that sandy sediments may efficiently trap and degrade organic matter irrespective of strong hydrodynamics and low microorganism abundances.

Transport and exchange processes in marine sediments

It has been hypothesized, that the supply of sands with particulate organic matter and its mineralization by the sediment biota is closely linked to transport processes that specifically take place in these coarse grained deposits (Webb and Theodor 1968; Boudreau et al. 2001; Huettel and Webster 2001). Therefore, this section will focus a comparison of exchange processes in muddy and sandy deposits with special emphasis on the effect that transport in sands may have on the processing of organic matter.

Transport in marine sediments takes place either via molecular diffusion without net water and sediment transport along concentration gradients or as mass flow with net water and sediment transport independent of concentration gradients. Transport processes that involve mass flow include pore-water transport due to the activity of fauna (bioirrigation) or physical forcing (pore-water advection) as well as sediment reworking through fauna (bioturbation) and bottom water hydrodynamics (bedform migration). Unlike molecular diffusion that applies only to solutes, transport by mass flow may include both solutes and particles.

Transport in muddy sediments

As the pore-water in fine-grained deposits (i.e. silty and muddy sediments) is practically unmovable, physical solute transport is restricted to molecular diffusion. Molecular diffusion is based on the thermally-induced random movement of the molecules that results in a net transport of molecules from sites where the solute in question is abundant (sources) to sites where the concentration is smaller (sinks). According to Fick's first law the resulting solute flux is proportional to the absolute height of the concentration gradient $\delta C / \delta x$.

$$J = -D \frac{\delta C}{\delta x}$$

The factor of proportionality is the temperature- and substance-dependent diffusion coefficient *D*. Fig. 3 shows two typical examples of oxygen concentration profiles as they develop in the presence of diffusive oxygen transport in muddy coastal sediments. Directly below the sediment-water interface the gradient is steepest (and fluxes are highest) as any oxygen that is consumed deeper in the sediment has to pass across this

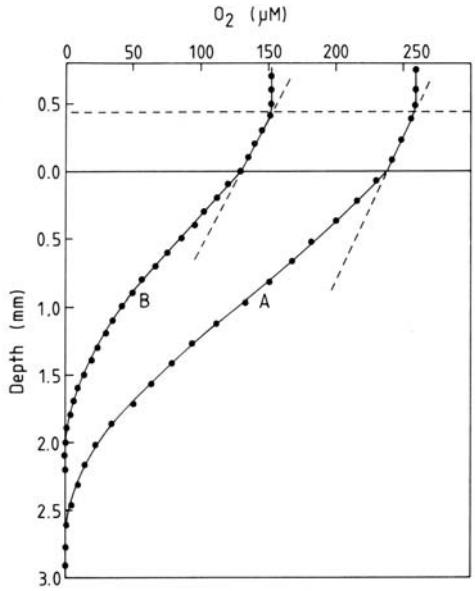

Fig. 3. Oxygen microgradients measured in Aarhus Bay sediment on (A) 14. November 1988 and (B) 5. July 1988. The diffusive boundary layers (DBLs) were 400 µm thick. A linear slope was fitted to the O_2 gradients within the DBL. From Rasmussen and Jørgensen (1992). © Inter-Research.

layer. The same flux has to cross the diffusive boundary layer (DBL) directly above the sediment, where transport is limited to diffusion too. While the oxygen uptake within the DBL is negligible, a concentration gradient across the DBL is still needed to maintain transport. Solute concentrations, therefore, decrease along the entire pathway between the source and the sink, also in regions without any solute uptake. Depending on the actual uptake rates, the maximum concentrations of the solute (e.g. bottom water oxygen concentration) will set a limit to both the maximum distance and the maximum fluxes that may be reached by means of diffusion (Jørgensen 2001). Oxygen, for example, rarely penetrates deeper than a few millimeters into coastal muddy deposits (Glud et al. 2003; Rasmussen and Jørgensen 1992). This means that the oxygen uptake by aerobic respiration will be restricted to the integrated oxygen consumption of the organisms in this uppermost sediment layer, because diffusion is unable to supply oxygen to the biota deeper in the sediment. Another characteristic of diffusion-dominated environments is that the established solute distributions are relatively stable with time. This is especially the case in deeper sediment layers: Diffusional transport of

solutes is fast only as long as distances are small (in the µm to small mm range) because the time it takes solutes to arrive at a certain point increases with the square of the distance. Geochemical transition zones (e.g. between the oxygenated surface layer and the anoxic sediment below) will tend to keep their position. In the presence of longer lasting changes in solute consumption and in the concentrations at the source, however, significant changes will take place. The two profiles in fig. 3 give an example of such a change. A comparison of the two profiles that were obtained in July (B) and November (A) at the same site shows how a seasonal increase in bottom water oxygen concentration and a decrease in sediment activity is reflected in an increase in oxygen penetration depth.

The solute exchange between the sediment and the bottom water may be largely intensified in the presence of bioirrigation, which extends the effective exchange area to the walls of the ventilated burrows (Aller 1988; Kristensen 1988). In coastal sediments, oxygen diffusion across the burrow walls typically equals diffusion across the sediment surface (Jahnke 2001). Furthermore, the three-dimensional structure and periodically flushing of the burrows will introduce spatial and temporal heterogeneity to the geochemical zonation (Aller 1994), as compared to the stable, horizontally laminated zonation that prevails in diffusion-controlled sediments in the absence of fauna. Sediment reworking through bioturbation also results in an intensified exchange of solutes (Aller 1982) and, additionally, in the transport of particles across the sediment water interface and within the sediments (Graf and Rosenberg 1997). A similar effect is expected if the upper sediment layer is physically reworked by supercritical bottom flow as it has been observed in time series of sediment surface topographies (e.g. Wheatcroft 1994).

Transport in sandy sediments

All transport processes that are described above are not restricted to muddy sediments but take place in sandy sediments, too. Due to the larger sediment grains, sands are permeable (i.e. the pore-water may move through the interstices), which allows for an additional exchange by means of physically induced mass flow of pore-water. This process is referred to as pore-water advection. The driving force behind advective pore-

water flow is always a pressure gradient. The pressure gradient is counteracted by friction in the porespace, which depends on viscosity and permeability. The relationship between pore-water flow velocity (u), spatial pressure gradient (∇p), sediment permeability (k) and porosity (φ), and pore-water viscosity (μ) is given by Darcy's law (Darcy 1856):

$$u = \frac{k}{\varphi \mu} \nabla p \, .$$

The permeability principally scales with grain size and sediment sorting is expected to range roughly between 10^{-12} and 10^{-9} m^2 in well sorted sands (median grain size 63 - 2000 µm) (Krumbein and Monk 1943).

Pressure gradients in aquatic sediments may originate from density gradients, hydrostatic pressure gradients along aquifers or between wave crests and troughs, and bottom-flow topography interactions. The resulting advective transport processes are referred to as density-driven convection, groundwater seepage, wave pumping, and current-induced advection.

Density-driven convection. Pore-water exchange by density-driven convection takes place where density differences exist between the pore-water and the overlying bottom water. Differences in salinity will result in haline convection which is likely to take place in estuaries or upwelling areas. Haline convection was investigated in the laboratory by Webster et al. (1996). They found that the resulting interfacial solute exchange can be much more effective than molecular diffusion.

Thermal convection is induced by temperature differences. Warm sub-surface waters that emerge from permeable sediments at hydrothermally active sites induce a pore-water circulation cell in the surrounding sediment that has strong effects on the distribution and interfacial fluxes of solutes (Dando et al. 2000). When intertidal sand flats that warmed up during air exposure are flooded, thermal convection may result in solute exchange that can be three orders of magnitude higher as compared to diffusion (Rocha 1998).

Groundwater seepage. Groundwater seepage takes place in areas where groundwater aquifers extend to the seafloor (Schlüter 2003). Moore (1996) estimated rates of groundwater seepage in the South Atlantic Bight from the excess ^{226}Ra

concentrations in the water column. They found that the input of groundwater to the South Atlantic Bight amounted to ~ 40 % of the river run-off during the study period. Depending on the origin of the groundwater, the discharge may result in significant benthic solute fluxes. In benthic chamber incubations in a sandy estuary within the same area, Jahnke et al. (2003) observed high nutrient efflux and suggested seeping of water through aquifers that extend beneath a nearby salt marsh. They proposed that the high fluxes of nutrient could originate from mineralization processes that occurred over larger areas adjacent to the estuary.

Wave pumping. Wave pumping is induced by the passage of surface gravity waves that introduce undulating hydrostatic pressure gradients at the seafloor that set the pore-water into oscillatory motion. Riedl et al. (1972) directly measured this effect and proposed that wave pumping should lead to intense interfacial pore-water exchange throughout the continental shelf. Their concept of a "subtidal pump" has received great attention as they estimated that wave pumping would filter the entire ocean volume through the shelf sands within only 14,000 years. Rutgers van der Loeff (1981) described solute exchange due to undulating hydrostatic pressure gradients in terms of enhanced diffusivity. Later studies focused on the sediment and wave characteristics needed to achieve significant interfacial solute exchange through wave pumping and added the concept of mechanical and rotational dispersion (Harrison et al. 1983; Webster and Taylor 1992). Precht and Huettel (2003) conducted solute exchange experiments in a wave tank and found that the effect of wave pumping on solute exchange might be lower than initially expected by Riedl et al. (1972). They pointed out that the effect of wave pumping on pore-water exchange is easily overestimated as it is hard to separate from advection induced by wave-driven oscillatory currents. Such current induced advection will mostly be present at the same time but is based on an entirely different principle (see below).

Current-induced advection. Current-induced advection is based on pressure gradients at the sediment surface that develop when topographical features like mounds or ripples protrude into unidirectional or oscillating bottom-flow. The upper graph of fig. 4 shows flow velocity profiles as measured along a mound in a flume. Well upstream of the mound the flow is undisturbed showing the logarithmic velocity

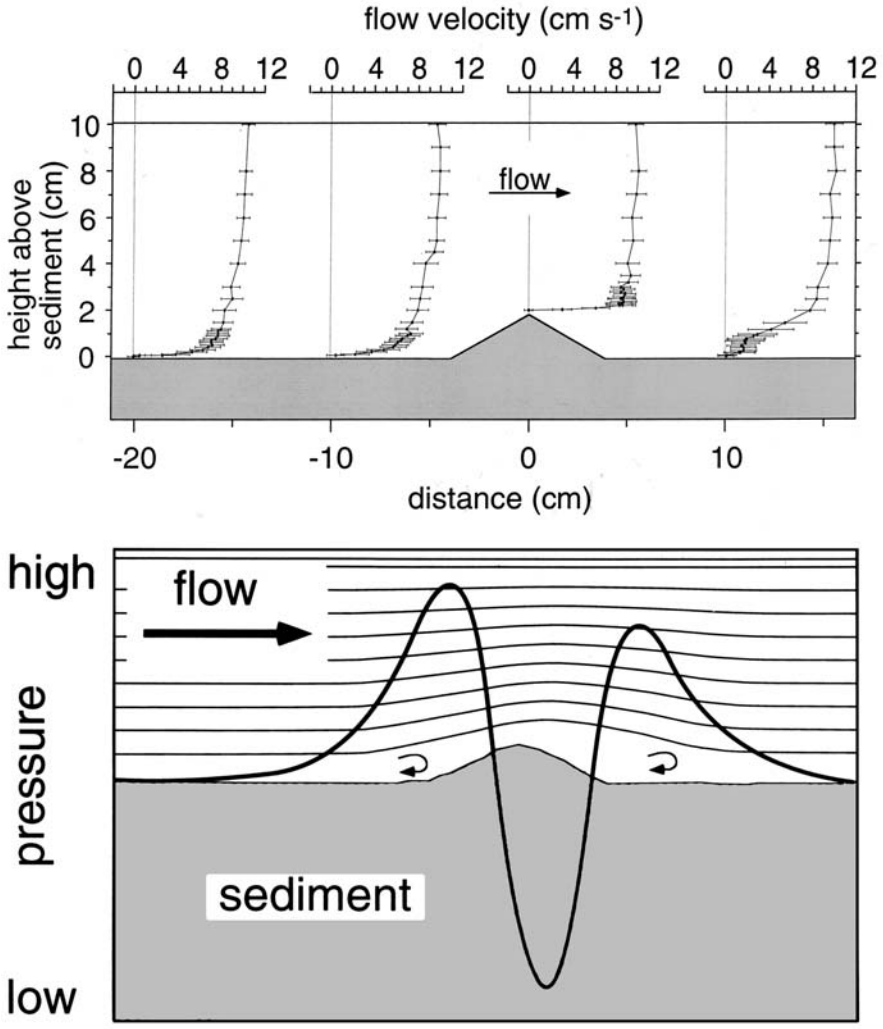

Fig. 4. Upper graph: Flow velocities recorded at a 20 mm high mound (slopes 30°). Error bars indicate standard deviations (n = 5). Lower graph: Schematic representation of water flow (thin lines) deflected by protruding topography and the associated pressure changes (thick line) at the sediment-water interface. From Huettel et al. (1996). © American Society of Limnology and Oceanography.

profile typical for boundary flows. Directly up- and downstream of the mound the profiles appear disturbed and flow velocities are reduced close to the sediment. On the contrary, the flow is accelerated where it passes the mound. A schematic representation of the bottom flow streamlines and the resulting pressure distribution is given in the lower graph of fig. 4. As the flow approaches the mound it is deflected upwards and low-speed fluid accumulates in a recirculation zone. This results in an increase in

pressure at the sediment surface. Right behind the top of the mound in the region of accelerated flow velocities the flow detaches from the surface of the mound and a pressure minimum develops due to flow separation (Hutchinson and Webster 1998). The second recirculation zone downstream is again associated with relatively high pressures. While investigations of pressure gradients due to current-topography interactions have been restricted to unidirectional bottom flow, oscillating flows due to surface gravity waves are expected to result in very similar pressure distributions with the difference that the time averaged low pressure area will be located exactly at the top of the roughness element (Precht and Huettel 2004).

The magnitude of the pressure gradient at the sediment surface was studied in laboratory flumes both at isolated roughness elements (mounds) (Huettel and Gust 1992a; Huettel et al. 1996) and sequential obstructions like ripples or dunes (Fehlman 1985; Vittal et al. 1977) and was found to scale both with flow velocity and obstacle height. Direct measurements of current-induced pressure gradients in the natural environment are still lacking. Based on laboratory findings, however, they can be expected to be mostly in the range of a few Pascal only (i.e., a few tenths of a millimeter of water column) (Glud et al. 1996; Huettel and Gust 1992a; Huettel et al. 1996; Thibodeaux and Boyle 1987).

The horizontal pressure gradients that develop along a current-exposed obstacle will force an inflow of bottom water in the high pressure regions up- and downstream of the obstacle and an outflow of pore-water at its downstream slope close to the crest. This results in a characteristic pore-water circulation pattern below the roughness element (fig. 5). The inflow in the high pressure regions is associated with relatively slow pore-water velocities and takes place over relatively large areas while the pore-water upwelling is relatively fast and restricted to a narrow outflow area. This pattern agrees to dye streamlines within the sediment porespace as observed in several flume studies (Huettel and Gust 1992a; Huettel et al. 1996; Savant et al. 1987; Thibodeaux and Boyle 1987).

Pore-water velocities associated with current-induced pressure gradients typically range from a few to several centimeters per hour (Huettel and Gust 1992a; Huettel et al. 1996; Savant et al. 1987). However, if intensely sculptured gravel beds are exposed to

fast bottom flow as it might be common in fluvial environments, interstitial flow velocities may reach up to tens of meters per hour (Thibodeaux and Boyle 1987).

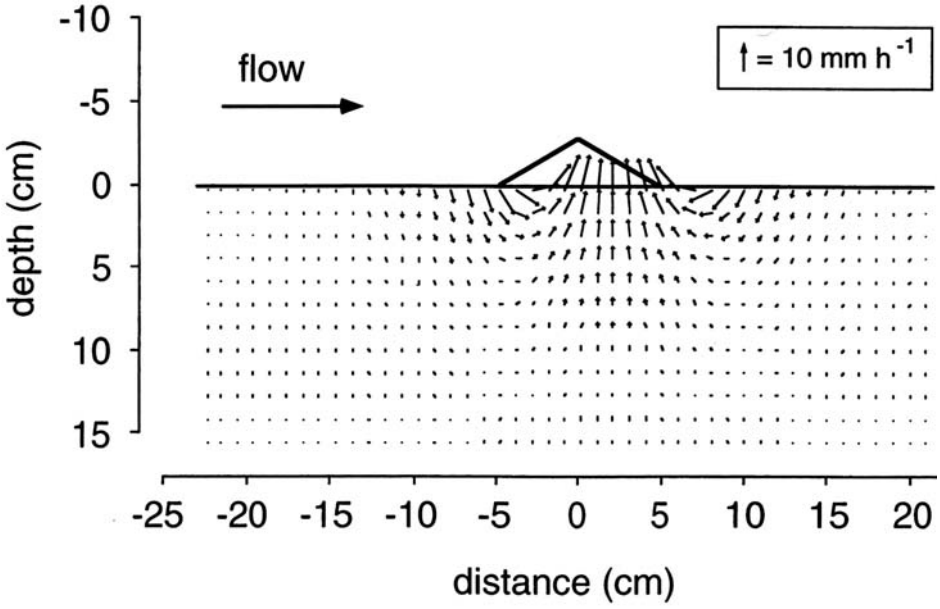

Fig. 5. Pore-water flow pattern generated with a source-sink model for the flow at a 28 mm high ripple. From Huettel et al. (1996). © American Society of Limnology and Oceanography.

Advective pore-water flow in the natural environment was reported by several investigators. Tracing of dye plumes that were injected into the sand at shallow rippled Mediterranean sites revealed the presence of pore-water advection in the presence of wave-induced oscillating bottom flow (Precht and Huettel 2004; Webb and Theodor 1968). In Mid Atlantic Bight sediments that were exposed to combined tidal and wave-driven currents, the presence of fast vertical pore-water transport became apparent from the short time it took iodide, released above the sediment surface, to arrive at the tip of a voltammetric sensor 20 mm below the sediment surface (Reimers et al. 2004).

Advective solute transport. Even relatively slow advective pore-water circulation at velocities of a few centimeter per hour proved to result in intense interfacial exchange of solutes. In flume experiments with stained pore-waters Huettel and Gust (1992a) observed interfacial pore-water exchange in the presence of small mounds (height ≤ 25 mm) and quantified the rates in terms of dye release to the overlying water.

Within one day the inflow of water pushed the stained pore-water downwards to a depth that exceeded the height of the mounds by a factor of two. In the low pressure area pore-water was transported upwards from > 100 mm sediment depth and released at the sediment surface. In the vicinity of the mounds, dye release exceeded diffusion by three orders of magnitude. Based on these measurements Huettel and Gust (1992a) estimated that advection induced by mounds at natural densities in the North Sea intertidal would affect the entire surface area and result in a 7-fold increase of fluxes as compared to diffusion. Using a similar experimental approach (Precht and Huettel 2003) quantified solute exchange across rippled beds in a wave tank under oscillating currents and found rates that were 50 times higher than diffusive exchange.

Advective exchange across the sediment-water interface will apply to any solute that is dissolved in the pore- or bottom water. This has significant consequences for the sedimentary biogeochemical processes. Oxygen and other electron acceptors can be supplied to the sediment biota at high rates while “waste products” like ammonium, hydrogen sulfide and dissolved inorganic carbon are efficiently removed. Enhanced solute exchange is considered to increase the potential for organic matter mineralization of microbiota (e.g. Aller and Aller 1998; Forster and Graf 1995). More specifically, the supply with oxygen and sulfate has been identified as a key factor that determines the mineralization rates (Enoksson and Samuelsson 1987; Froelich et al. 1979; Jørgensen and Sorensen 1985). Evidence for the potential of oxygen to intensify organic matter mineralization in sands was further provided by Dauwe et al. (2001) who incubated North Sea sands and measured enhanced rates of organic matter mineralization in the presence of oxygen as compared to anoxic conditions. Besides a generally enhanced supply, advection may also facilitate the transfer of electron acceptors to the individual bacteria as the assimilation of solutes by surface-associated bacteria may largely increase in the presence of fluid flow (Logan and Kirchman 1991). Advection may thus be expected to result in sedimentary conditions that are favorable for an intense metabolic activity of the microbial community.

Field evidence for an advective supply with electron acceptors has been provided by Lohse et al. (1996). They observed deep oxygen penetration in freshly retrieved

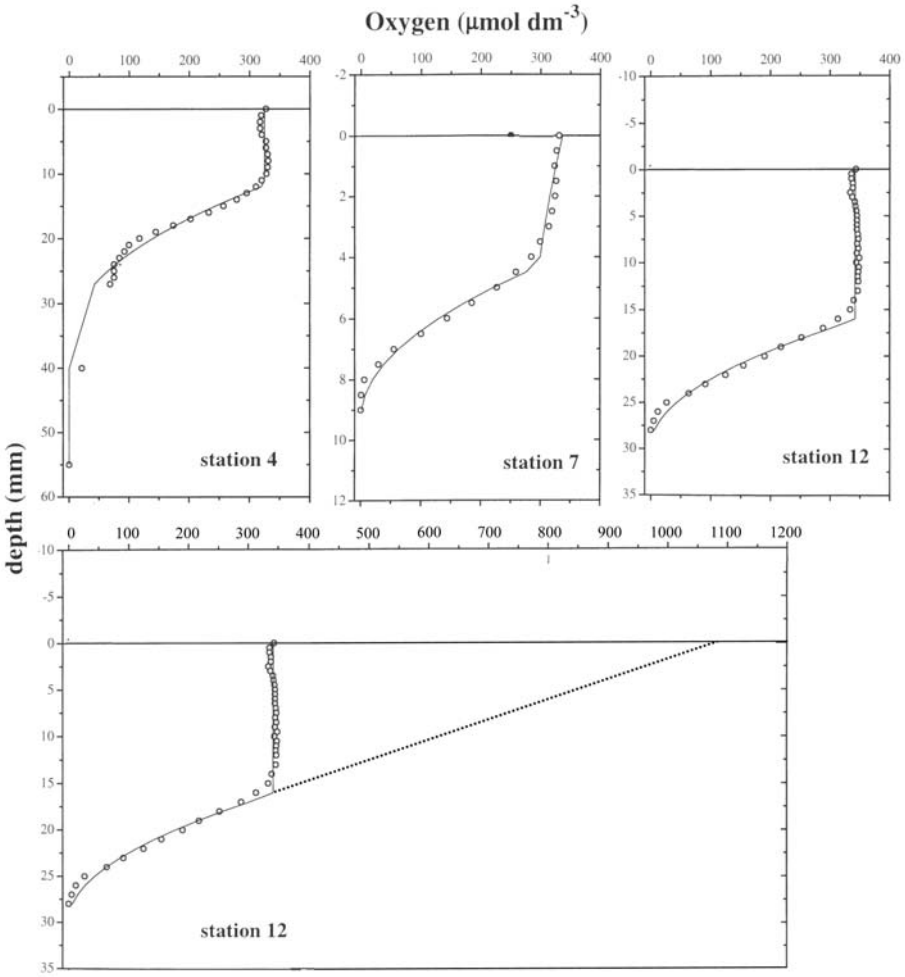

Fig. 6. Upper three graphs: oxygen distributions in freshly retrieved sediment cores from medium- (4) and fine-sand stations (7 and 12) in February. Thin lines represent fits of a diffusion-analogue model approach. Lower graph: extended version of the upper right graph. The dotted line extends the maximum gradient to the sediment surface (intercept with the sediment surface at 1080 µmol L^{-1}). Modified after Lohse et al. (1996). © Inter-Research.

North Sea sand cores and found that the oxygen profiles divided into a lower part showing the strong gradients known from diffusion dominated environments and an upper part where advective supply maintained high oxygen concentrations (upper panel of fig. 6). This is in agreement with profiles obtained in advectively flushed zones in laboratory flumes (Forster et al. 1996; Ziebis et al. 1996). The deep oxygenation in the presence of advection thus represents a combination of advective and diffusive supply. Advective inflow of bottom water keeps pore-water concentrations high in the upper

sediment horizon and allows diffusive transport into deeper sediment layers. The dotted line in the lower graph of fig. 6 that extends the maximum gradient in the presumably diffusion-dominated lower sediment layer represents the oxygen gradient that would be needed to transport oxygen to that layer by means of diffusion. This gradient that does not even account for any uptake in the upper sediment layer would be impossible as it would require a bottom water oxygen concentration of > 300 % air saturation.

Further field evidence for an advective supply of oxygen was inferred from the temporal variability in sediment oxygen distribution with particularly deep penetration in times of rough hydrodynamic conditions (i.e. fast bottom-flow) (Falter and Sansone 2000; Reimers et al. 1996). Indications for an efficient advective removal of "waste products" like dissolved inorganic nitrogen species, phosphate, and silicate has been inferred from low pore-water concentrations, from the general shape of the concentration profiles, and from correlations between solute distributions and hydrodynamic conditions (e.g., D'Andrea et al. 2002; Gehlen et al. 1995; Marinelli et al. 1998; McLachlan et al. 1985). Direct evidence of advective solute release was provided by Oldham (1999) who observed a doubling of water column ammonium concentrations in a sandy estuary in response to a wind-driven increase in bottom flow velocity and turbulence.

The combination of advective solute transport and biogeochemical reactions in the sediment is expected to result in a heterogeneous spatial distribution of biologically active solutes within the sands. With respect to oxygen this has been demonstrated by Ziebis et al. (1996) who exposed a medium sand with biogenic mounds to unidirectional flume flow. Advective pore-water flushing resulted in a severalfold larger oxygenated sediment volume as compared to a diffusive setting and in a complex and largely extended transition zone between the oxygenated and the anoxic part of the sediment (fig. 7). A similar oxygen distribution was observed below ripples that have been exposed to oscillating currents in a wave tank (Precht et al. 2004). Such complex zonations are not restricted to oxygen but also found with respect to other reactive solutes. Huettel et al. (1998) observed high nitrate concentrations due to enhanced nitrification up- and downstream of the mounds, where the inflow of bottom water

ventilated the sediment. On the other hand, high concentrations of ammonia, Fe(II) and Mn(II) were present in upwelling zones.

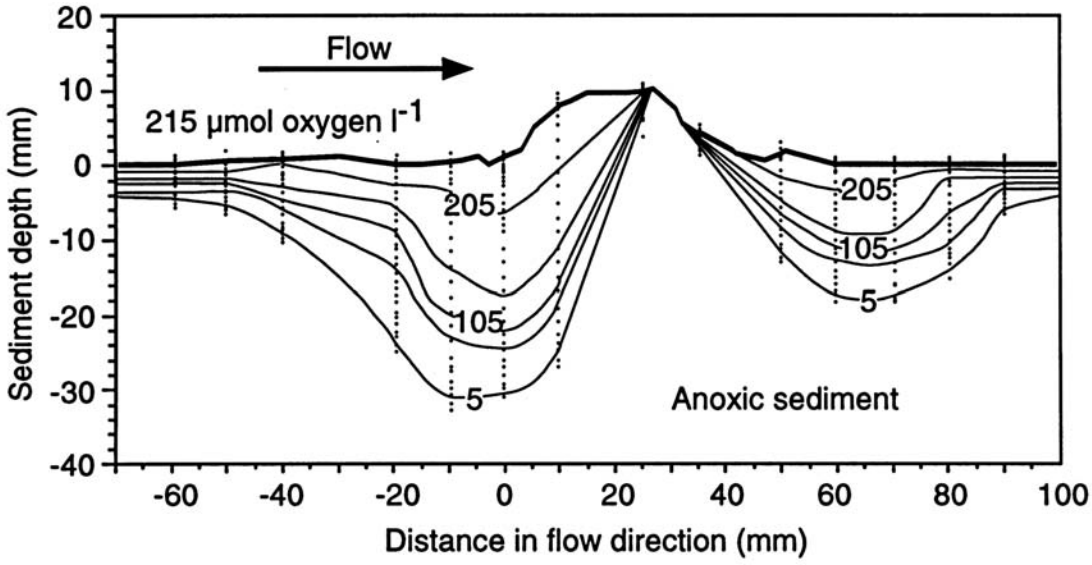

Fig. 7. Oxygen penetration around a small sediment mound, exposed to flow. Points of equal oxygen concentration were connected to illustrate the distribution. Vertical dotted lines indicate the 14 measured oxygen profiles. From Ziebis et al. (1996). © Inter-Research.

Due to the dynamic nature of the factors that drive pore-water advection in the natural environment, distributions of solutes and biogeochemical transition zones in sandy sediments are expected to change constantly. Bottom water hydrodynamics, sediment surface topography, and permeability are subject to temporal changes at any time scale from seconds to seasons (Huettel et al. 2003). Short term effects within the range of seconds to minutes apply to hydrodynamics and include changes in velocity and direction of bottom-flow due to turbulences and wave-driven oscillatory currents as well as pressure undulations that result from the passage of surface gravity waves. Changes in currents at time scales from minutes to days will result from tidal cycles and local wind fields. At a similar time scale, topographies may also change significantly. Ripples have been observed to migrate at velocities of more than 1 cm min^{-1} (Sleath 1984) and the burrowing activity of benthic fauna may completely restructure sediment topographies within a matter of hours to days (Clifton and Hunter 1973; Wheatcroft

1992). An example for long term variations are seasonal differences in storm frequency which will in turn have a strong effect on the prevailing topographies (Li and Amos 1999).

The time scales of permeability changes are more difficult to assess. Changes in the abundances and activity of benthic biota will cover different time scales (e.g. diurnal activity patterns, reaction to food pulses, growth, reproduction) and may both reduce permeability (by secretion of adhesive exopolysaccharides by bacteria and benthic algae) or increase it (by sediment reworking and burrow construction). Permeability will also change in response to hydrodynamic conditions as these determine how frequently clogging of the pores and sediment consolidation is eliminated by resuspension.

Temporal changes of advective transport as they result from the above-mentioned processes may strongly affect the sedimentary environment (Rutherford et al. 1993). An increase or decrease of bottom flow will affect mainly the rates of advection while the general circulation pattern will persist (Rutherford et al. 1995) which will primarily shift the transition zones (e.g. the oxic-anoxic boundary) vertically (Ziebis et al. 1996). If changes include flow direction or surface topography, these will alter both the pressure distribution and pore-water circulation pattern and, hence, the entire biogeochemical zonation (Precht and Huettel 2003; Precht et al. 2004). For example, sediment regions and benthic organisms that have been exposed to anoxic pore-waters in an upwelling zone below a ripple crest may receive oxygenated bottom-water once the ripple has been shifted by half its wavelength. Such dynamic changes in biogeochemical zonation potentially intensifies sediment metabolism. Bacteria in transition zones between oxidized and anaerobic sediment regions generally show high activities (Fenchel and Blackburn 1979). A fast exchange of oxidized and reduced reactants across short distances may favor both aerobic and anaerobic metabolism as reduced products from anaerobic decay (e.g., sulfide and ammonia) will be readily available for re-oxidization by aerobic processes (e.g., sulfide oxidation and nitrification). Particularly intense sediment metabolism is known to be associated to periodic re-exposures to oxygen resulting in a more efficient and faster organic matter mineralization as it would take place under constant conditions (Aller 1994; Aller and Aller 1998; Hulthe et al. 1998).

Advective particle transport. As mentioned above, advective pore-water flow will not only transport dissolved but also suspended matter. By this means, advection may supply particulate organic material to the sediment biota. Huettel et al. (1996) added neutrally buoyant tracer particles to the flume water and observed that, within less than one day, these were transported with the pore-water down to a sediment depth > 20 mm. As the pore-water velocities decreased with sediment depth the particles became trapped and accumulated in distinct layers perpendicular to the direction of the pore-water streamlines. Several experiments with tracer particles and phytoplankton cells confirmed the ability of advection to transport organic particles several centimeters into sandy sediments and identified grain size and permeability as the key factors that determine the flux and penetration depth of particles (Ehrenhauss and Huettel 2004; Ehrenhauss et al. 2004; Huettel and Rusch 2000; Rusch and Huettel 2000). It is likely that advective particle transport and trapping represents a key process for the incorporation of organic matter into sandy sediments. Even if rough hydrodynamic forces exclude any gravitational settling, this process allows an access of the sandy sediment biota to the pool of organic particles like organic detritus, microalgae, and bacteria, that are carried along with the overlying water. Advective particle transport also represents a likely explanation for the efficient trapping of organic particles in Mid Atlantic Bight sediments that was suggested by Bacon et al. (1994) based on their ^{210}Pb budget.

Experimental results suggest that the supply with organic particles intensifies the metabolic activity of the sands and that the particles that are trapped in the interstices are degraded much faster compared to those that are suspended in the overlying water. This became evident from a fast decrease in numbers of previously trapped microalgal cells (Huettel and Rusch 2000), a decrease in oxygen concentration in the upper sediment and an increase in total oxygen uptake (Forster et al. 1996), and enhanced rates of nutrient and dissolved organic carbon release (Ehrenhauss and Huettel 2004; Ehrenhauss et al. 2004). The enhanced degradation was attributed to mechanical stress and an intensified contact of the organic particles with the bacteria on the sand grains as well as with their exoenzymes (Clement et al. 1997; Huettel and Rusch 2000). Furthermore, as bottom-water inflow extends deeper into the sediment than particle

transport, the layers of particle accumulation will be permanently percolated with pore-water that supplies oxygen and other electron acceptors to the sediment community.

Field evidence for particle trapping in the natural environment has been inferred from incubations of washed and sieved sand cores in the North Sea intertidal and the shallow Red Sea (Huettel and Rusch 2000; Rasheed et al. 2003; Rusch and Huettel 2000). Especially in coarse grained sediment cores an increase of particulate organic matter with time was observed and attributed to advective particle transport. D'Andrea et al. (2002) suggested advective transport of algae and phytodetritus into the sediment to explain the high chlorophyll *a* concentrations down to several centimeters sediment depth in intertidal sands. Other studies reported a correlation of photopigment concentrations in sandy sediments to those of the overlying water column (Burford et al. 1994; Jenness and Duineveld 1985), which could possibly be explained by advective transport of algae into the sediment. Finally, subsurface maxima of silicate and ammonium that are regularly observed in South Atlantic Bight sands (Marinelli et al. 1998), might originate from the mineralization of diatoms that were transported into the sediment by advection and trapped in discrete accumulation layers.

The role of sands in the shelf ecosystem

The present knowledge of advective processes in sands strongly supports a hypothesis that was already put forward by Webb and Theodor (1968): *"If the upper layer of such [permanently submerged] sands is continuously irrigated through wave action, then it should act as a filter for suspended organic particles. The micro-organisms on the surface of the sand grains and interstitial organisms should utilize both particulate and suspended organic substances in the water. On the other hand, nutrients released by the micro-organisms would be returned to the sea by this circulation. Estimations of organic carbon and nitrogen in coarse grained marine deposits are almost always very low and this has led to the view that productivity in such deposits is also low. But it is equally possible that low values for carbon and nitrogen are the result of a high rate of turnover and that these sands are in fact an important source of nutrients in shallow seas".*

However, most of the knowledge on advection still results from investigations under laboratory conditions while few field studies are still rare. Especially with respect to the potential of advection to intensify metabolic activities and organic matter mineralization rates in permeable sands direct evidence is still restricted to the laboratory. Forster et al. (1996) exposed a medium sand with mounds to unidirectional flume flow and found the total oxygen uptake to increase linearly with flow velocity and hence, advection (fig. 8).

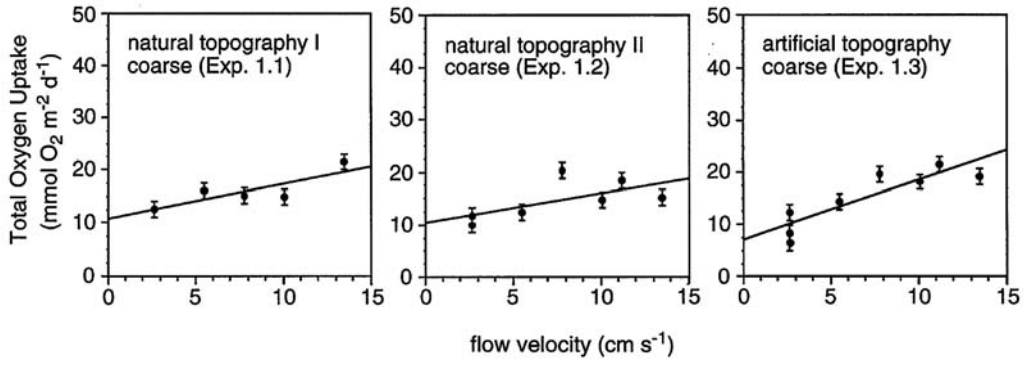

Fig. 8. Total oxygen uptake as a function of flow velocity in sediments with different surface topographies. Error bars show ± 1.5 mmol m^{-2} d^{-1}. Modified after Forster et al. (1996). © Inter-Research.

Booij et al. (1991) incubated sands in circular chambers where pressure gradients and pore-water circulation develop dependent on the stirring speed (Glud et al. 1996; Huettel and Gust 1992b). Similarly to the results obtained in the flume an increase in advection (i.e., in stirring speed) resulted in an increase in oxygen uptake. The observed increase in oxygen uptake strongly suggests that advection enhanced organic matter mineralization in these sands, as oxygen is the terminal electron acceptor for all heterotrophic processes including anaerobic pathways of organic matter degradation (Canfield 1993; Thamdrup et al. 1994).

Ziebis et al. (1996) stressed that a lot more information on conditions for advective transport in the natural environment is needed to assess the significance of advection-related processes on the continental shelf. If, and to which extent advection intensifies organic matter mineralization in natural sands will determine the contribution of the vast sand areas for the cycling of organic matter and nutrients on the continental shelf and the role of the continental shelf for the global carbon cycle. There is thus a strong need for in situ measurements of organic matter mineralization in sands. This is complicated by methodological constraints. Chamber incubations are expected to result in erroneous flux estimates as long as pressure gradients within the chamber do not match natural conditions (Glud et al. 1996; Jahnke et al. 2000). Therefore, information is needed not only on the pressure distribution within the used chamber but also on the prevailing natural pressure gradients. Flux calculations based on microprofiles cannot be based on the gradient within the diffusive boundary layer as a continuous DBL above the sediment surface is absent in the presence of interfacial flows (Guess 1998). From the gradients within the sediment it is impossible to calculate reliable fluxes because an accurate mathematical representation of solute transport in flow-dominated sediments is not yet available (Boudreau et al. 2001). Therefore, studies on sediment metabolism and organic matter mineralization in natural sands will have to include both in situ measurements and the development of appropriate methods.

Aim of the thesis

This thesis focuses on advective pore-water exchange in natural shelf sands and its potential to contribute to solute supply and organic matter mineralization. Special emphasis was placed on the factors that determine the significance of advective processes in natural shelf environments. Three neighboring stations with fine-, medium- and coarse-grained sand were chosen in order to assess the effect of sediment permeability. A substantial part of the work was dedicated to the development of appropriate methods to study advection in the field. Autonomous benthic chambers were designed and used for a direct quantification of solute fluxes. Measurements of surface topographies and bottom currents were performed to estimate pressure gradients and rates of pore-water advection at the respective sites.

The first manuscript characterizes the autonomous benthic chamber system. It is based on a chamber design that was previously used to investigate various advection-related processes in the laboratory. Upon stirring a well defined pressure gradient develops at the sediment surface that resembles pressure gradients along ripples or mounds that are exposed to bottom flow. The characterization of the new chamber focuses on the pressure distribution at the sediment water interface at different stirrer settings. This is crucial for the selection of appropriate settings for the in situ flux studies as well as for the interpretation of the results.

The second manuscript shows benthic fluxes of oxygen and nutrients that were measured with the novel chamber system at the three stations. The study focuses on the effect of advection on oxygen uptake in sands with emphasis on the role of sediment permeability. In order to extrapolate the results to a larger area, reported grain size distributions of the German Bight are used to assess sediment permeabilities for the entire region.

Acoustic altimetry and laser scanning have been used to map small-scale surface topographies in situ. The third manuscript evaluates the respective methods and compares the surface topographies of the three stations. Rates of advective pore-water exchange are estimated based on the dimensions of the observed roughness elements and near-bottom flow velocities.

The fourth manuscript introduces a new method that allows a non-invasive quantification of the oxygen uptake of aquatic sediments based on concurrent measurements of oxygen concentrations and turbulences well above the sediment. The new method represents a promising tool for future oxygen flux studies, especially in sandy areas where interfacial fluxes largely depend on the hydrodynamics above the sediment-water interface and artifacts are most easily introduced.

Introduction to the study area

Investigations mainly took place in the subtidal off the Island of Spiekeroog in the German Bight, which represents the south-eastern corner of the North Sea. The North Sea is a shelf sea with an average water depth of 70 m and comprises approximately 2 % of the global continental shelf. Exchange with the north-eastern Atlantic takes place through the English Channel and the Norwegian Sea. The hydrodynamic of the North Sea is dominated by tidal currents. In combination with wind-driven currents this results in a general anti-clockwise circulation (Otto et al. 1990). The North Sea sediments are dominated by relict sands (fig. 9).

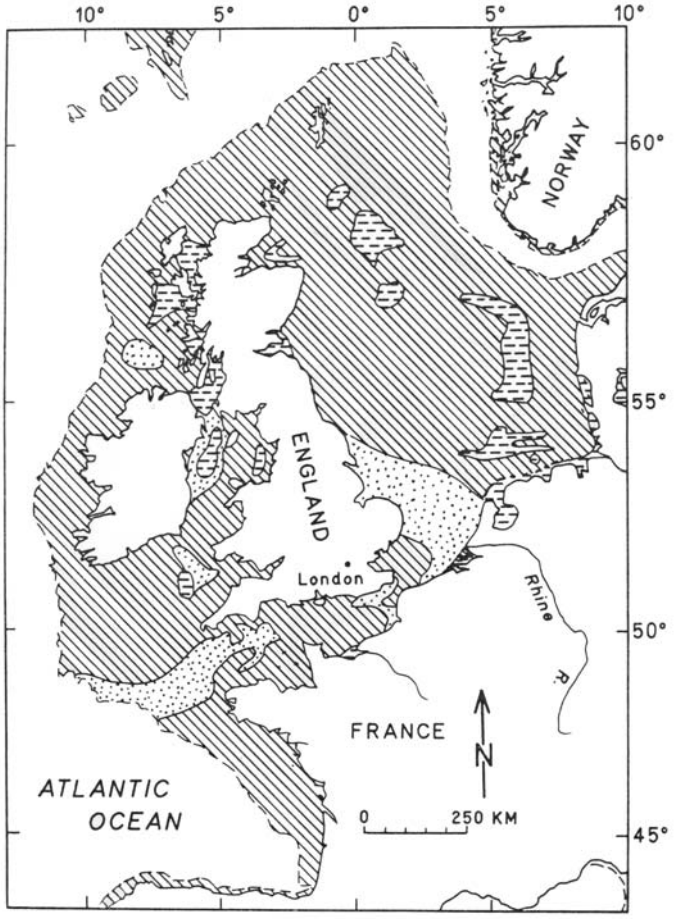

Fig. 9. Sediments off western Europe. Diagonal hatching indicates relict sediment, dots show areas of modern sands, dashed horizontal lines depict areas of modern silts. The curved dashed line represents the seaward edge of the continental shelf. From Emery (1968). © American Association of Petroleum Geologists.

Modern sandy and silty sediments that have been deposited in equilibrium with recent hydrodynamic conditions are restricted to relatively small areas. The majority of the primary production in North Sea waters is expected to be mineralized in the water column and in the surficial sediments (De Haas et al. 2002). Carbon burial is considered to be small and export to adjacent deeper areas (Skagerrak, Norwegian Channel, Norwegian Sea) is expected to amount to only a few percent of the net primary production (De Haas and Van Weering 1997). Primary productivity is particularly intense in the southern North Sea with an estimated annual rate of 370 g C m^{-2} yr^{-1} (Wollast 1991).

The island of Spiekeroog is part of the chain of Frisian Islands that extends between the Jade Estuary and the Dutch Island of Texel. These barrier islands separate the backbarrier environment with the mainland shoreline and the Wadden See tidal flats from the open waters of the German Bight. Due to strong tidal forcing, the water column in the German Bight is mixed throughout the year in most areas shallower than 30 m (Dietrich et al. 1975). The area seawards of Spiekeroog, where the study area is located, represents a mesotidal, high-energy environment. With a mean tidal range of 2.5 m tidal forces are among the highest found along the North Sea barrier islands (Postma 1982). This results in strong tidal currents with peak flow velocities of up to 50 cm s^{-1} at 1 m above the seafloor (Antia 1993). Surface gravity waves add to the hydrodynamic forcing. Even under relatively calm conditions they still impose significant oscillatory currents at the seafloor at least down to 20 m water depth (Antia 1993).

References

Aller, R.C. 1982. The effects of macrobenthos on chemical properties of marine sediment and overlying water, p. 53-102. *In* P. L. McCall and M. J. S. Tevesz [eds.], Animal-sediment relations. The biogenic alteration of sediments. Topics in geobiology. Plenum Press.

Aller, R.C. 1988. Benthic fauna and biogeochemical processes in marine sediments: the role of burrow structures, p. 301-338. *In* T. H. Blackburn and J. Sørensen [eds.], Nitrogen cycling in coastal marine environments. John Wiley.

Aller, R.C. 1994. Bioturbation and remineralization of sedimentary organic matter: effects of redox oscillation. Chem. Geol. **114:** 331-345.

Aller, R.C., and J.Y. Aller. 1998. The effect of biogenic irrigation intensity and solute exchange on diagenetic reaction rates in marine sediments. J. Mar. Res. **56:** 905-936.

Anderson, R.F., G.T. Rowe, P.F. Kemp, S. Trumbore, and P.E. Biscaye. 1994. Carbon budget for the mid-slope depocenter of the Middle Atlantic Bight. Deep-Sea Res. Part II **41:** 669-703.

Antia, E.E. 1993. Sedimentology, morphodynamics and facies association of a mesotidal barrier island shoreface (Spiekeroog, southern North Sea), p. 370, Berichte aus dem Fachbereich Geowissenschaften. Univ. Bremen, Geowissenschaften.

Antoine, D., J.-M. André, and A. Morel. 1996. Oceanic primary production 2. Estimation at global scale from satellite (coastal zone color scanner) chlorophyll. Global Biogeochem. Cycles **10:** 57-69.

Bacon, M.P., R.A. Belastock, and M.H. Bothner. 1994. ^{210}Pb balance and implications for particle transport on the continental shelf, U.S. Middle Atlantic Bight. Deep-Sea Res. Part II **41:** 511-535.

Bearman, G. 1989. Waves, tides and shallow-water processes, 1 ed. Pergamon Press.

Bergamaschi, B.A., E. Tsamakisa, R.G. Keila, T.I. Eglinton, D.B. Montluçona, and J.I. Hedgesa. 1997. The effect of grain size and surface area on organic matter, lignin and carbohydrate concentration, and molecular compositions in Peru Margin sediments. Geochim. Cosmochim. Acta **61:** 1247-1260.

Berner, R.A. 1982. Burial of organic carbon and pyrite sulfur in the modern ocean: its geochemical and environmental significance. Am. J. Sci. **282:** 451-473.

Booij, K., W. Helder, and B. Sundby. 1991. Rapid redistribution of oxygen in a sandy sediment induced by changes in the flow velocity of the overlying water. Neth. J. Sea Res. **28:** 149-165.

Böttcher, M.E., B. Hespenheide, E. Llobet-Brossa, C. Beardsley, O. Larsen, A. Schramm, A. Wieland, G. Böttcher, U.G. Berninger, and R. Amann. 2000. The biogeochemistry, stable isotope geochemistry, and microbial community structure of a temperate intertidal mudflat: an integrated study. Cont. Shelf Res. **20:** 1749-1769.

Boudreau, B.P., M. Huettel, S. Forster, R.A. Jahnke, A. McLachlan, J.J. Middelburg, P. Nielsen, F. Sansone, G. Taghon, W.R. Van Raaphorst, I. Webster, J.M. Weslawski, P. Wiberg, and B. Sundby. 2001. Permeable marine sediments: overturning an old paradigm. EOS Trans. Am. Geophys. Union **82:** 133-136.

Brockmann, U.H., R.W.P.M. Laane, and H. Postma. 1990. Cycling of nutrient elements in the North Sea. Neth. J. Sea Res. **26:** 239-264.

Burford, M.A., B.G. Long, and P.C. Rothlisberg. 1994. Sedimentary pigments and organic carbon in relation to microalgal and benthic faunal abundance in the Gulf of Carpentaria. Mar. Ecol. Prog. Ser. **103:** 111-117.

Cahoon, L.B. 1999. The role of benthic microalgae in neritic ecosystems, p. 47-86. *In* A. Ansell, R. N. Gibson and M. Barnes [eds.], Oceanography and Marine Biology. An Annual Review. Oceanogr. Mar. Biol. Annu. Rev. Taylor & Francis.

Cahoon, L.B., J.E. Nearhoof, and C.L. Tilton. 1999. Sediment grain size effect on benthic microalgal biomass in shallow aquatic ecosystems. Estuaries **22:** 735-741.

Canfield, D.E. 1993. Organic matter oxidation in marine sediments, p. 333-363. *In* R. Wollast, F. T. Mackenzie and L. Chou [eds.], Interactions of C, N, P, & S biogeochemical cycles & global change. NATO ASI Series. Springer.

Chamley, H. 1990. Sedimentology. Springer.

Clement, T.P., B.M. Peyton, R.S. Skeen, D.A. Jennings, and J.N. Petersen. 1997. Microbial growth and transport in porous media under denitrification conditions: Experiments and simulations. J. contaminant Hydrol. **24:** 269-285.

Clifton, H.E., and R.E. Hunter. 1973. Bioturbational rates and effects in carbonate sand, St. John, U.S. Virgin Islands. J. Geol. **81:** 253-268.

Conley, D.J., and R.W. Johnstone. 1995. Biogeochemistry of N, P, and Si in Baltic sediments: response to a simulated deposition of a spring diatom bloom. Mar. Ecol. Prog. Ser. **122:** 265-276.

Dando, P.R., S. Aliani, H. Arab, C.N. Bianchi, M. Brehmer, S. Cocito, S.W. Fowler, J. Gundersen, L.E. Hooper, R. Kolbl, J. Kuever, P. Linke, K.C. Makropoulos, R. Meloni, J.C. Miquel, C. Morri, S. Muller, C. Robinson, H. Schlesner, S. Sievert, R. Stohr, D. Stuben, M. Thomm, S.P. Varnavas, and W. Ziebis. 2000. Hydrothermal studies in the Aegean Sea. Phys. Chem. Earth B: Hydrol. Oceans Atmos. **25:** 1-8.

D'Andrea, A.F., R.C. Aller, and G.R. Lopez. 2002. Organic matter flux and reactivity on a South Carolina sandflat: The impacts of porewater advection and macrobiological structures. Limnol. Oceanogr. **47:** 1056-1070.

Darcy, H. 1856. Les fontaines publiques de la ville de Dijon. Victor Dalmont.

Dauwe, B., J.J. Middelburg, and P.M.J. Herman. 2001. Effect of oxygen on the degradability of organic matter in subtidal and intertidal sediments of the North Sea area. Mar. Ecol. Prog. Ser. **215:** 13-22.

De Haas, H., and T.C.E. Van Weering. 1997. Recent sediment accumulation, organic carbon burial and transport in the northeastern North Sea. Mar. Geol. **136:** 173-187.

De Haas, H., T.C.E. Van Weering, and H. De Stieger. 2002. Organic carbon in shelf seas: sinks or sources, processes and products. Cont. Shelf Res. **22:** 691-717.

DeFlaun, M.F., and L.M. Mayer. 1983. Relationships between bacteria and grain surfaces in intertidal sediments. Limnol. Oceanogr. **28:** 873-881.

Denny, M.W. 1988. Biology and the mechanics of the wave-swept environment. Princeton University Press.

Dietrich, G., K. Kalle, W. Krauss, and G. Siedler. 1975. Allgemeine Meereskunde : eine Einfuehrung in die Ozeanographie. Borntraeger.

Ehrenhauss, S., and M. Huettel. 2004. Advective transport and decomposition of chain-forming planktonic diatoms in permeable sediments. J. Sea Res. **52**: 179-197.

Ehrenhauss, S., U. Witte, S.I. Bühring, and M. Huettel. 2004. Effect of advective pore water transport on distribution and degradation of diatoms in permeable North Sea sediments. Mar. Ecol. Prog. Ser. **271**: 99-111.

Eisma, D., and J. Kalf. 1987. Distribution, organic content and particle size of suspended matter in the North Sea. Neth. J. Sea Res. **21:** 265-285.

Emery, K.O. 1968. Relict sediments on continental shelves of world. Am. Assoc. Pet. Geol. Bull. **52:** 445-464.

Enoksson, V., and M.O. Samuelsson. 1987. Nitrification and dissimilatory ammonium production and their effects on nitrogen flux over the sediment-water interface in bioturbated coastal sediments. Mar. Ecol. Prog. Ser. **36:** 181-189.

Falter, J.L., and F.J. Sansone. 2000. Hydraulic control of pore water geochemistry within the oxic-suboxic zone of a permeable sediment. Limnol. Oceanogr. **45:** 550-557.

Fehlman, M.H. 1985. Resistence components and velocity distributions of open channel flows over bedforms. Colorado State University.

Fenchel, T., and T.H. Blackburn. 1979. Bacteria and mineral cycling. Academic Press.

Fleming, K., P. Johnston, D. Zwartz, Y. Yokoyama, K. Lambeck, and J. Chapell. 1998. Refining the eustatic sea-level curve since the last glacial maximum using far and intermediate field sites. Earth Planet. Sci. Lett. **163:** 327-342.

Forster, S., and G. Graf. 1995. Impact of irrigation on oxygen flux into the sediment: intermittent pumping by *Calianassa subterranea* and 'piston-pumping' by *Lanice conchilega*. Mar. Biol. **123:** 335-346.

Forster, S., M. Huettel, and W. Ziebis. 1996. Impact of boundary layer flow velocity on oxygen utilization in coastal sediments. Mar. Ecol. Prog. Ser. **143:** 173-185.

Froelich, P.N., G.P. Klinkhammer, M.L. Bender, N.A. Luedtke, G.R. Heath, D. Cullen, P. Dauphin, D. Hammond, B. Hartman, and V. Maynard. 1979. Early oxidation of organic matter in pelagic sediments of the eastern equatorial Atlantic: suboxic diagenesis. Geochim. Cosmochim. Acta **43:** 1075-1090.

Galloway, J.N., R.W. Howarth, A.F. Michaels, S.W. Nixon, J.M. Prospero, and F.J. Dentener. 1996. Nitrogen and phosphorus budgets of the North Atlantic Ocean. Biogeochemistry **35:** 3-25.

Gehlen, M., H. Malschaert, and W.R. Van Raaphorst. 1995. Spatial and temporal variability of benthic silica fluxes in the southeastern North-Sea. Cont. Shelf Res. **15:** 1675-1696.

Glud, R.N., S. Forster, and M. Huettel. 1996. Influence of radial pressure gradients on solute exchange in stirred benthic chambers. Mar. Ecol. Prog. Ser. **141:** 303-311.

Glud, R.N., J.K. Gundersen, H. Røy, and B.B. Jørgensen. 2003. Seasonal dynamics of benthic O_2 uptake in a semienclosed bay: Importance of diffusion and faunal activity. Limnol. Oceanogr. **48:** 1265-1276.

Graf, G., and R. Rosenberg. 1997. Bioresuspension and biodeposition: a review. Journal of Marine Systems **11:** 269-278.

Guess, S. 1998. Oxygen uptake at the sediment-water interface simultaneously measured using a flux chamber method and microelectrodes: must a diffusive boundary layer exist? Est. Coast. Shelf Sci. **46:** 143-156.

Harrison, W.D., D. Musgrave, and W.S. Reeburgh. 1983. A wave-induced transport process in marine sediments. J. Geophys. Res. C **88:** 7617-7622.

Huettel, M., and G. Gust. 1992a. Impact of bioroughness on interfacial solute exchange in permeable sediments. Mar. Ecol. Prog. Ser. **89:** 253-267.

Huettel, M., and G. Gust. 1992b. Solute release mechanisms from confined sediment cores in stirred benthic chambers and flume flows. Mar. Ecol. Prog. Ser. **82:** 187-197.

Huettel, M., H. Røy, E. Precht, and S. Ehrenhauss. 2003. Hydrodynamical impact on biogeochemical processes in aquatic sediments. Hydrobiologia **494:** 231-236.

Huettel, M., and A. Rusch. 2000. Transport and degradation of phytoplankton in permeable sediment. Limnol. Oceanogr. **45:** 534-549.

Huettel, M., and I.T. Webster. 2001. Porewater flow in permeable sediments, p. 144-179. *In* B. P. Boudreau and B. B. Jørgensen [eds.], The benthic boundary layer: transport processes and biogeochemistry. Oxford Univ. Press.

Huettel, M., W. Ziebis, and S. Forster. 1996. Flow-induced uptake of particulate matter in permeable sediments. Limnol. Oceanogr. **41:** 309-322.

Huettel, M., W. Ziebis, S. Forster, and G.W. Luther, III. 1998. Advective transport affecting metal and nutrient distribution and interfacial fluxes in permeable sediments. Geochim. Cosmochim. Acta **62:** 613-631.

Hulthe, G., S. Hulth, and P.O.J. Hall. 1998. Effect of oxygen on degradation rate of refractory and labile organic matter in continental margin sediments. Geochim. Cosmochim. Acta **62:** 1319-1328.

Hutchinson, P.A., and I.T. Webster. 1998. Solute uptake in aquatic sediments due to current-obstacle interactions. J. Environ. Eng. **124:** 419-426.

Jahnke, R.A. 2001. Constraining organic matter cycling with benthic fluxes, p. 302-319. *In* B. P. Boudreau and B. B. Jørgensen [eds.], The benthic boundary layer: transport processes and biogeochemistry. Oxford Univ. Press.

Jahnke, R.A., C.R. Alexander, and J.E. Kostka. 2003. Advective pore water input of nutrients to the Satilla River Estuary, Georgia, USA. Est. Coast. Shelf Sci. **56:** 641-653.

Jahnke, R.A., J.R. Nelson, R.L. Marinelli, and J.E. Eckman. 2000. Benthic flux of biogenic elements on the Southeastern US continental shelf: influence of pore water advective transport and benthic microalgae. Cont. Shelf Res. **20:** 109-127.

Jenness, M.I., and G.C.A. Duineveld. 1985. Effects of tidal currents on chlorophyll *a* content of sandy sediments in the southern North-Sea. Mar. Ecol. Prog. Ser. **21:** 283-287.

Jørgensen, B.B. 2001. Life in the diffusive boundary layer, p. 348-373. *In* B. P. Boudreau and B. B. Jørgensen [eds.], The benthic boundary layer: transport processes and biogeochemistry. Oxford Univ. Press.

Jørgensen, B.B., and J. Sorensen. 1985. Seasonal cycles of O_2, NO_3^- and SO_4^{2-} reduction in estuarine sediments - the significance of a NO_3^- reduction maximum in spring. Mar. Ecol. Prog. Ser. **24:** 65-74.

Kawamata. 1998. Effect of wave-induced oscillatory flow on grazing by a subtidal sea urchin Strongylocentrotus nudus (A. Agassiz). J. Exp. Mar. Biol. Ecol. **224:** 31-48.

Keil, R.G., D.B. Montlucon, F.G. Prahl, and J.I. Hedges. 1994a. Sorptive preservation of labile organic matter in marine sediments. Nature **370:** 549-552.

Keil, R.G., E. Tsamakis, C.B. Fuh, J.C. Giddings, and J.I. Hedges. 1994b. Mineralogical and textural controls on the organic composition of coastal marine sediments: hydrodynamic separation using SPLITT-fractionation. Geochim. Cosmochim. Acta **58:** 879-893.

Kristensen, E. 1988. Benthic fauna and biogeochemical processes in marine sediments: microbial activity and fluxes, p. 275-299. *In* T. H. Blackburn and J. Sørensen [eds.], Nitrogen cycling in coastal marine environments. John Wiley.

Krumbein, W.C., and G.D. Monk. 1943. Permeability as a function of the size parameters of unconsolidated sand. Trans. Am. Inst. Min. Metall. Eng. **151:** 153-163.

Lambeck, K., and J. Chapell. 2001. Sea level change through the last glacial cycle. Science **292:** 679-686.

Li, M.Z., and C.L. Amos. 1999. Field observations of bedforms and sediment transport thresholds of fine sand under combined waves and currents. Mar. Geol. **158:** 147-160.

Liu, K.K., K. Iseki, and S.Y. Chao. 2002. Continental margin carbon fluxes, p. 187-239. *In* R. B. Hanson, H. W. Ducklow and J. G. Field [eds.], The changing carbon cycle: A midterm synthesis of the Joint Global Ocean Flux Study. University Press.

Llobet-Brossa, E., R. Rosselló-Mora, and R. Amann. 1998. Microbial community composition of wadden sea sediments as revealed by flourescence *in situ* hybridization. Appl. Environ. Microbiol. **64:** 2691-2696.

Logan, B.E., and D.L. Kirchman. 1991. Uptake of dissolved organics by marine bacteria as a function of fluid motion. Mar. Biol. **111:** 175-181.

Lohse, L., E.H.G. Epping, W. Helder, and W.R. Van Raaphorst. 1996. Oxygen pore water profiles in continental shelf sediments of the North Sea: Turbulent versus molecular diffusion. Mar. Ecol. Prog. Ser. **145:** 63-75.

Malone, T.C., T.S. Hopkins, P.G. Falkowski, and T.E. Whitledge. 1983. Production and transport of phytoplankton biomass over the continental shelf of the New York Bight. Cont. Shelf Res. **1:** 305-337.

Marinelli, R.L., R.A. Jahnke, D.B. Craven, J.R. Nelson, and J.E. Eckman. 1998. Sediment nutrient dynamics on the South Atlantic Bight continental shelf. Limnol. Oceanogr. **43:** 1305-1320.

Mayer, L.M. 1994. Surface area control of organic carbon accumulation in continental shelf sediments. Geochim. Cosmochim. Acta **58:** 1271-1284.

McCave, I.N. 1972. Transport and escape of fine-grained sediment from shelf areas, p. 225-248. *In* D. J. P. Swift, D. B. Duane and O. H. Pilkey [eds.], Shelf sediment transport : process and pattern. Dowden, Hutchinson & Ross.

McCave, I.N. 2003. Sedimentary settings on continental margings - an overview, p. 1-14. *In* G. Wefer, D. Billett, D. Hebbeln, B. B. Jørgensen, M. Schlüter and T. C. E. Van Weering [eds.], Ocean Margin Systems. Springer.

McLachlan, A., I.G. Eliot, and D.J. Clarke. 1985. Water filtration through reflective microtidal beaches and shallow sublittoral sands and its implications for an inshore ecosystem in western Australia. Est. Coast. Shelf Sci. **21:** 91-104.

Menard, H.W., and S.M. Smith. 1966. Hypsometry of ocean basin provinces. J. Geophys. Res. **71:** 4305-&.

Meybeck, M. 1993. C, N, P, and S in rivers: from sources to global inputs, p. 163-193. *In* R. Wollast, F. T. Mackenzie and L. Chou [eds.], Interactions of C, N, P, & S biogeochemical cycles & global change. Springer.

Milligan, T.G., and P.S. Hill. 1998. A laboratory assessment of the relative importance of turbulence, particle composition, and concentration in limiting maximal floc size and settling behaviour. J. Sea Res. **39:** 227-241.

Milliman, J.D., D.A. Ross, and O.H. Pilkey. 1972. Sediments of the continental margin off the eastern United States. Geological Society of America Bulletin **83:** 1315-1334.

Milliman, J.D., and C.P. Summerhayes. 1975. Upper continental margin sedimentation off Brazil. Schweizerbart.

Moore, D.C. 1996. Large groundwater inputs to coastal waters revealed by Ra-226 enrichments. Nature **380:** 612-614.

Moore, L.W., H. Matheny, T. Tyree, D. Sabatini, and S.J. Klaine. 1988. Agricultural runoff modeling in a small West Tennessee watershed. J. Water Pollut. Control. Fed. **60:** 242-249.

Nelson, J.R., J.E. Eckman, C.Y. Robertson, R.L. Marinelli, and R.A. Jahnke. 1999. Benthic microalgal biomass and irradiance at the sea floor on the continental shelf of the South Atlantic Bight. Cont. Shelf Res. **19:** 477-505.

Nittrouer, C.A., and L.D. Wright. 1994. Transport of Particles across Continental Shelves. Rev. Geophys. **32:** 85-113.

Oldham, C.E. 1999. Porewater nutrient fluxes in a shallow fetch-limited estuary. Mar. Ecol. Prog. Ser. **183:** 39-47.

Otto, L., J.T.F. Zimmerman, G.K. Furnes, M. Mork, R. Saetre, and G. Becker. 1990. Review of the physical oceanography of the North Sea. Neth. J. Sea Res. **26:** 161-238.

Postma, H. 1982. Hydrography of the Wadden Sea: movements and properties of water and particulate matter, Report of the Wadden Sea Working Group. A. A. Balkema.

Precht, E., U. Franke, L. Polerecky, and M. Huettel. 2004. Oxygen dynamics in permeable sediments with wave-driven pore water exchange. Limnol. Oceanogr. **49**: 693-705.

Precht, E., and M. Huettel. 2003. Advective pore-water exchange driven by surface gravity waves and its ecological implications. Limnol. Oceanogr. **48:** 1674-1684.

Precht, E., and M. Huettel. 2004. Rapid wave-driven advective pore water exchange in a permeable coastal sediment. J. Sea Res. **51:** 93-107.

Rasheed, M., M.I. Badran, and M. Huettel. 2003. Particulate matter filtration and seasonal nutrient dynamics in permeable carbonate and silicate sands of the Gulf of Aqaba, Red Sea. Coral Reefs **22:** 167-177.

Rasmussen, H., and B.B. Jørgensen. 1992. Microelectrode studies of seasonal oxygen-uptake in a coastal sediment - role of molecular diffusion. Mar. Ecol. Prog. Ser. **81:** 289-303.

Reimers, C.E., S.M. Glenn, and E.L. Creed. 1996. The dynamics of oxygen uptake by shelf sediments. EOS Trans. Am. Geophys. Union **76:** 88.

Reimers, C.E., H.A. Stecher III, G.L. Taghon, C.M. Fuller, M. Huettel, A. Rusch, N. Ryckelynck, and C. Wild. 2004. *In-situ* measurements of advective solute transport in permeable shelf sands. Cont. Shelf Res. **24:** 183-201.

Richardson, K. 1996. Conclusion, research and eutrophication control, p. 243-267. *In* B. B. Jørgensen and K. Richardson [eds.], Eutrophication in coastal marine ecosystems. Coastal and estuarine studies. American Geophysical Union.

Riedl, R.J., N. Huang, and R. Machan. 1972. The subtidal pump, a mechanism of intertidal water exchange by wave action. Mar. Biol. **13:** 210-221.

Rocha, C. 1998. Rhythmic ammonium regeneration and flushing in intertidal sediments of the Sado estuary. Limnol. Oceanogr. **43:** 823-831.

Rowe, G.T., S. Smith, P. Falkowski, T. Whitledge, R. Theroux, W. Phoel, and H. Ducklow. 1986. Do continental shelves export organic matter? Nature **324:** 559-561.

Rowe, G.T., R. Theroux, W. Phoel, H. Quinby, R. Wilke, D. Koschoreck, T.E. Whitledge, P.G. Falowski, and C. Fray. 1988. Benthic carbon budgets for the continental shelf south of New England. Cont. Shelf Res. **8:** 511-527.

Rusch, A., and M. Huettel. 2000. Advective particle transport into permeable sediments - evidence from experiments in an intertidal sandflat. Limnol. Oceanogr. **45:** 525-533.

Rusch, A., M. Huettel, C.E. Reimers, G.L. Taghon, and C.M. Fuller. 2003. Activity and distribution of bacterial populations in Middle Atlantic Bight shelf sands. FEMS Microbiol. Ecol. **44:** 89-100.

Rutgers van der Loeff, M.M. 1981. Wave effects on sediment water exchange in a submerged sand bed. Neth. J. Sea Res. **15:** 100-112.

Rutherford, J.C., J.D. Boyle, A.H. Elliott, T.V.J. Hatherell, and T.W. Chiu. 1995. Modeling benthic oxygen uptake by pumping. J. Environ. Eng. **121:** 84-95.

Rutherford, J.C., G.J. Latimer, and R.K. Smith. 1993. Bedform mobility and benthic oxygen uptake. Water Res. **27:** 1545-1558.

Savant, S.A., D.D. Reible, and L.J. Thibodeaux. 1987. Convective transport within stable river sediments. Water Resour. Res. **23:** 1763-1768.

Schlüter, M. 2003. Fluid flow in continental margin sediments, p. 205-217. *In* G. Wefer, D. Billett, D. Hebbeln, B. B. Jørgensen, M. Schlüter and T. C. E. Van Weering [eds.], Ocean marin systems. Springer.

Shum, K.T., and B. Sundby. 1996. Organic matter processing in continental shelf sediments - the subtidal pump revisited. Mar. Chem. **53:** 81-87.

Sleath, J.F.A. 1984. Sea bed mechanics. Wiley-Interscience.

Smetacek, V.S., U. Bathmann, E.-M. Nöthig, and R. Scharek. 1991. Coastal Eutrophication: Causes and consequences. *In* R. F. C. Mantoura, J.-M. Martin and R. Wollast [eds.], Ocean Margin processes in global change. John Wiley and Sons.

Sternberg, R.W., and L.H. Larsen. 1976. Frequency of sediment movement on the Washington continental shelf: a note. Mar. Geol. **21:** M37-M47.

Thamdrup, B., H. Fossing, and B.B. Jørgensen. 1994. Manganese, iron, and sulfur cycling in a coastal marine sediment, Aarhus Bay, Denmark. Geochim. Cosmochim. Acta **58:** 5115-5129.

Thibodeaux, L.J., and J.D. Boyle. 1987. Bedform-generated convective transport in bottom sediment. Nature **325:** 341-343.

Tréguer, P., D.M. Nelson, A.J. Van Bennekom, D.J. DeMaster, A. Leynaert, and B. Quéguiner. 1995. The silica balance in the world ocean: a reestimate. Science **268:** 375-379.

Vittal, N., K.G.R. Raju, and R.J. Garde. 1977. Resistance of two-dimensional triangular roughness. Journal of Hydraulic Research **15:** 19-36.

Walsh, J.J. 1991. Importance of continental margins in the marine biogeochemical cycling of carbon and nitrogen. Nature **350:** 53-55.

Walsh, J.J., E.T. Premuzic, J.S. Gaffney, G.T. Rowe, G. Harbottle, R.W. Stoenner, W.L. Balsam, P.R. Betzer, and S.A. Macko. 1985. Organic storage of CO_2 on the continental slope off the Mid-Atlantic Bight, the southeastern Bering Sea, and the Peru Coast. Deep-Sea Research Part a-Oceanographic Research Papers **32:** 853-883.

Walsh, J.J., G.T. Rowe, R. Iverson, and C.P. McRoy. 1981. Biological export of shelf carbon is a sink of the global CO_2 cycle. Nature **291:** 196-201.

Webb, J.E., and J. Theodor. 1968. Irrigation of submerged marine sands through wave action. Nature **220:** 682-683.

Webster, I.T., S.J. Norquay, F.C. Ross, and R.A. Wooding. 1996. Solute exchange by convection within estuarine sediments. Est. Coast. Shelf Sci. **42:** 171-183.

Webster, I.T., and J.H. Taylor. 1992. Rotational dispersion in porous media due to fluctuating flow. Water Resour. Res. **28:** 109-119.

Wheatcroft, R.A. 1992. Experimental tests for particle size dependent bioturbation in the deep ocean. Limnol. Oceanogr. **37:** 90-104.

Wheatcroft, R.A. 1994. Temporal variation in bed configuration and one-dimensional bottom roughness at the mid shelf STRESS site. Cont. Shelf Res. **14:** 1167-1190.

Wollast, R. 1991. The coastal organic carbon cycle: fluxes, sources, and sinks., p. 365-382. *In* M. R. F. C, M. J. M. and R. Wollast [eds.], Ocean margin processes in global change. John Wiley & Sons.

Wollast, R. 1998. Evaluation and comparison of the global carbon cycle in the coastal zone and in the open ocean, p. 213-252. *In* K. H. Brink and A. R. Robinson [eds.], The Sea - Vol. 10: The global coastal ocean: processes and methods. John Wiley & Sons.

Wollast, R. 2003. Continental margins - review of geochemical settings, p. 15-31. *In* G. Wefer, D. Billett, D. Hebbeln, B. B. Jørgensen, M. Schlüter and T. C. E. Van Weering [eds.], Ocean marin systems. Springer.

Zabel, M., and C. Hensen. 2003. The importance of mineralization processes in surface sediments at continental margins, p. 253-267. *In* G. Wefer, D. Billett, D. Hebbeln, B. B. Jørgensen, M. Schlüter and T. C. E. Van Weering [eds.], Ocean marin systems. Springer.

Ziebis, W., M. Huettel, and S. Forster. 1996. Impact of biogenic sediment topography on oxygen fluxes in permeable seabeds. Mar. Ecol. Prog. Ser. **140:** 227-237.

Overview of the enclosed manuscripts

Four manuscripts are enclosed in this thesis. All four manuscripts focus on transport and metabolic activity in natural sediments. The first manuscript characterizes a new field-going benthic chamber system, while the second presents flux data that have been obtained with the chambers at sandy North Sea sites. The third manuscript evaluates natural rates of pore-water exchange at the same sites based on in situ measurements of the physical preconditions of advective pore-water transport. The fourth manuscript introduces a novel non-invasive approach for the quantification of sediment oxygen uptake. When the thesis was submitted for assessment, one manuscript (# 4) was published in an peer-reviewed journal, two manuscripts had been submitted (# 1 & 2) and one was in the final phase of preparation (# 3).

1.

Pore-water advection and solute fluxes in permeable marine sediments (I): Calibration and performance of the novel benthic chamber system SANDY

Felix Janssen, Paul Faerber, Markus Huettel, Volker Meyer & Ursula Witte

This study was initiated by U. Witte. Felix Janssen was responsible for the development and field testing of the novel chamber system. He investigated the chamber and optode performance the laboratory, evaluated the data, and wrote the manuscript with editorial help and input of U. Witte and M. Huettel.

The manuscript is now published in Limnology and Oceanography (**50**: 768-778).

2.

Porewater advection and solute fluxes in permeable marine sediments (II): Organic matter mineralization at three sandy sites with different permeabilities (German Bight, North Sea)

Felix Janssen, Markus Huettel & Ursula Witte

U. Witte initiated this study. F. Janssen organized and coordinated the cruises, carried out the chamber deployments and did the laboratory measurements. He evaluated the data and wrote the manuscript with editorial help and input by U. Witte and M. Huettel.

The manuscript is now published in Limnology and Oceanography (**50**: 779-792).

3.

Sediment surface topographies and bottom water flow:
an in situ case-study on the fundamentals of pore-water advection.

Felix Janssen, Hans Røy, Ursula Werner & Ursula Witte

This study was initiated by U. Witte and F. Janssen. F. Janssen organized and coordinated the cruises, and carried out the topography and current measurements. He evaluated the data which also included oxygen microprofiles provided by U. Werner and wrote the manuscript with editorial help and input by U. Witte, H. Røy, U. Werner, and M. Huettel.

4.

Oxygen uptake by aquatic sediments measured with a novel non-invasive eddy-correlation technique

Peter Berg, Hans Røy, Felix Janssen, Volker Meyer, Bo Barker Jørgensen, Markus Huettel & Dirk de Beer

This study was initiated by P. Berg and B. B. Jørgensen. F. Janssen participated in the construction of the eddy-correlation device and in the organization of the field campaigns. He was responsible for all benthic chamber measurements and evaluated the chamber-derived data. F. Janssen wrote the first version of the corresponding part in the manuscript and provided editorial help and input for the entire manuscript.

The Manuscript is published in Marine Ecology Progress Series (**262**: 75-83).

Pore-water advection and solute fluxes in permeable marine sediments (I): Calibration and performance of the novel benthic chamber system SANDY

Felix Janssen [1], Paul Faerber [1], Markus Huettel [1,2], Volker Meyer [1] & Ursula Witte [1,3]

[1] Max Planck Institute for Marine Microbiology, Celsiusstrasse 1, D-28359 Bremen, Germany

[2] Present address: Florida State University, Department of Oceanography, 0517 OSB, West Call Street, Tallahassee, Florida 32306-4320, USA

[3] Present address: University of Aberdeen, Oceanlab, Newburgh, Aberdeen AB41 6AA, Scotland, UK

Acknowledgements

We thank B. B. Jørgensen for the support of this work. R. Rimek is thanked for his dedicated work on the design of the SANDY system. The construction was very much improved by the technical assistance of A. Cremer, S. Meyer, and T. Kumbier. G. Herz and O. Eckhoff are greatfully acknowledged for manufacturing the system. We also like to thank G. Schuessler, K. Neumann, and C. Wigand for pressure and sulfate measurements and for the fabrication of optodes. F. Aspetsberger helped a lot in the optode measurements. H. Røy is thanked for fruitful discussions on diffusive exchange in benthic chambers. This study was financed by the Max Planck Society.

Abstract

The autonomous benthic chamber system SANDY has been developed specifically to study solute fluxes in permeable aquatic sediments in situ. In such permeable sands, that cover most of the continental shelves, advective pore-water transport can dominate solute exchange across the sediment water interface. Measurements of benthic solute fluxes by means of the SANDY system allow one to take the contribution of this advective exchange into account. The innovative features of the system include a unique mechanical chamber drive that permits gentle and deep penetration of hard consolidated sands with minimum disturbance and a programmable stirring mechanism that is able to generate well-defined pressure gradients at the enclosed sediment surface. Setting the stirring rate accordingly, these pressure gradients can be adjusted to mimic those occurring under natural conditions due to the interaction of surface topography and boundary layer flow. Solute fluxes, measured at a specific "advective stirrer setting" can be compared to those obtained at a "non-advective" setting where pressure gradients are absent and solute exchange is restricted to diffusion and bioirrigation. Rates of pore-water exchange that have been measured at contrasting stirrer settings in natural coarse grained deposits demonstrate the feasibility of this approach and confirm that the SANDY chambers represent ideal model systems to study advection-related processes in permeable shelf sediments in situ. For the first time, the SANDY system allows a systematic investigation of fluxes of oxygen and other solutes in permeable shelf sands, which is crucial for an improved understanding of the role of the continental shelf for the global cycles of matter.

Introduction

Sandy deposits represent the predominant sediment type in shelf areas worldwide (Emery 1968; Emery and Uchupi 1972). The large pore spaces of sands give rise to high permeabilities which in turn allow for a transport of water through the sediment - a process referred to as pore-water advection (Huettel and Webster 2001). The principal driving forces of advection are pressure gradients at the sediment surface that develop when topographical features like mounds or ripples protrude into unidirectional or oscillating bottom water flow (Huettel and Gust 1992a; Precht and Huettel 2003). While pressure gradients induced by local roughness elements at the seafloor are expected to be in the range of a few Pascal only (Thibodeaux and Boyle 1987; Huettel et al. 1996) they can have a large impact on exchange processes across the sediment water interface. In a flume study Huettel and Gust (1992a) found that rates of advective solute transport around small mounds exceeded molecular diffusion by up to three orders of magnitude. By means of this intensified transport, advection potentially stimulates both chemical reactions and the metabolic activity of biota within the sediment (Boudreau et al. 2001; Huettel et al. 2003). The combination of enhanced transport and activity results in enhanced interfacial fluxes of biologically relevant solutes such as oxygen, nutrients, and heavy metals as has been observed in laboratory incubations of permeable sands (Booij et al. 1991; Forster et al. 1996; Huettel et al. 1998). If advection similarly intensifies metabolic activities and solute fluxes of naturally occurring sands this may substantially affect organic matter turnover in shelf environments including rates of carbon mineralization, nutrient recycling, and recycled primary production (Huettel et al. 2003).

Despite this potential relevance, the significance of advection to solute fluxes in natural permeable sediments is still largely unresolved. As in muddy sediments, in situ flux measurements of sands may be obtained by means of benthic chamber deployments (Jahnke et al. 2000). Enclosing the sediment excludes currents and waves and replaces the former natural pressure distribution with artificial pressure gradients that result from stirrer induced flow cells within the chamber water. These gradients need no sediment topography to develop and are found in benthic chambers of any size and geometry (Tengberg et al. 2005). For a given chamber design the magnitude of the pressure

gradient, and hence the rates of pore-water advection, depend on the stirring speed (Glud et al. 1996). Consequently, fluxes obtained in permeable sands will most likely depend on the chamber settings. Chamber-derived fluxes will thus deviate from natural fluxes unless the pressure gradient in the chamber perfectly meets environmental conditions (Glud et al. 1996; Jahnke et al. 2000; Boudreau et al. 2001).

Natural pressure gradients, on the other hand, are expected to vary greatly between sites as they scale both with the strength of the prevailing hydrodynamic forces and the height and spacing of the existing roughness elements (Huettel and Gust 1992a; Huettel et al. 1996). Even at a single spot a "typical" pressure gradient does not exist because tidal, wave-, and wind-driven currents and the sediment topography constantly change at time scales from seconds to seasons (Grant 1983; Wheatcroft 1994). Given the variability of natural settings, the opportunity to adjust the actual pressure gradient by changing the stirring rate makes chambers valuable experimental tools for flux studies on permeable sediments. Huettel and Rusch (2000) stated that centrally stirred cylindrical chambers can be used to mimic natural pressure gradients (e.g., that along a ripple of a particular height exposed to flow of a particular velocity). A chamber with a known pressure distribution can thus be used to investigate how interfacial solute fluxes depend on the intensity of advective transport. The observed fluxes at a specific "advective stirrer setting" will result from a combination of solute transport through advection, diffusion, and through bioirrigation of the enclosed macrofauna. The difference between this bulk flux and fluxes that are obtained at a "non-advective setting" (i.e., at very low pressures) would then allow one to quantify the net flux that was based upon advection alone.

In several studies, mostly in the laboratory, cylindrical chambers have been used to investigate advective transport and associated biological processes and rates (Booij et al. 1991; Glud et al. 1996; Heise and Gust 1999; Huettel and Rusch 2000; Rasheed et al. 2003; Wild et al. 2004). Until now, however, no field-going system was available for in situ studies on continental shelf sands. This publication describes the novel autonomous chamber system SANDY, designed specifically to investigate the significance of advection to solute fluxes in natural permeable beds. The hydraulic properties of the chamber at different stirrer settings are characterized with respect to pressure distribution and diffusive boundary layer (DBL) thickness as the fundamentals of solute

exchange *via* advection and diffusion. In order to precisely quantify oxygen fluxes the SANDY system is equipped with fiberoptic oxygen sensors ("optodes"). The reliability of the optode device is assessed with respect to accuracy and temporal stability of the oxygen measurements. This paper introduces and characterizes the new benthic chamber system SANDY with special emphasis on conditions of interfacial solute and pore-water exchange within the chamber. The companion paper presents oxygen and nutrient flux data that have been obtained with the SANDY system on natural sands of different permeabilities (Janssen et al. 2005).

Material and methods

System description

Chamber technique. The SANDY chamber units are constructed as compact, self contained modules and can be attached to any suitable supporting frame. The entire SANDY system consists of two chamber modules, four syringe water samplers with seven glass syringes each, electronics and batteries all mounted to a stainless steel tripod. A description of both the supporting frame and water samplers can be found in Witte and Pfannkuche (2000).

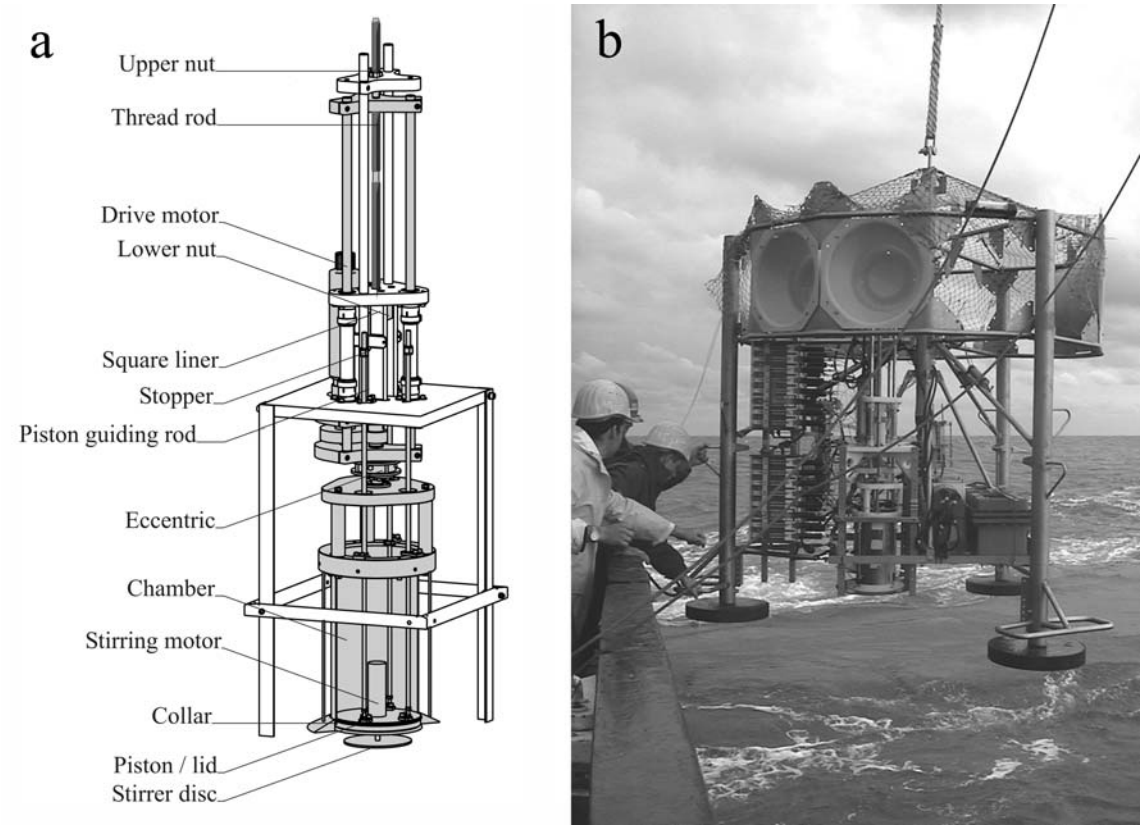

Fig. 1. Panel a shows details of the SANDY chamber module. All gray parts move up and down with the chamber drive. Parts of the chamber wall and the collar are removed to show the piston / lid and the stirrer. The chamber has an inner diameter 200 mm, the stirrer disc (156 mm diameter x 4 mm) is mounted 20 mm below the lid. The parts consist either of stainless steel (chamber, rods, nuts, pressure housing, frame) or of plastic (mainly Homopolymer Acetal (POM) and Polycarbonate: lid, stirrer disc, stoppers, guides, mountings). Panel b shows the entire chamber system containing two SANDY modules and four water samplers (to the left of the chamber modules).

Figs. 1 a & b show the chamber module and give an impression of the entire system. In the starting position the cylindrical stainless steel chamber is closed from below with a piston that later serves as the chamber lid and holds the stirrer disc (fig. 1 a). An external collar surrounds the chamber at the same vertical level but is free to slide upwards as soon as the chamber enters the sediment. The whole chamber drive (i.e., all gray parts) is moved vertically by a 24 V DC drive motor that turns the threaded rod. Initially the threaded rod turns in two nuts. The upper one holds the drive in position while the lower one, sitting at the top of the square liner, is free to slide downwards.

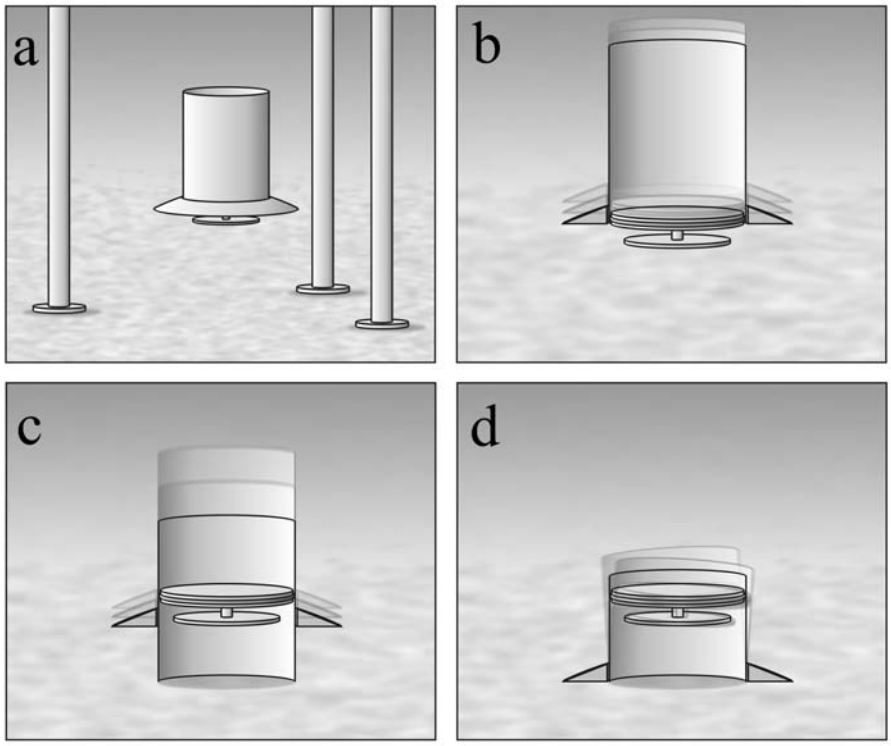

Fig. 2 a-d. Sketch of the chamber deployment. In fig. a-d the front part of the chamber wall is removed to show the position of the lid. Refer to the text for details.

Fig. 2 illustrates the deployment principle, technical details refer to fig. 1 a. To exclude sediment erosion by a shock wave at the moment the frame arrives at the seafloor, the chamber is initially situated well above the sediment surface (approximately 220 mm) (fig. 2 a). Controlled by the onboard electronics the drive motor starts turning, and chamber, collar, and lid slowly approach the sediment. Once the lid reaches its ultimate distance to the sediment (typically 120 mm) it is kept in position by the vertically

adjustable stoppers on the piston guiding rods (fig. 2 b). In order to rapidly enclose the sediment, the threaded rod now leaves the upper nut thereby releasing the chamber drive. Within approximately one second the chamber slides down and penetrates the upper sediment layer without any displacement of the overlying water (fig. 2 c). Still turning the threaded rod in the lower nut, the motor forces the chamber slowly further down until the lower rim arrives at its final depth (typically 150 mm below the surface; fig. 2 d). Deep intrusion into the sediment is facilitated by the eccentric that moves the upper part of the chamber along a small circular path resulting in a slight rotating tilting of the chamber of about 1 ° in all directions. After the incubation, the drive motor turns the opposite direction pulling the chamber out of the sediment. The initial chamber to sediment distance, the chamber intrusion depth, and the lid to sediment distance can all be adjusted.

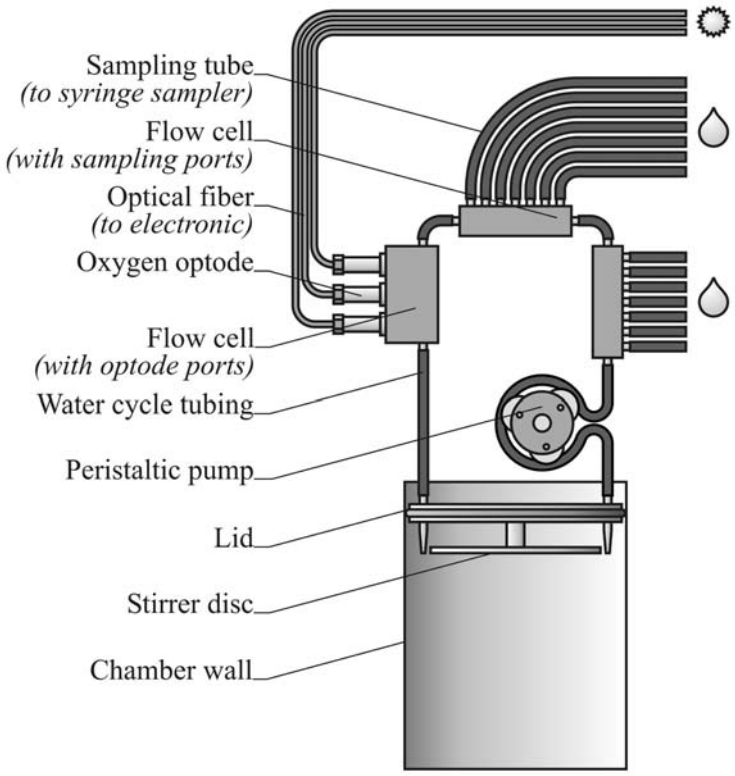

Fig. 3. Schematic of the chamber water circuit (not to scale) including flow cells with ports for the connection of 3 optodes and 2 syringe samplers

The stirrer disc is coupled to a 12 V DC motor through a magnetic clutch. To minimize flow obstructions within the chamber, sampling ports and sensors are inserted into a water circuit (gastight Viton® tubing, 30 ml total volume) with in- and outflow located next to the stirrer disc (fig. 3). The circuit is permanently flushed with chamber water at 20 ml min^{-1} by means of a peristaltic pump (Masterflex L/S® pumphead).

Electronics. A central electronics device controls chambers and water samplers and performs measurements of oxygen. The speed of the stirrer disc is permanently monitored by means of a photoelectric sensor and adjusted according to the selected stirring rate. The optode setup consists of a light emitting diode (intensity modulated sinusoidally at 20 kHz) for excitation of the oxygen sensitive ruthenium fluorophore at the tip of the optode, a wavelength division fiber coupler, and a photomultiplier tube (PMT) (Klimant et al. 1995; Glud et al. 1999). The luminescence lifetime is determined based on the phase angle shift between the oscillation of the excitation light and the luminescence of the fluorophore (Holst et al. 1997). Phase angle measurements are performed by the "Diver board" (Joanneum Research-Institute, Graz, Switzerland), a miniaturized version of the setup described by Gruber et al. (1995). The actual phase angle readings (0 to 2 π) are stored once every second at 14 bit resolution. A custom-built fiberoptic rotary switch switches between the six optodes. A fluorescent paint of negligible lifetime applied to a seventh position of the switch serves as an internal reference in order to correct for phase angle changes due to warm-up of the LED and the PMT.

Hydraulic properties of the chamber

The SANDY chamber bas been characterized with respect to radial pressure distributions and chamber hydrodynamics. Special emphasis was placed on two particular stirrer settings that are subsequently referred to as "advective" and "non-advective" stirring mode: stirring continuously at 40 rpm and intermittently at 20 rpm (15 s clockwise, 15 s pause, 15 s counterclockwise, 15 s pause…). All measurements took place in acrylic chambers of exactly the same size and geometry as the SANDY chambers. The chambers were filled with de-ionized water of room temperature (18° C) and, unless otherwise stated, measurements were performed at 100 mm distance between the lower surface of the stirrer disc and the bottom (i.e., at 120 mm overlying water height).

Radial pressure gradient. The radial pressure gradient was calibrated for a wide range of water column heights and stirring rates including the advective- and non-advective stirrer setting. The chambers were closed from below by means of a plastic bottom that was covered by a 250 µm nylon mesh to introduce a roughness comparable to that of sandy sediment. An array of seven pressure ports along the radius of the bottom was used for pressure measurements relative to the chamber center by means of a wet/wet differential pressure transducer (Effa GA 63) according to Huettel and Gust (1992b) and Glud et al. (1996).

Chamber water mixing. The dispersal of a cloud of fluorescence dye was monitored at the non-advective stirrer setting. Five bare optic fibers (multimode, 140µm outer diameter) with uncoated tips were introduced from below through three ports in the gauze covered plastic bottom (see fig. 6 for details). The fibers were connected to a fluorometer, which is an intensity based model of the optode device described above. For the range of concentrations used, the fluorescence intensity scaled linearly with the dye concentration (data not shown). While stirring in the non-advective mode, 40 ml of a 50 mg l^{-1} sodium fluorescein solution (C.I. 45350) was added to a chamber water circuit similar to that of the SANDY system and the dye concentrations at the fiber tips were monitored.

Diffusive boundary layer (DBL) thickness. The average DBL thickness was assessed using the alabaster dissolution method as described by Santschi et al. (1991) and Santschi et al. (1983). An alabaster ($CaSO_4 \cdot 2\ H_2O$) layer covered the bottom of six chambers (three replicates per stirring mode). After filling the chambers with de-ionized water, the stirrers were run for 1 d at the respective modes and 13 samples (3 ml) per chamber were taken from the chamber water circuit. An additional sample was taken from one of the chambers after stirring another 30 d at 40 rpm to determine the sulfate concentration at saturation. Sulfate concentrations were measured with an Ion Chromatograph (Waters IC-Pak™ anion column and mod. 430 conductivity detector). The DBL thickness was then determined by fitting the sulfate concentration time series with an exponential equation that describes the $CaSO_4$ accumulation in an enclosed water volume in relation to the boundary layer thickness (Buchholtz-Ten Brink et al. 1989). The effective molecular diffusivities of Ca^{2+} and SO_4^{2-} at 18° C were taken from

Li and Gregory (1974) and corrected for cross-coupled diffusion as described in Santschi et al. (1991).

Optode performance

Oxygen concentration within a bottle of freshwater was kept at 100 % air saturation (295.2 µmol L^{-1}) by bubbling with air. By means of a peristaltic pump, the water was circulated between the bottle and a flow cell that contained six optodes. The bottle as well as the flow cell were placed in a temperature controlled water bath at 18.2° C. To investigate measurement accuracy and reproducibility, a series of phase angle readings was conducted at fixed positions of the fiberoptic switch (4 min for each sensor). The number of replicates that was needed to reach a certain accuracy was determined by calculating the running average of consecutive readings for different averaging periods. The drift of the optode measurements including the effect of the initial warm-up of the electronics was quantified during a 24 h measurement series. Linear regressions were applied to measurements of the first and last 4 hours in order to determine the initial and long term drift rates, respectively. To calibrate the optodes an oxygen concentration series (0 - 100 % air saturation, 8 steps) was prepared by bubbling the water with air, nitrogen, and mixtures of both as obtained with a gas mixer (Digamix, Woesthoff). Calibration was then performed by fitting a modified Stern-Volmer equation (Holst et al. 1997) to series of luminescence lifetime *vs*. oxygen concentration.

Results

Hydraulic properties of the chamber

Pressure gradient. The rotation of the stirrer disc resulted in a radial pressure gradient with pressure rising from the center to the outer rim of the chamber bottom. The upper curve in the left graph of fig. 4 shows the pressure gradient at the advective stirrer setting (40 rpm) and a disc to bottom distance of d = 100 mm. The overall pressure difference Δp between the center and the outer rim of the chamber increased with stirrer speed (right graph). Within the stirring rates investigated (10 to 80 rpm) the relationship could be approximated by a power function of the form $\Delta p\ (\omega) = 9.33\ 10^{-6}\ \omega^{2.28}$ (r^2 = 0.99) where ω is the angular velocity in degrees per second.

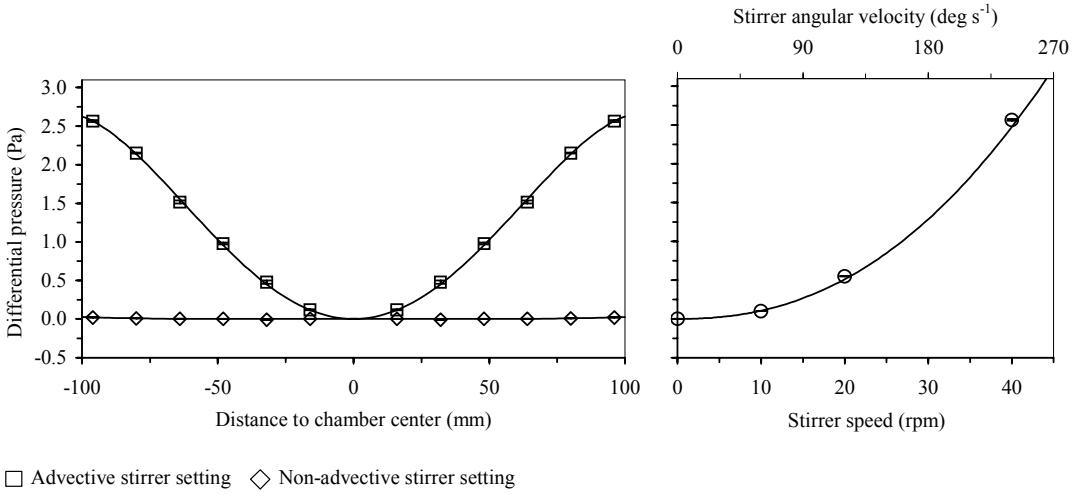

Fig. 4. Left graph: radial pressure distribution at the chamber bottom at stirring rates of 40 rpm (continuously; squares) and 20 rpm (intermittent; diamonds). Pressures were measured relative to the center port at 6 ports along the chamber radius (r = 16 to 96 mm, 16 mm spacing) and mirrored to the opposite side (-16 to -96 mm). The whiskers show standard deviations of three measurements. The line represents a 4th order polynomial fit. Right graph: the relation between the overall pressure difference (center port to most distant port) and stirrer speed (up to 80 rpm; 80 rpm data point not shown). The curve represents a power function (refer to text for details).

The pressure gradient was also affected by changes in the disc to bottom distance (fig. 5). While the general shape was maintained (left graph) the overall pressure difference Δp decreased steadily with increasing distance (right graph). The relation

was found to be well represented by a reciprocal power function of the form $\Delta p\,(d) = (8.12\ 10^{-4}\ d^{1.24} + 0.15)^{-1}$ ($r^2 = 0.99$) where d is the distance between the lower surface of the stirrer disc and the chamber bottom in millimeters.

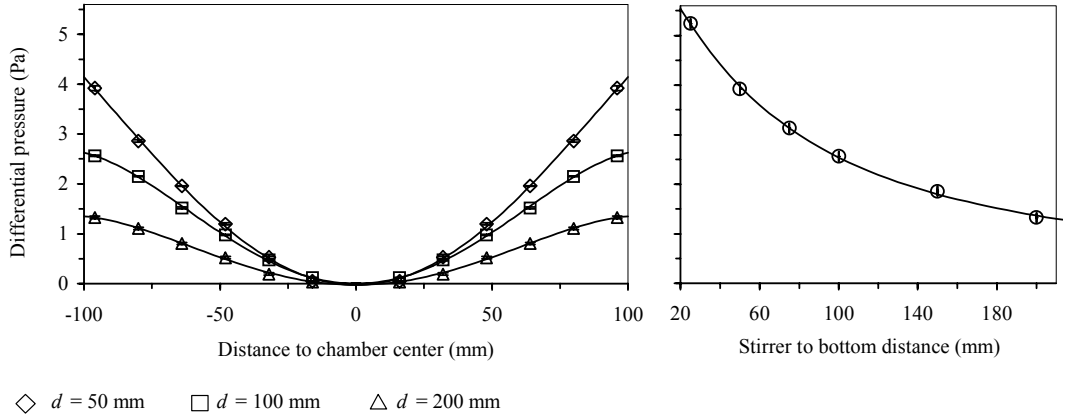

Fig. 5. Left graph: radial pressure distribution at the chamber bottom at stirrer to bottom distances of d = 50 mm (diamonds), 100 mm (squares), and 200 mm (triangles) at stirring speeds of 40 rpm (refer to legend of fig. 4 for details on the arrangement of the pressure ports). The whiskers show standard deviations of three measurements. The lines represent 4th order polynomial fits. Right graph: relation between the overall pressure difference (center port to most distant port) and stirrer to bottom distance. The curve represents a reciprocal power function (refer to text for details).

The lower curve in the left graph of fig. 4 shows the radial pressure distribution at the non-advective setting (d = 100 mm). The overall pressure difference at this stirring mode was below 1 % of the value obtained at 40 rpm. This proportion slightly increased with decreasing disc to bottom distance to a maximum value of 2.5 % at d = 25 mm (i.e., the least distance investigated).

Mixing. Fig. 6 shows the fluorescein concentrations at the respective fiber tips while stirring in the non-advective stirring mode. A constant reading at all five tips (i.e., a homogenous dye distribution) was reached within a few minutes after dye injection.

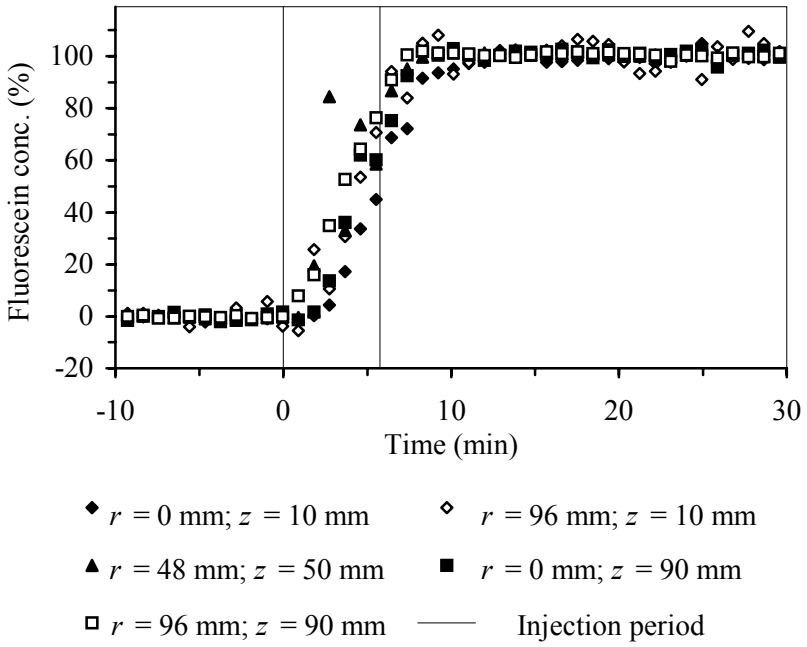

Fig. 6. Fluorescein concentrations at five different locations within the chamber water relative to the maximum values that have been reached after 60 min. The positions of the fiber tips are given relative to the center of the bottom (r = 0 mm, z = 0 mm). The vertical lines mark the period of time where the fluorescein injection took place.

DBL properties. The fitted exponential equations proved to be good approximations of the measured sulfate concentration time series ($r^2 > 0.97$ in all cases). The corresponding DBL thicknesses (average ± s.d.) were 211 ± 4 and 617 ± 24 µm at the advective and non-advective stirrer setting, respectively. From these DBL thicknesses the shear velocity u_* (cm s^{-1}) was calculated according to the empirical relationship of Tengberg et al. (2004), that was determined from alabaster dissolution rates and skin friction measurements in stirred chambers: $z = 76.18\ u_*^{-0.933}$. This resulted in average shear velocities of 0.34 and 0.11 cm s^{-1}, respectively, at the advective and non-advective stirrer setting.

Optode performance

Accuracy. Single oxygen measurements as calculated from individual phase angle readings deviated considerably from the true oxygen concentration in the aerated bottle. Average absolute deviations (± s.d.) of 100 successive oxygen measurements of all six

sensors were 0.9 % ± 0.1 % air saturation or 2.7 ± 0.3 µmol L^{-1} with maximum deviations of 2.8 ± 0.3 % air saturation. However, calculating moving averages at growing averaging periods revealed that an averaging period of n = 12.2 ± 2.1 was sufficient to reduce the maximum deviation of all sensors below 1 % air saturation. For the least precise sensor an averaging period of n = 14 was required.

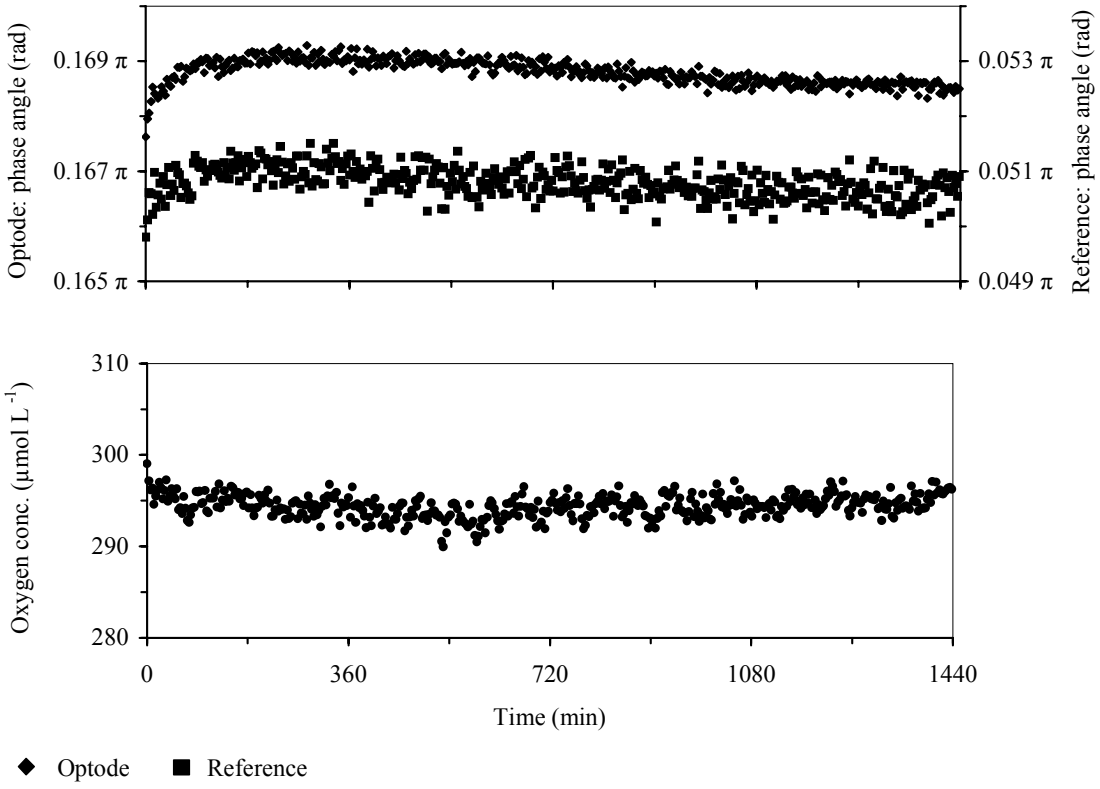

Fig. 7. Upper graph: 24 h time series of luminescence lifetimes as recorded at 100 % oxygen saturation (diamonds) and the internal reference (squares). Each data point represents the average value of 15 readings. Lower graph: apparent oxygen concentrations as calculated from reference-corrected phase angles of the same sensor.

Drift. A 24 h time series of the phase angles of one of the sensors and the internal reference is given in fig. 7 (upper graph). A substantial initial increase later gives way to a slow linear decrease. Subtracting the phase angle of the reference from that of the sensor reduces the drift substantially. The lower graph in fig. 7 shows the remaining drift of the same sensor converted to oxygen concentrations. In the 'warm-up' period a slight phase angle increase of the sensor resulted in an apparent oxygen decrease while

the opposite was true later on. Generally, highest drift rates occurred during warm up but varied considerably between the six sensors (average (± s.d.) 0.025 ± 0.316 µmol L^{-1} h^{-1}) with a maximum rate of -1.4 µmol L^{-1} h^{-1} for the least stable sensor. Later on, the rates were both linear and consistent between sensors with an average of 0.21 ± 0.07 µmol L^{-1} h^{-1} during the last four hours.

Discussion

In order to minimize alteration of the physical and biogeochemical sediment properties and to get reliable flux estimates it is generally preferable measurements in situ. This is particularly important when dealing with sandy sediments where the permeability results in a close coupling between bottom water hydrodynamics and sediment biogeochemistry. Waves and currents result in pressure gradients and pore-water advection which in turn determine biogeochemical conditions within the sediment, e.g., solute distributions, redox potential, and oxygenation (Ziebis et al. 1996; Huettel et al. 1998; Precht et al. 2004). When sandy sediments are removed from the natural environment, advective solute transport ceases. As biogeochemical reactions continue, conditions within the sediment start to change. Lohse et al. (1996) found that an enhanced oxygenation of the upper sediment layer of freshly retrieved sand cores which they attributed to advection vanished completely within one hour. In addition, the sampling of undisturbed sandy sediment cores is particularly difficult, as the sediment stratification is easily disturbed and pore-water tends to drain due to the low cohesion of coarse grained sediments (Marinelli et al. 1998). In situ incubations avoid these difficulties and minimize the delay between enclosure and incubation.

Construction, deployment, and hydraulic properties of the chamber system SANDY

Although in situ deployments of autonomous benthic chambers are today performed almost routinely down to abyssal depths (Tengberg et al. 1995) a system that suited the specific requirements of deployments on sands in shallow high energy environments was still missing. Video observations during test deployments of hand held chambers at current velocities of up to 50 cm s^{-1} revealed that the sediment surface was eroded if the chamber approached the sediment too slowly. In addition, the surrounding sediment was washed away within tens of minutes after the chamber entered the sediment. Apart from these difficulties, most of the existing benthic chambers, being mainly designed for soft and muddy sediments, are probably unable to penetrate hard, consolidated sands to an adequate depth.

The specific construction of the SANDY chamber solves these problems and permits chamber studies on sands even under harsh hydrodynamic conditions. The initial height

of the chamber above the sediment prevents an impact by the shock wave while the system is deployed at the seafloor. The lid and the surrounding collar prevent an acceleration of the water flow beneath the chamber and, thus, erosion of the sediment surface. The fast penetration of the sediment without displacement of the water above the sediment keeps the sediment surface in place, and the slightly eccentric movement of the chamber facilitates deep intrusion of the sediment at minimum disturbance. In combination with the protection of the adjacent sediment surface by the collar, the deep intrusion counteracts washout during the incubation. Attached to a rigid frame, the SANDY system is a robust instrument that can be deployed from any research vessel and works entirely autonomous.

Once the sediment is enclosed, the stirrer induced hydraulic properties within the chamber water replace the former natural conditions. Knowledge of the chamber characteristics is crucial in order to relate the obtained solute fluxes to the prevailing pressure gradients. The general shape of the pressure gradient corresponded to gradients of similar chambers (Glud et al. 1996; Huettel and Rusch 2000). Despite the fact that a concentrical pressure distribution has no genuine natural equivalent, both the pressure gradient and pore-water flow field within cylindrical chambers show strong similarities to conditions along topographical features that are exposed to bottom water flow (Huettel and Rusch 2000). Topography-induced pore-water flow fields are characterized by comparatively narrow areas of funneled pore-water release near the top of the roughness elements that are flanked both up- and downstream by larger regions of bottom water intrusion (Huettel and Gust 1992a). This is also the case in circular chambers where water enters the sediment in the large outer region of the chamber from where it follows the pressure gradient along curved paths towards the small central outflow area (Huettel and Gust 1992b; Huettel and Rusch 2000).

Pressure differences as measured at different stirring rates, confirmed that the SANDY chamber may be used to mimic natural advection phenomena of various intensities. Applying the empirical relationships between the overall pressure difference, the rotational speed of the stirrer disc and its distance to the sediment it is possible to predict the pressure distribution at any setting. However, the pressure gradients that were measured along the plastic chamber bottom represent maximum values as they would develop along the surface of impermeable sediments. If the permeability is high

enough to allow for advection the ensuing pore-water flow tends to relieve the pressure gradient. As the pore-water flow velocity increases with sediment permeability (Darcy 1856) the same is true with respect to the extent of pressure relief. Transferred to pore-water exchange in chamber incubations on various sands it is evident that exchange rates at the same stirrer settings cannot be expected to scale linearly with sediment permeability. This agrees to results obtained by Glud et al. (1996) who incubated sediments in similar chambers and reported a logarithmic relationship between pore-water exchange and permeabilities. Natural pressure gradients (e.g., along a ripple of a certain height exposed to flow of a certain velocity) are likewise affected by the actual permeability. Incubations at similar stirrer settings on sediments of different permeabilities thus mimic the effect of specific natural conditions rather than that of a specific pressure gradient.

The advective and non-advective stirring modes were investigated in more detail. The pressure gradient at the advective setting represents moderate conditions of pore-water exchange. The corresponding overall pressure difference (2.9 Pa at d = 100 mm) is equal to that which has been measured at 10 mm high mounds that were exposed to unidirectional bottom flow at velocities of approximately 20 cm s^{-1} (Huettel et al. 1996). Investigations of the non-advective stirring mode focused on whether benthic fluxes due to diffusion and bioirrigation may be quantified at this setting. A comparison of these "background fluxes" to fluxes obtained at the advective setting allows one to evaluate the significance of advective transport as compared to diffusion and bioirrigation. The absence of any significant radial pressure gradient at the non-advective setting confirmed that advection would be virtually absent at this stirrer setting. The fast dye cloud dispersal, on the other hand, confirmed that this stirring mode was still sufficient to keep the overlying water homogeneously mixed. This ensures that changes in solute concentration above the sediment surface as they result from interfacial fluxes are passed on to the sampling ports and sensors.

Changing the stirrer settings affects not only the pressure gradient but also the flow and turbulence properties above the sediment surface. If differences in flow and turbulence properties would change interfacial fluxes between stirrer settings, these changes could be misinterpreted as effects of advection. An effect that could strongly bias fluxes would be sediment resuspension at the advective stirring mode.

Resuspension results in pore-water discharge from the eroded sediment layer and exposure of formerly covered, deeper sediment layers to the overlying water. Oxygen uptake rates in laboratory chambers were found to increase severalfold once the upper sediment layer became resuspended (Glud et al. 1995; Sloth et al. 1996). A significant resuspension-effect was also described with respect to fluxes of carbon dioxide, nutrients, DOC, and heavy metals both due to pore-water release and adsorption / desorption processes (see Tengberg et al. (2003), and references therein). No resuspension, however, was observed in test runs of the acrylic chambers at 40 rpm, demonstrating that shear velocity was still subcritical for the sediment used (washed and sieved well sorted fine silicate sand, 220 µm median grain size). As Sands of this grain size are particularly sensitive to erosion (Hjulström's curve in Sundborg 1956) suspension is not expected to occur at the advective stirring mode at sands of any grain size. This is in agreement with the average shear velocity as calculated from the alabaster dissolution experiments (0.34 cm s^{-1}). According to the "Inman curve" (Miller et al. 1977) and the "threshold conditions for granular material" (Julien 1995) 2-3 times higher shear velocities are needed to erode fine Sand particles.

Several authors stressed that chamber-derived diffusive fluxes may be affected by the thickness of the DBL that develops at the enclosed sediment surface (e.g., Santschi et al. 1983; Hall et al. 1989; Broström and Nilsson 1999). A thicker DBL at the non-advective setting could result in a reduced diffusive solute transport that would erroneously be attributed to the absence of advection. Average DBL thicknesses differed almost by a factor of 3 between the respective stirring modes. The alabaster layer, however, was impermeable and prevented any advective transport. If the chambers were deployed on permeable sands (i.e., the sediments the system was meant for) a DBL would most likely be absent. Oxygen profiling in permeable sands that were exposed to unidirectional flow failed to resolve any DBL above the sediment surface even in the absence of surface topography (Forster et al. 1996; Ziebis et al. 1996; Guess 1998). This was attributed to flow across the interface due to advection along minute roughness elements and bottom shear-induced dispersion within the uppermost sediment layer. Exchange across the sediment surface at the advective stirrer setting thus probably faces no DBL which is a natural characteristic of advection controlled environments rather than an artifact. At the non-advective setting, on the other hand, a

DBL is likely to develop as advection is missing and dispersion is limited at reduced flow and turbulence conditions. DBL thicknesses as determined at the respective stirrer settings are both within the range of values that have been reported from shallow water environments (Glud et al. 1996; Jørgensen 2001). At the non-advective setting interfacial solute fluxes thus probably take place via diffusion across a DBL of common thickness which corresponds to conditions in diffusion dominated environments. Bioirrigative solute transport would add to the respective exchange rates at both stirrer settings.

A DBL artifact, however, might be expected if investigations of advection-related fluxes are extended towards fine and very fine sands of low permeability. While the resistance of the DBL applies to any solute (Santschi et al. 1991) further discussion will focus on oxygen fluxes as an important parameter of benthic activity that is particularly well-studied (e.g., Jørgensen and Revsbech 1985; Jørgensen and Des Marais 1990; Glud et al. 1994). The expected difference in diffusive oxygen uptake at both stirrer settings was quantified based on the equations provided by Rasmussen and Jørgensen (1992) assuming steady state conditions and constant rates of oxygen removal throughout the sediment depth as long as any oxygen is present (T = 15°C, S = 35, $[O_2]_{\text{bottom water}}$ = 100 % air saturation). For diffusive oxygen fluxes of 10, 20, and 30 mmol m^{-2} d^{-1} at 40 rpm (average DBL 211 µm) the predicted reduction at 20 rpm (average DBL 617 µm) is 0.54, 2.1 and 4.8 mmol m^{-2} d^{-1} or 5.4, 10.7, and 16.0 %. Natural oxygen fluxes are expected to be mostly in the lower proportion of this range. Based on a compilation of reported carbon oxidation rates in shelf sediments Canfield and Teske (1996) give a median oxygen flux of 13.7 mmol m^{-2} d^{-1}. The diffusive oxygen uptake rate can be expected to be only a fraction of this oxygen demand. Hence, even in incubations on impermeable sands it is unlikely that a DBL-effect on the diffusive solute fluxes introduces a significant artifact at least with respect to oxygen.

Another aspect to consider is the effect that natural topographical features at the surface of the enclosed sediment (e.g., ripples or mounds) will have on the exchange rates. Interactions of the rotational flow with roughness elements could induce localized pressure fields leading to advection that could possibly add to pore-water exchange along the radial pressure gradient. An investigation of exchange across sculptured sediment surfaces (sloping surface, simple trough and crest with a triangular cross-

section) indicated an opposite effect. Observation of dye concentrations in the chamber water as a tracer of pore-water exchange revealed that the sculptured surfaces generally reduced the rates by 10 to 30 % as compared to a smooth and horizontal surface (data not shown). As the radial pressure gradient results from the centrifugal force of the rotating water column (Greenspan 1969), it is likely that the roughness elements disturb the regular flow pattern, which in turn reduces the resulting pressure difference.

In conclusion, the characterization of the hydraulic properties of the chamber confirmed that differences in solute fluxes between both stirrer settings can be attributed to advection. The potential of the chamber to study the impact of advection on solute fluxes of natural sandy sediments is confirmed by rates of pore-water exchange as they have been measured at the respective stirrer settings in situ (fig. 8).

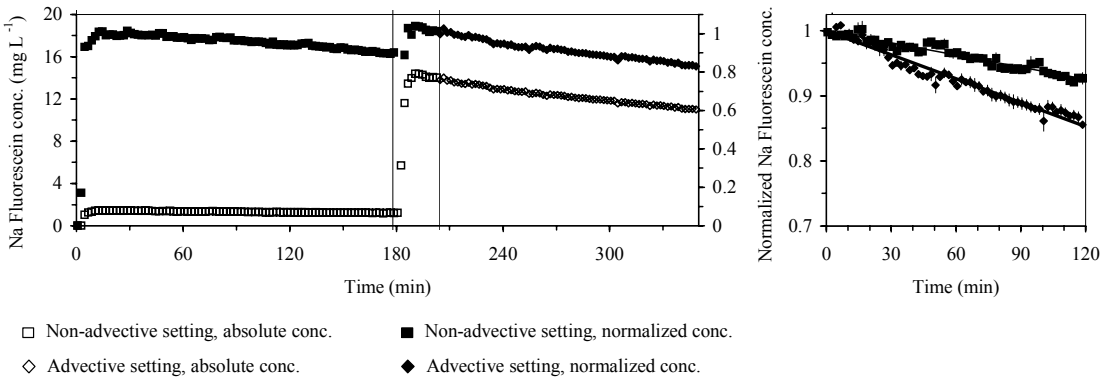

Fig. 8. Left graph: in situ time series of fluorescein concentrations in the chamber water. The vertical lines mark the respective tracer injections (42 ml of 100 and 1000 mg L^{-1} sodium fluorescein solution, respectively) and the stirrer mode change (at 204 min). Concentrations are expressed as absolute values (open symbols) and normalized to the maximum concentration at the beginning of the respective parts (filled symbols). The data represent averages of two fluorometer channels. Right graph: Direct comparison of the normalized fluorescein concentrations during the first 120 min of the same incubation at the advective- (diamonds) and the non-advective stirring mode (squares). The error bars represent the range of the concentrations as measured by the two channels.

Deployments took place on a coarse sand station off the Island of Spiekeroog (German Bight, North Sea; 16 m water depth, permeability 7.46 x 10^{-11} m^2; for details

on the station see Janssen et al. (2005). The same fluorometer that was employed in the dye cloud dispersion experiment was used to monitor the decrease of tracer dye (i.e., sodium fluorescein concentration) as a measure of interfacial solute transport. From the respective slopes it is obvious that rates of decrease were smaller at the non-advective setting than those at the advective mode where an additional loss took place by advection. The net rates of advective transport as calculated from the difference between the respective slopes amounted to 91.4 ± 11.5 L m^{-2} d^{-1} (average of the three incubations ± s.d.). This agrees with pore-water exchange rates measured with similar chambers in laboratory incubations (fig. 5 in Glud et al. 1996). Exposing macrofauna-free sand of a similar permeability to a fivefold lower overall pressure difference (0.52 Pa) than that of the advective stirring mode resulted in a six times lower advective pore-water exchange (approximately 15 L m^{-2} d^{-1}, calculated from diffusion-corrected tracer loss; R. Glud, personal communication).

Among the solute fluxes that have been investigated with benthic chambers, the flux of oxygen has received special attention (e.g., Jahnke 1996; Smith et al. 1997; Witte and Pfannkuche 2000). Oxygen uptake represents aerobic organic matter degradation as well as anaerobic decay (indirectly as oxygen demand for the re-oxidation of reduced electron acceptors; Canfield et al. 1993; Thamdrup et al. 1994) and is a commonly used measure of the benthic activity and total organic matter mineralization (Viollier et al. 2003). Concentrations of oxygen in the chamber water may be recorded continuously by means of electrochemical or fiberoptical sensors (Revsbech 1989; Klimant et al. 1995). A comparison of a Clark type electrode and an intensity-based optode revealed that optodes are superior with respect to long term stability but have a higher noise level than electrodes (Glud et al. 1999). The authors anticipated that an introduction of lifetime-based optodes will further enhance the quality of measurements. The lifetime based optode device that is part of the SANDY system was successfully employed during two deep-sea campaigns (Witte et al. 2003a; Witte et al. 2003b). A thorough testing of the system under controlled laboratory conditions was performed as part of this study, as both measurement accuracy and stability are crucial for SANDY deployments in order to resolve any advection-induced changes of sediment oxygen uptake.

Averaging 14 replicate phase angle readings proved to be sufficient to reduce the maximum variation below 1 % oxygen saturation. A complete cycle of 14 readings of all seven channels (6 optodes plus reference) plus the time needed for switching takes about 2.5 min. This in an adequate temporal resolution as the oxygen depletion within the chamber water takes place slowly and steadily and chamber deployments usually last for several hours. The introduction of an optical switch improves reliability as it allows replicate measurements within the chambers without any noticeable reduction in accuracy. Although repositioning of the fiberoptic switch resulted in up to a few percent variation of luminescence intensity, phase angles and thus oxygen determinations were unaffected (data not shown). This emphasizes the robustness of phase angle-based optode measurements. It can be expected, that the system has a greater tolerance than intensity based systems also with respect to other sources of signal intensity changes (e.g., fiber bending, photobleaching of the luminophore or drift of excitation light intensity).

The phase angle drift was small and, after an initial warm-up period both linear and similar for all sensors. A linear drift introduces a bias to absolute fluxes while it leaves relative changes unaffected. As the main focus of SANDY deployments lies on the changes of fluxes in response to the advection intensity, switching on the electronics some hours prior to the deployment solves the drift problem. The bias that is introduced to absolute fluxes proved to be relatively low. Assuming an overlying water height of 120 mm (i.e., 100 mm stirrer to bottom distance) the persisting drift after the initial warm-up would have led to an oxygen uptake underestimate of 0.61 mmol m^{-2} d^{-1} ± 0.20 mmol m^{-2} d^{-1} (20-24 h, average of all sensors ± s.d.). This is below 5 % of the typical oxygen demand of 13.7 mmol m^{-2} d^{-1} of coastal sediments (Canfield and Teske 1996).

An important issue with respect to field work is that the sensor calibration is readily performed. The easiest way is a simultaneous calibration based solely on oxygen concentrations of the samples withdrawn during deployments and the optode measurements at the time of sampling. This avoids any shipboard calibration effort and excludes problems related to temperature differences between calibration and measurement that would result in erroneous oxygen determinations (Holst et al. 1997). Fig. 9 shows a calibration based on data from five consecutive chamber deployments

that took place within a period of 4.5 days in the southeastern North Sea (June 2001, water temperature 13° C). The calibration curve is in good agreement with the data set (r^2 = 0.97) confirming the suitability of this approach and the excellent long term stability of the optodes.

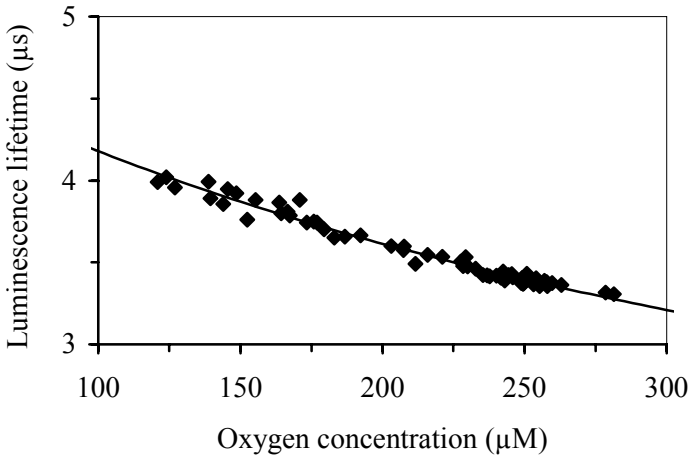

Fig. 9. An example of a simultaneous calibration based on oxygen concentrations of the syringe samples and lifetimes that were measured at the time of sampling.

Conclusion and outlook

The SANDY system proved to be suited to study of the effects of pore-water advection on solute fluxes in permeable sediments in situ. A specially designed chamber drive minimizes sediment disturbance which facilitates the incubation of sediments in their natural state. The characterization of the hydraulic properties of the chamber and in situ measurements of pore-water exchange rates confirmed that sequential incubations at contrasting stirrer settings allow the quantification of advection-related solute fluxes. Phase angle-based optode measurements provide stable and accurate recordings of chamber water oxygen concentration. This facilitates detailed studies of oxygen uptake as a measure of organic matter mineralization.

Many scientific issues related to transport and reactions in permeable sediments can be addressed with the SANDY system. An example is the application of a sequence of different stirrer settings to investigate the effect of permanently changing pressure gradients as they are encountered when tidal currents interact with a given sediment

topography. Increasing the stirrer speed until the flow becomes supercritical allows studies on sand resuspension events as they are frequently encountered in sandy environments. The addition of dissolved or particulate organic substrates to the chamber water establishes a variety of further topics with regard to the reaction of sands to organic matter pulses. Adding contaminants would help to assess the importance of sands as biofilters and their sensitivity to anthropogenic impacts.

Part two of this publication focuses on the potential of advection to stimulate sediment oxygen uptake. Results from a fine- medium- and coarse grained sandy site are compared in order to assess the role of advection in sediments of different permeability (Janssen et al. 2005).

References

Booij, K., W. Helder, and B. Sundby. 1991. Rapid redistribution of oxygen in a sandy sediment induced by changes in the flow velocity of the overlying water. Neth. J. Sea Res. **28**: 149-165.

Boudreau, B.P., M. Huettel, S. Forster, R.A. Jahnke, A. McLachlan, J.J. Middelburg, P. Nielsen, F. Sansone, G. Taghon, W.R. Van Raaphorst, I. Webster, J.M. Weslawski, P. Wiberg, and B. Sundby. 2001. Permeable marine sediments: overturning an old paradigm. EOS Trans. Am. Geophys. Union **82**: 133-136.

Broström, G., and J. Nilsson. 1999. A theoretical investigation of the diffusive boundary layer in benthic flux chamber experiments. J. Sea Res. **42**: 179-189.

Buchholtz-Ten Brink, M.R., G. Gust, and D. Chavis. 1989. Calibration and performance of a stirred benthic chamber. Deep-Sea Res. Part I **36**: 1083-1101.

Canfield, D.E., B.B. Jørgensen, H. Fossing, R.N. Glud, J. Gundersen, N.B. Ramsing, B. Thamdrup, J.W. Hansen, L.P. Nielsen, and P.O.J. Hall. 1993. Pathways of organic carbon oxidation in three continental margin sediments. Mar. Geol. **113**: 27-40.

Canfield, D.E., and A. Teske. 1996. Late Proterozoic rise in atmospheric oxygen concentration inferred from phylogenetic and sulphur-isotope studies. Nature **382**: 127-132.

Darcy, H. 1856. Les fontaines publiques de la ville de Dijon. Victor Dalmont.

Emery, K.O. 1968. Relict sediments on continental shelves of the world. Am. Assoc. Pet. Geol. Bull. **52**: 445-464.

Emery, K.O., and E. Uchupi. 1972. Western North Atlantic Ocean: topography, rocks, structures, water, life, and sediments. Vol. 17, *Am. Assoc. Pet. Geol. Mem.* The American Association of Petroleum Geologists.

Forster, S., M. Huettel, and W. Ziebis. 1996. Impact of boundary layer flow velocity on oxygen utilization in coastal sediments. Mar. Ecol. Prog. Ser. **143**: 173-185.

Glud, R.N., S. Forster, and M. Huettel. 1996. Influence of radial pressure gradients on solute exchange in stirred benthic chambers. Mar. Ecol. Prog. Ser. **141**: 303-311.

Glud, R.N., J.K. Gundersen, N.P. Revsbech, and B.B. Jørgensen. 1994. Effects on the Benthic Diffusive Boundary-Layer Imposed by Microelectrodes. Limnol. Oceanogr. **39**: 462-467.

Glud, R.N., J.K. Gundersen, N.P. Revsbech, B.B. Jørgensen, and M. Huttel. 1995. Calibration and performance of the stirred flux chamber from the benthic lander Elinor. Deep-Sea Res. Part I **42**: 1029-1042.

Glud, R.N., I. Klimant, G. Holst, O. Kohls, V. Meyer, M. Kuhl, and J.K. Gundersen. 1999. Adaptation, test and in situ measurements with O_2 microopt(r)odes on benthic landers. Deep-Sea Res. Part I **46**: 171-183.

Grant, J. 1983. The relative magnitude of biological and physical sediment reworking in an intertidal community. J. Mar. Res. **41**: 673-689.

Greenspan, H.P. 1969. The theory of rotating fluids, *Cambridge monographs on mechanics and applied mathematics*. Cambridge Univ. Press.

Gruber, W.R., P. O'Leary, and O.S. Wolfbeis. 1995. Detection of fluorescence lifetime based on solid-state technology, and its application to optical sensing, p. 148-158. *In* J. R. Lakowicz, [eds.]. Advances in Fluorescence Sensing Technology II. SPIE-The International Society for Optical Engineering.

Guess, S. 1998. Oxygen uptake at the sediment-water interface simultaneously measured using a flux chamber method and microelectrodes: must a diffusive boundary layer exist? Est. Coast. Shelf Sci. **46**: 143-156.

Hall, P.O.J., L.G. Anderson, M.M.R. Vanderloeff, B. Sundby, and S.F.G. Westerlund. 1989. Oxygen-uptake kinetics in the benthic boundary layer. Limnol. Oceanogr. **34**: 734-746.

Heise, S., and G. Gust. 1999. Influence of the physiological status of bacteria on their transport into permeable sediments. Mar. Ecol. Prog. Ser. **190**: 141-153.

Holst, G., R.N. Glud, M. Kuhl, and I. Klimant. 1997. A microoptode array for fine-scale measurement of oxygen distribution. Sens. Actuat. B **38**: 122-129.

Huettel, M., and G. Gust. 1992a. Impact of bioroughness on interfacial solute exchange in permeable sediments. Mar. Ecol. Prog. Ser. **89**: 253-267.

Huettel, M., and G. Gust. 1992b. Solute release mechanisms from confined sediment cores in stirred benthic chambers and flume flows. Mar. Ecol. Prog. Ser. **82**: 187-197.

Huettel, M., H. Røy, E. Precht, and S. Ehrenhauss. 2003. Hydrodynamical impact on biogeochemical processes in aquatic sediments. Hydrobiologia **494**: 231-236.

Huettel, M., and A. Rusch. 2000. Transport and degradation of phytoplankton in permeable sediment. Limnol. Oceanogr. **45**: 534-549.

Huettel, M., and I.T. Webster. 2001. Porewater flow in permeable sediments, p. 144-179. *In* B. P. Boudreau and B. B. Jørgensen, [eds.]. The benthic boundary layer: transport processes and biogeochemistry. Oxford Univ. Press.

Huettel, M., W. Ziebis, and S. Forster. 1996. Flow-induced uptake of particulate matter in permeable sediments. Limnol. Oceanogr. **41**: 309-322.

Huettel, M., W. Ziebis, S. Forster, and G.W. Luther III. 1998. Advective transport affecting metal and nutrient distribution and interfacial fluxes in permeable sediments. Geochim. Cosmochim. Acta **62**: 613-631.

Jahnke, R.A. 1996. The global ocean flux of particulate organic carbon: Areal distribution and magnitude. Global Biogeochem. Cycles **10**: 71-88.

Jahnke, R.A., J.R. Nelson, R.L. Marinelli, and J.E. Eckman. 2000. Benthic flux of biogenic elements on the Southeastern US continental shelf: influence of pore water advective transport and benthic microalgae. Cont. Shelf Res. **20**: 109-127.

Janssen, F., M. Huettel, and U. Witte. 2005. Pore-water advection and solute fluxes in permeable marine sediments (II): Benthic respiration at three sandy sites with different permeabilities (German Bight, North Sea). Limnol. Oceanogr. **50**: 779-792.

Jørgensen, B.B. 2001. Life in the diffusive boundary layer, p. 144-179. *In* B. P. Boudreau and B. B. Jørgensen, [eds.]. The benthic boundary layer: transport processes and biogeochemistry. Oxford Univ. Press.

Jørgensen, B.B., and D.J. Des Marais. 1990. The Diffusive Boundary-Layer of Sediments - Oxygen Microgradients over a Microbial Mat. Limnol. Oceanogr. **35**: 1343-1355.

Jørgensen, B.B., and N.P. Revsbech. 1985. Diffusive boundary layers and the oxygen uptake of sediments and detritus. Limnol. Oceanogr. **30**: 111-122.

Julien, P.Y. 1995. Erosion and sedimentation. Cambridge Univ. Press.

Klimant, I., V. Meyer, and M. Kuhl. 1995. Fiberoptic oxygen microsensors, a new tool in aquatic biology. Limnol. Oceanogr. **40**: 1159-1165.

Li, Y.H., and S. Gregory. 1974. Diffusion of ions in sea-water and in deep-sea sediments. Geochim. Cosmochim. Acta **38**: 703-714.

Lohse, L., E.H.G. Epping, W. Helder, and W.R. Van Raaphorst. 1996. Oxygen pore water profiles in continental shelf sediments of the North Sea: Turbulent versus molecular diffusion. Mar. Ecol. Prog. Ser. **145**: 63-75.

Marinelli, R.L., R.A. Jahnke, D.B. Craven, J.R. Nelson, and J.E. Eckman. 1998. Sediment nutrient dynamics on the South Atlantic Bight continental shelf. Limnol. Oceanogr. **43**: 1305-1320.

Miller, M.C., I.N. McCave, and P.D. Komar. 1977. Threshold of sediment motion under unidirectional currents. Sedimentology **24**: 507-527.

Precht, E., and M. Huettel. 2003. Advective pore-water exchange driven by surface gravity waves and its ecological implications. Limnol. Oceanogr. **48**: 1674-1684.

Precht, E., U. Franke, L. Polerecky, and M. Huettel. 2004. Oxygen dynamics in permeable sediments with wave-driven pore water exchange. Limnol. Oceanogr. **49**: 693-705.

Rasheed, M., M.I. Badran, and M. Huettel. 2003. Influence of sediment permeability and mineral composition on organic matter degradation in three sediments from the Gulf of Aqaba, Red Sea. Est. Coast. Shelf Sci. **57**: 369-384.

Rasmussen, H., and B.B. Jørgensen. 1992. Microelectrode studies of seasonal oxygen-uptake in a coastal sediment - role of molecular diffusion. Mar. Ecol. Prog. Ser. **81**: 289-303.

Revsbech, N.P. 1989. An oxygen microsensor with a guard cathode. Limnol. Oceanogr. **34**: 474-478.

Santschi, P.H., R.F. Anderson, M.Q. Fleisher, and W. Bowles. 1991. Measurements of diffusive sublayer thicknesses in the ocean by alabaster dissolution, and their implications for the measurements of benthic fluxes. J. Geophys. Res. C **96**: 10641-10657.

Santschi, P.H., P. Bower, U.P. Nyffeler, A. Azevedo, and W.S. Broecker. 1983. Estimates of the resistance to chemical transport posed by the deep-sea boundary layer. Limnol. Oceanogr. **28**: 899-912.

Sloth, N.P., B. Riemann, L.P. Nielsen, and T.H. Blackburn. 1996. Resilience of pelagic and benthic microbial communities to sediment resuspension in a coastal ecosystem, Knebel Vig, Denmark. Est. Coast. Shelf Sci. **42**: 405-415.

Smith, K.L., R.C. Glatts, R.J. Baldwin, S.E. Beaulieu, A.H. Uhlman, R.C. Horn, and C.E. Reimers. 1997. An autonomous, bottom-transecting vehicle for making long time-series measurements of sediment community oxygen consumption to abyssal depths. Limnol. Oceanogr. **42**: 1601-1612.

Sundborg, A. 1956. The river Klaralven; a study of fluvial processes. Geografiska annaler **38**: 125-316.

Tengberg, A., E. Almroth, and P. Hall. 2003. Resuspension and its effects on organic carbon recycling and nutrient exchange in coastal sediments: in situ measurements using new experimental technology. J. Exp. Mar. Biol. Ecol. **285**: 119-142.

Tengberg, A., F. De Bovee, P. Hall, W. Berelson, D. Chadwick, G. Cicer, P. Crassous, A. Devol, S. Emerson, J. Gage, R.N. Glud, F. Graziottini, J. Gundersen, D. Hammond, W. Helder, K. Hinga, O. Holby, R. Jahnke, A. Khripounoff, S. Lieberman, V. Nuppenau, D. Smallman, B. Wehrli, and P. De Wilde. 1995. Benthic chamber and profiling landers in oceanography - a review of design, technical solutions and functioning. Prog. Oceanog. **35**: 253-294.

Tengberg, A., P.O.J. Hall, U. Andersson, B. Lindén, O. Styrenius, G. Boland, F. de Bovee, B. Carlsson, S. Ceradini, A. Devol, G. Duineveld, J.-U. Friemann, R.N. Glud, A. Khripounoff, J. Leather, P. Linke, L. Lund-Hansen, G. Rowe, P. Santschi, P. De Wilde, and U. Witte. 2005. Intercalibration of benthic flux chambers II. Hydrodynamic characterization and flux comparisons of 14 different designs. Mar. Chem. **94**: 147–173.

Tengberg, A., H. Stahl, G. Gust, V. Muller, U. Arning, H. Andersson, and P. O. J. Hall. 2004. Intercalibration of benthic flux chambers I. Accuracy of flux measurements and influence of chamber hydrodynamics. Prog. Oceanog. **60**: 1-28.

Thamdrup, B., H. Fossing, and B.B. Jørgensen. 1994. Manganese, iron, and sulfur cycling in a coastal marine sediment, Aarhus Bay, Denmark. Geochim. Cosmochim. Acta **58**: 5115-5129.

Thibodeaux, L.J., and J.D. Boyle. 1987. Bedform-generated convective transport in bottom sediment. Nature **325**: 341-343.

Viollier, E., C. Rabouille, S.E. Apitz, E. Breuer, G. Chaillou, K. Dedieu, Y. Furakawa, C. Grenz, P. Hall, F. Janssen, J.L. Morford, J.-C. Poggiale, S. Roberts, T. Shimmield, M. Taillefert, A. Tengberg, F. Wenzhöfer, and U. Witte. 2003. Benthic biogeochemistry: state of the art technologies and guidelines for the future of *in situ* survey. J. Exp. Mar. Biol. Ecol. **285-286**: 5-31.

Wheatcroft, R.A. 1994. Temporal variation in bed configuration and one-dimensional bottom roughness at the mid shelf STRESS site. Cont. Shelf Res. **14**: 1167-1190.

Wild, C., M. Rasheed, U. Werner, U. Franke, R. Johnstone, and M. Huettel. 2004. Degradation and mineralization of coral mucus in reef environments. Mar. Ecol. Prog. Ser. **267**: 159-171.

Witte, U., N. Aberle, M. Sand, and F. Wenzhöfer. 2003a. Rapid response of a deep-sea benthic community to POM enrichment: an *in situ* experimental study. Mar. Ecol. Prog. Ser. **251**: 27-36.

Witte, U., and O. Pfannkuche. 2000. High rates of benthic carbon remineralisation in the abyssal Arabian Sea. Deep-Sea Res. Part II **47**: 2785-2804.

Witte, U., F. Wenzhöfer, S. Sommer, A. Boetius, P. Heinz, N. Aberle, M. Sand, A. Cremer, W.-R. Abraham, B.B. Jørgensen, and O. Pfannkuche. 2003b. *In situ* experimental evidence of the fate of a phytodetritus pulse at the abyssal sea floor. Nature **424**: 763-766.

Ziebis, W., M. Huettel, and S. Forster. 1996. Impact of biogenic sediment topography on oxygen fluxes in permeable seabeds. Mar. Ecol. Prog. Ser. **140**: 227-237.

Porewater advection and solute fluxes in permeable marine sediments (II): Organic matter mineralization at three sandy sites with different permeabilities (German Bight, North Sea)

Felix Janssen [1], Paul Faerber [1], Markus Huettel [1,2], Volker Meyer [1] & Ursula Witte [1,3]

[1] Max Planck Institute for Marine Microbiology, Celsiusstrasse 1, D-28359 Bremen, Germany

[2] Present address: Florida State University, Department of Oceanography, 0517 OSB, West Call Street, Tallahassee, Florida 32306-4320, USA

[3] Present address: University of Aberdeen, Oceanlab, Newburgh, Aberdeen AB41 6AA, Scotland, UK

Acknowledgements

B. B. Jørgensen is acknowledged for the support of this work. We are indebted to the captains and crews of RV HEINCKE and UTHOERN for their great support during cruises. S. Bühring, S. Ehrenhauss, A. Kamp, M. Keller, H. Woyt, and A. M. Alraei are gratefully acknowledged for their help during cruise preparation as well as on board. Special thanks to the technicians whose skills and dedication made this work possible: V. Meyer, P. Färber, J. Langreder, G. Herz, A. Kutsche, O. Eckhoff, S. Meyer, and F. Nowottny. A. Cremer and O. Pfannkuche are thanked for providing various equipment as well as technical assistance. C. Wigand is thanked for manufacturing the oxygen optodes. We are further indebted to S. Menger and G. Schüssler for TOC and bromide measurements, and to C. Deutscher for grain size analysis. K. Motamedi from the Federal Maritime and Hydrographic Agency of Germany is gratefully acknowledged for making grain size data of the German Bight available. Funding of this study was provided by the Max Planck Society.

Abstract

This study reports in situ measurements of oxygen consumption in permeable sandy shelf sediments that were obtained under controlled conditions of advective pore-water exchange. The measurements were conducted with the novel autonomous benthic chamber system SANDY, which is able to establish defined radial pressure gradients in the chamber, leading to water circulation through the pore space of the enclosed permeable sediment. The oxygen flux measurements revealed that organically poor shelf sands can have oxygen consumption rates that are similar to those found in fine grained sediments with much higher organic contents. For the first time, it is demonstrated in situ that advection can substantially enhance oxygen consumption rates of highly permeable sandy sediments. This effect is attributed to an advective supply of oxygen to the sediment in addition to the transport by diffusion and bioirrigation. These findings provide evidence for the potential of advection to enhance mineralization rates and emphasize that advection has to be considered when assessing carbon cycling in shelf areas. On the other hand, advection had no significant impact on oxygen consumption in finer sediments that would still be classified as permeable sands. Extrapolated to the German Bight as a whole, considerable pore-water advection can be expected to occur in 60 % of the total area. The fraction of this area where advection is strong enough to significantly enhance organic matter mineralization is still largely unresolved and needs further investigation. In the remaining 40 % of the German Bight area, however, an effect of advection on oxygen uptake and mineralization can be largely excluded.

Introduction

Until the 1980ies the biogeochemistry of coastal sands has received little attention. Because organic matter content and bacterial numbers decrease with increasing grain size (Emery and Uchupi 1972; DeFlaun and Mayer 1983) it seemed that coarse grained sandy deposits lack both the substrates and the organisms to sustain significant biological activity. Sands were therefore considered to be biogeochemical deserts that did not significantly contribute to the cycling of organic matter (Boudreau et al. 2001).

A new perception of sandy sediments developed when systematic investigations increased the understanding of solute transport in these sediments (Savant et al. 1987; Thibodeaux and Boyle 1987; Huettel and Gust 1992a). Permeabilities in excess of 10^{-12} m^2, as common for sandy sediments, were found to allow for significant pore-water advection, i.e., flow of water through the sediment interstices. While transport in silty and muddy deposits is restricted to molecular diffusion, bioturbation, and bioirrigation, advective pore-water flow through sandy sediments creates an additional solute transport mechanism. The main driving forces of advection are pressure gradients along the sediment surface. These develop whenever unidirectional or oscillating bottom flows are deflected by topographical features of the sediment surface, e.g., ripple and mounds (Huettel and Gust 1992a; Huettel et al. 1996; Precht and Huettel 2003). Other factors that can lead to pore-water flow include undulating pressures at the seafloor due to the passage of surface gravity waves referred to as “wave pumping” (Riedl et al. 1972; Rutgers van der Loeff 1981; Shum and Sundby 1996), groundwater seepage and fluid venting (Dando et al. 2000; Burnett et al. 2001), gas bubble emergence (Dando et al. 1991), and temperature or salinity gradients (Webster et al. 1996; Rocha 2000).

Horizontal pressure differences induced locally by roughness elements at the seafloor are expected to be in the range of a few Pascal only (Thibodeaux and Boyle 1987; Huettel and Gust 1992a; Huettel et al. 1996). Nevertheless, they can lead to pore-water transport down to > 10 cm sediment depth and to solute exchange at rates exceeding those of molecular diffusion by up to 3 orders of magnitude (Huettel and Gust 1992a; Huettel et al. 1996). This enhances the supply with oxygen and other electron acceptors, which is considered to increase the mineralization activity of

sediment biota (Froelich et al. 1979; Jørgensen and Sorensen 1985; Enoksson and Samuelsson 1987). At the same time waste products such as reduced electron acceptors and remnants of organic matter mineralization (carbon dioxide and nutrients) are efficiently removed (McLachlan et al. 1985; Gehlen et al. 1995; Huettel et al. 1998; Rocha 1998). Furthermore, advection may contribute to the supply of fresh particulate organic matter to the sediment, even if the hydrodynamic forces prevent any gravitational settling of particles. Through advective pore-water flow, unicellular algae, bacteria, and organic detritus are carried down several centimeters into the sediment were they become trapped (Pilditch et al. 1998; Huettel and Rusch 2000; Fries and Trowbridge 2003).

The nonlocal advective transport of solutes and particles in combination with the biogeochemical reactions within the sediment result in a complex distribution of biologically relevant substances such as oxygen, nutrients, heavy metals and organic matter (Ziebis et al. 1996; Huettel et al. 1998; Precht et al. 2004). The resulting biogeochemical transition zones (e.g., the redox discontinuity layer) are larger than those of horizontally laminated beds and highly dynamic as they are coupled to current speed and direction, and to sediment surface topography, all of which continuously change on time scales from seconds to seasons (Ziebis et al. 1996; Huettel et al. 2003; Precht et al. 2004). These transition zones, particularly if oscillating, are considered to be sites of intense metabolic activity (Aller 1994; Aller and Aller 1998; Huettel et al. 1998). On account of these findings sands may be envisioned as biocatalytical filters with the ability to mineralize organic matter at high rates (Boudreau et al. 2001; Huettel and Webster 2001; Huettel et al. 2003).

Experimental evidence for an enhanced organic matter mineralization in the presence of advection was provided by Forster et al. (1996). In a flume study they found the total oxygen uptake (TOU) of a coarse sandy sediment with surface topography to increase with the flow velocity, i.e., with increasing rates of pore-water advection. The significance of this process for natural environments, however, is still unresolved because no instrument was available that could measure the effect of advection on oxygen uptake in situ. A better understanding is crucial because of the potential ecological relevance of sands. Sandy beds cover more than two thirds of the continental shelf seafloor (Emery 1968; Emery and Uchupi 1972). Hence, they represent the

dominant sediment type in a particularly productive part of the marine environment, where up to one third of the entire pelagic primary production is thought to take place (Walsh 1988; Jørgensen 1996) and additional organic matter is supplied through benthic primary production (Cahoon 1999; Nelson et al. 1999). Dating back to the early 1980ies there is an ongoing discussion about whether this production is mainly remineralized on the shelf or transported to deeper waters (Walsh et al. 1981; Malone et al. 1983; Rowe et al. 1986; Bacon et al. 1994). To gain further insight into the fate of organic matter on the shelf, and the role of sandy sediments for the carbon cycling in coastal areas in situ evidence of the significance of advection for organic matter mineralization is needed.

In order to conduct flux investigations in permeable sands in situ, the autonomous chamber system SANDY was developed (see part I of this publication; Janssen et al. 2005). These chambers allow the simulation of naturally occurring advective pore-water exchange, as pressure gradients within the chamber display strong similarities to those produced by flow-topography interactions. In the current study, sediment total oxygen uptake (TOU) in the presence and absence of advection is compared to evaluate the impact of advection on rates of organic matter mineralization. In order to assess the effect of permeability on oxygen and nutrient fluxes, the chambers were deployed on fine, medium, and coarse North Sea shelf sands located in close proximity to each other.

Material and methods

Study area

All investigations were carried out at three stations seawards of the barrier island of Spiekeroog in the southeastern North Sea. The distance between the northernmost and southernmost station was 2.8 km (fig. 1).

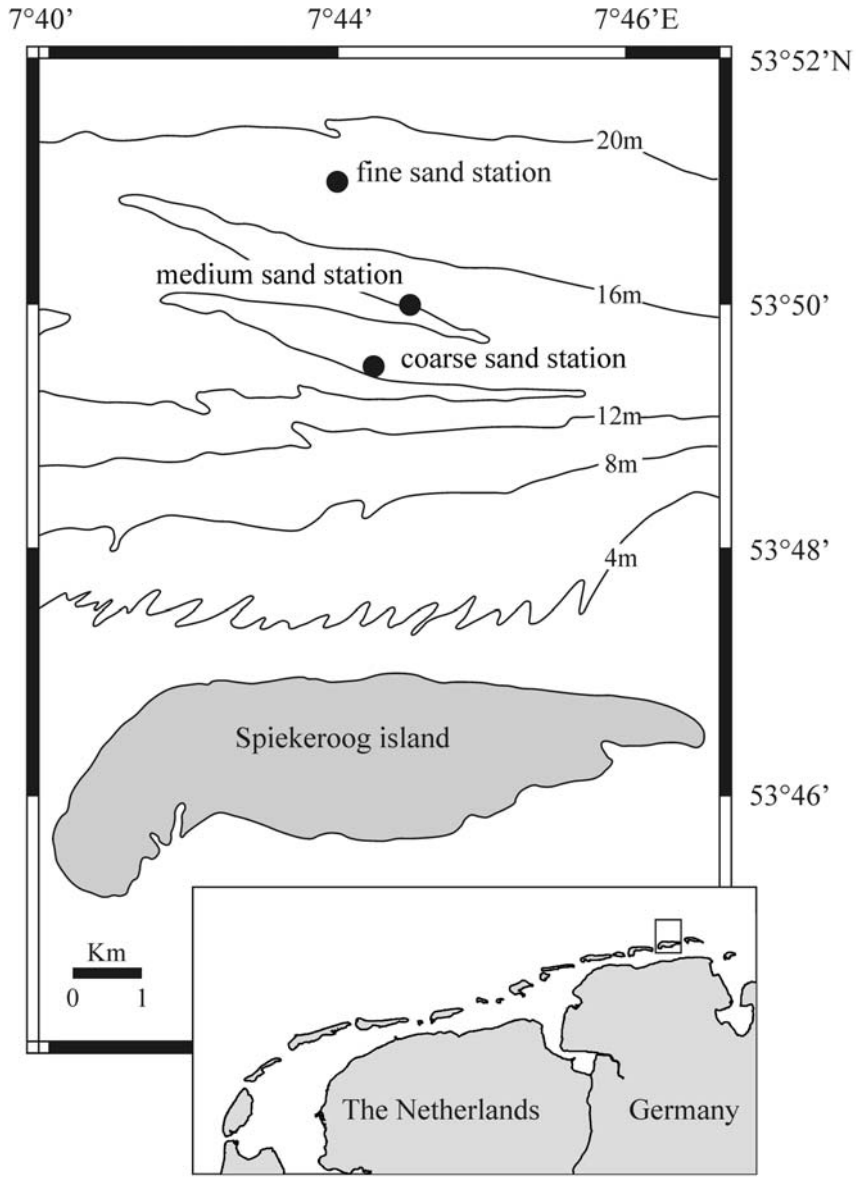

Fig. 1. Upper graph: location of the three stations and the bathymetry of the area (redrawn after Antia 1993). Lower graph: The chain of West and East Frisian Islands. The box marks the area around the Island of Spiekeroog.

The study area is located in a mesotidal high-energy environment with a mean tidal range of 2.5 m (Postma 1982). Tides result in average bottom water current velocities (measured 15 cm above the seafloor) of approximately 20 cm s^{-1} with peak flow velocities of up to 35 cm s^{-1} (Janssen et al. in prep.). Wave driven oscillatory currents add to the water motion above the bed. Significant wave heights of 1 - 2 m as they prevail under relatively calm conditions are expected to result in oscillatory current velocities of up to 56 ± 25 and 18 ± 12 cm s^{-1} at water depths of 10 and 20 m, respectively according to an evaluation of wave recordings of Dette (1977) and Niemeyer (1979) in Antia (1993).

Tab. 1. Station data and sediment characteristics. Sediment samples were taken in polycarbonate cores of 36 mm inner diameter by means of a miniaturized multiple corer. Sediments were fractionated by dry sieving after rinsing the sediment on a 63 µm mesh to remove silt and clay particles. Grain size parameters were determined graphically (Lindholm 1987). Total organic carbon (TOC) and total nitrogen (TN) were measured by automated combustion (Fisons Instruments NA 1500 elemental analyzer) in freeze dried and ground samples that were acidified within silver sample cups to remove carbonates.

				Bulk sediment characteristics [1)]		
Sediment type	Position	Water depth (m)	Permeability (10^{-11} m^2)	Median grain size (µm) / Sorting[2)]	Porosity / Solids density (g cm^{-3})	TOC (% DW) / TOC:TN[3)]
Fine	53°51.0'N 7°44.0'E	19	0.30 ± 0.17	163 ± 20 / 0.58 ± 0.03	0.37 ± 0.009 / 2.70 ± 0.02	0.122 ± 0.023 / 8.0 ± 2.6
Medium	53°50.0'N 7°45.0'E	16	2.63 ± 0.33	299 ± 8 / 0.46 ± 0.02	0.34 ± 0.006 / 2.68 ± 0.02	0.023 ± 0.002 / 7.4 ± 2.6
Coarse	53°49.5'N 7°44.5'E	16	7.46 ± 1.34	672 ± 78 / 0.80 ± 0.11	0.33 ± 0.006 / 2.71 ± 0.02	0.030 ± 0.006 / 8.8 ± 2.8

[1)] Averages ± SD of 3 (grain size parameters, physical properties) and 6 replicates (TOC & TN)
[2)] Sorting (i.e., the graphic SD) is given in phi units
[3)] Molar ratio

Most of the seafloor within the study area is covered with quarternary sandy deposits (Figge 1981). Hydrodynamic forces and animal activity lead to the formation of ripples and discrete topographical features like mounds or pits at the sediment surface. Average heights of roughness elements as detected in 0.5 m long sediment surface profiles that

were obtained at all three stations were typically in the range of 10 - 20 mm with maximum elevations of 30 - 35 mm (Janssen et al. in prep.).

The three stations were selected for their different sediment properties (tab. 1). Median grain sizes increased from the northern, past the central, to the southern station by more than a factor of four. According to Wentworth (1922), the sediments are classified as fine, medium, and coarse sand, and the respective stations are subsequently referred to as fine-, medium-, and coarse sand station. The permeabilities of the three stations reflect the differences in grain size (fig. 2).

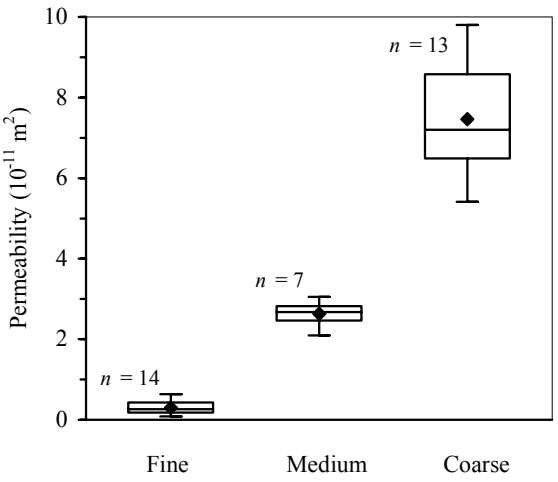

Fig. 2. Permeabilities of the surficial sediments at the three stations as determined on board using 80-190 mm long cores of 36 mm inner diameter. Measurements took place at in situ temperature with the constant head method (Klute and Dirksen 1986). The diamond represents the mean, the median is given by the horizontal line. The box marks the upper and lower quartile, the whiskers the total range of values.

Relative to the fine sand station, the resistance to water transport through the porespace was approximately 9 and 25 times less at the medium- and the coarse sand station, respectively. The total organic carbon (TOC) content (tab. 1) was generally low, but significantly higher at the fine sand station as compared to both other stations ($p = 0.005$; Wilcoxon two group test). Differences in TOC between the medium- and coarse sand stations were insignificant ($p = 0.066$). In contrast to the grain size median, which was almost constant within the upper sediment layer at all three stations, the TOC content tended to decrease with sediment depth (fig. 3).

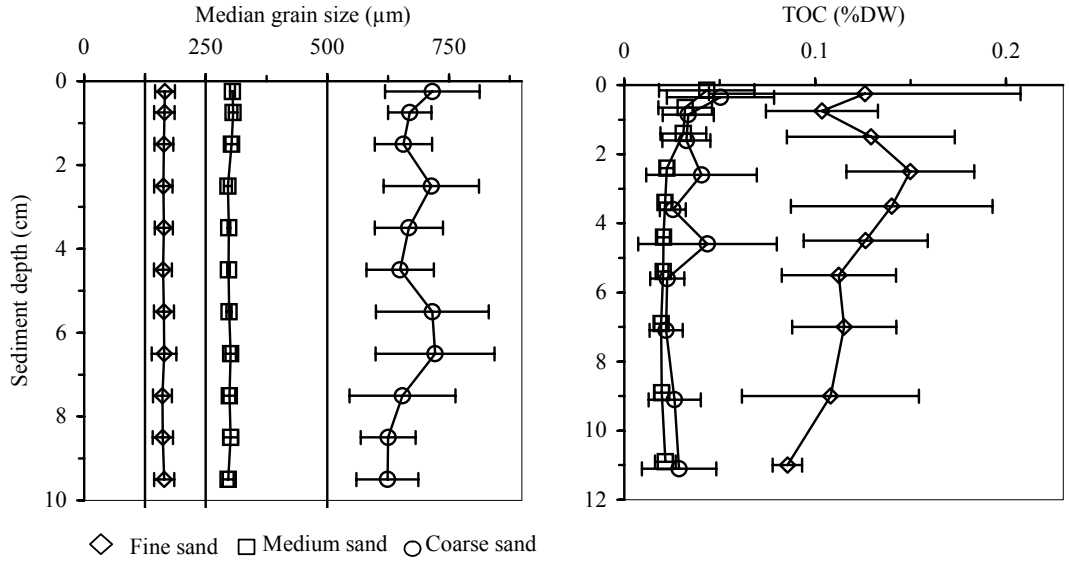

Fig. 3. Median grain sizes (left) and total organic carbon content, TOC (right) vs. sediment depth. Marks represent the average (whiskers: s.d.) of three (grain size) and six replicates (TOC), respectively. Points are positioned in the center of the respective sediment layer. Depth intervals: 0-1 cm in 0.5 cm steps, 1-10 cm in 1 cm steps (porosity and grain size); 0-1 cm in 0.5 cm steps, 1-6 cm in 1 cm steps, 6-12 cm in 2 cm steps (TOC). In the right graph points have been slightly shifted vertically to facilitate discrimination between neighboring data points. Vertical lines in the left graph represent the lower limits of the Udden-Wentworth size classes: fine, medium, and coarse sand (from left to right).

Chamber deployments

Oxygen and nutrient fluxes at the three stations were determined with the chamber system SANDY that has been designed specifically for in situ flux studies in sandy sediments. A detailed description of the system and a characterization of the hydraulic properties of the chamber can be found in Janssen et al. (2005). The SANDY system is based on a cylindrical chamber with a central stirrer disc similar to the chamber described by Huettel and Gust (1992b). Stirring results in a radial pressure gradient along the sediment surface that scales with the stirring rate (Glud et al. 1996). As the chamber isolates the sediment from all natural hydrodynamic forces, this permits to expose the enclosed sediment to defined pressure gradients. Given that the permeability is sufficiently high, the pressure gradient causes an advective circulation of chamber water through the sediment porespace along curved paths from the outer rim of the

chamber towards a central outflow area (Huettel and Rusch 2000). Further details of flow and pressure fields in cylindrical chambers can be found in Khalili et al. (1997) and Basu and Khalili (1999).

Deployments of the SANDY system took place during four cruises with the research vessels HEINCKE and UTHOERN (tab. 2).

Tab. 2. General cruise and deployment data. The right column specifies the origin of the flux measurements presented in this study.

Vessel (cruise ID)	Date	Water temp. (°C)	Stations of SANDY incubations and number of replicates presented in this study
HEINCKE (#148)	07 - 15 Jun. 2001	13	fine: TOU (n=5),NH_4^+(n=4),NO_3^-(n=5),PO_4^{3-}(n=5),SO_4^{4-}(n=4) coarse: TOU (n=3),NH_4^+(n=4),NO_3^-(n=3),PO_4^{3-}(n=4),SiO_4^{4-}(n=3)
HEINCKE (#154)	24 - 30 Sep. 2001	16	fine: NH_4^+(n=3),NO_3^-(n=2),PO_4^{3-}(n=3),SiO_4^{4-}(n=3) medium: TOU(n=2),NH_4^+(n=3),NO_3^-(n=3),PO_4^{3-}(n=3),SiO_4^{4-}(n=2) coarse: NH_4^+(n=3),NO_3^-(n=3),PO_4^{3-}(n=1),SiO_4^{4-}(n=3)
UTHOERN	22 - 27 Oct. 2001	14	fine: TOU(n=1),NH_4^+(n=2),NO_3^-(n=1),PO_4^{3-}(n=2),SiO_4^{4-}(n=2) medium: TOU(n=4),NH_4^+(n=5),NO_3^-(n=5),PO_4^{3-}(n=7),SiO_4^{4-}(n=7) coarse: TOU(n=1),NH_4^+(n=4),NO_3^-(n=4),PO_4^{3-}(n=4),SiO_4^{4-}(n=4)
UTHOERN	10 - 13 Nov. 2001	11	fine: NH_4^+(n=2),NO_3^-(n=2),PO_4^{3-}(n=2),SiO_4^{4-}(n=2) medium: TOU(n=2) coarse: TOU(n=1),NH_4^+(n=1),PO_4^{3-}(n=1),SiO_4^{4-}(n=1)

Two chambers, controlling electronics, battery, and ballast weights were mounted to a three-legged frame (Witte and Pfannkuche 2000) that was deployed and recovered by means of a rope with an attached surface marker buoy (Janssen et al. 2005). After the SANDY system was lowered to the seafloor, the stainless steel chambers (200 mm inner diameter) were driven into the sediment. Each chamber was equipped with one or two syringe water samplers with seven sampling and one injection syringe each (Witte and Pfannkuche 2000). The latter was used to add a neutrally buoyant sodium bromide solution to the chamber water (1.2 - 1.5 g NaBr per chamber at the beginning of the deployment). The bromide concentration of the first syringe sample permitted determination of the enclosed water volume (on average (± s.d.) 3.3 ± 0.6 L in all chamber incubations that were used to quantify TOU). The remaining syringe samples

were withdrawn at preset intervals over the time course of the deployment. Three fiberoptic oxygen sensors referred to as "optodes" (Klimant et al. 1995) continuously measured the oxygen concentration in the overlying water of each chamber. Optodes as well as water sampling ports were not placed directly in the chamber, but in a gastight water circuit that was permanently flushed with the overlying chamber water by means of a peristaltic pump.

In order to investigate the impact of advective pore-water exchange on TOU, two different stirrer settings were applied consecutively within each deployment. During the first half of the deployment (1.5 to 2.5 h) the stirrer was run at 40 rpm ("advective setting") to produce a pressure gradient and the associated advective pore-water flow. Given an average distance (± s.d.) of 85 ± 19 mm between the stirrer disc and the sediment surface in all deployments (as inferred from the average chamber water volume), the overall pressure difference between the outer rim and the center of the enclosed sediment was 2.9 ± 0.5 Pa with a maximum radial pressure gradient of 0.044 Pa mm^{-1} at r = 62 mm (see Janssen et al. 2005). At the beginning of the second half of the deployment the mode was changed to intermittent stirring at 20 rpm (15 s clockwise, 15 s pause, 15 s counterclockwise, 15 s pause etc.). Pore-water advection stopped at this "non-advective setting", which excluded the development of any significant pressure gradient (Janssen et al. 2005). The advective setting thus represented a scenario where advective pore-water exchange adds to the transport of oxygen and other solutes by diffusion and bioirrigation, while the non-advective setting allowed an assessment of oxygen fluxes in the absence of advection.

Sample analysis and data treatment.

Subsamples for oxygen, nutrients, and bromide were taken from the syringes immediately after retrieval of the SANDY system. Oxygen concentrations of the samples were determined on board via Winkler titration (Strickland and Parsons 1968). The optodes were calibrated by fitting a modified Stern-Volmer equation (Holst et al. 1997) to the oxygen concentrations of the samples vs. the luminescence lifetime readings of the optodes that were recorded at the time of sampling. Samples from several successive deployments were included in the calibrations in order to improve accuracy.

Bromide and nutrient samples were filtered (Minisart® 0.2 µm cellulose acetate syringe filters) and either frozen (bromide) or kept at 4° C (nutrients) after addition of mercury(I)chloride (110 ppm final concentration). Bromide was measured with an Ion Chromatograph (Sykam anion column LC A14 & UV detector S 3200). Nutrient concentrations (ammonium, nitrite, nitrate + nitrite, phosphate, and silicate) were determined with a continuous flow auto-analyzer (Skalar SanPlus) following the methods given by Clesceri et al. (1989).

TOU and nutrient fluxes were determined from linear regressions of concentrations of oxygen (averages of 2 - 3 optodes) and nutrients (syringe samples) vs. time. TOU in the presence and absence of advection was calculated separately using the oxygen decrease during the last 1 - 1.5 h of the advective setting and the first 1 - 1.5 h directly after switching to the non-advective setting. In the case of nutrient fluxes, all samples taken in the time course of the deployment were included in the regression as changes in the nutrient concentrations were relatively small and poorly resolved by the small number of samples. Therefore, nutrient fluxes do not differentiate between the respective stirrer settings but focus on general station characteristics. Flux determination was generally restricted to deployments where no evidence of chamber leakage was found in the bromide data. TOU was only determined in incubations where oxygen at both stirrer settings decreased linearly with time. Nutrient fluxes were only used if the syringe sample concentrations followed any recognizable trend (increase, decrease, or stagnancy). Statistical analyses were performed with the software JMP® 4.0.0 (SAS Institute Inc.). Simultaneous comparisons between all three stations were carried out with the Kruskal-Wallis test while the Wilcoxon two-group test was used for pairwise comparisons.

Results

TOU in the presence and absence of advection

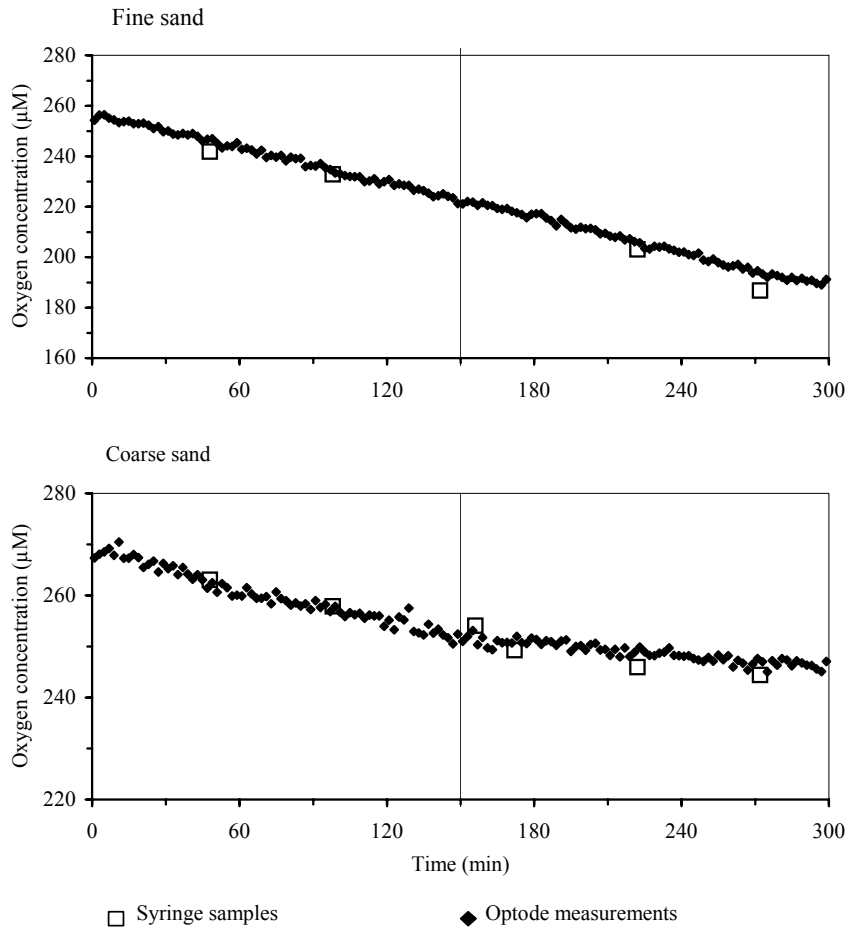

Fig. 4. Example of oxygen depletion with time at the fine (upper graph) and the coarse sand station (lower graph). The filled diamonds represent the optode measurements, the open squares give the oxygen concentrations of the syringe samples. Note the different scales of the y-axis.

Advective pore-water exchange increased TOU at the medium and coarse sand station, while no advective enhancement of TOU was detected at the less permeable fine sand station. Examples of chamber water oxygen concentration time series measured at the fine and coarse sand station are shown in fig. 4. At the fine sand station the change from the advective to the non-advective stirrer setting at t = 150 min did not affect the rate of oxygen decrease in the chamber water (fig. 4, upper graph). At the coarse sand station,

on the other hand, the rate decreased immediately after the change in stirring mode (fig. 4, lower graph).

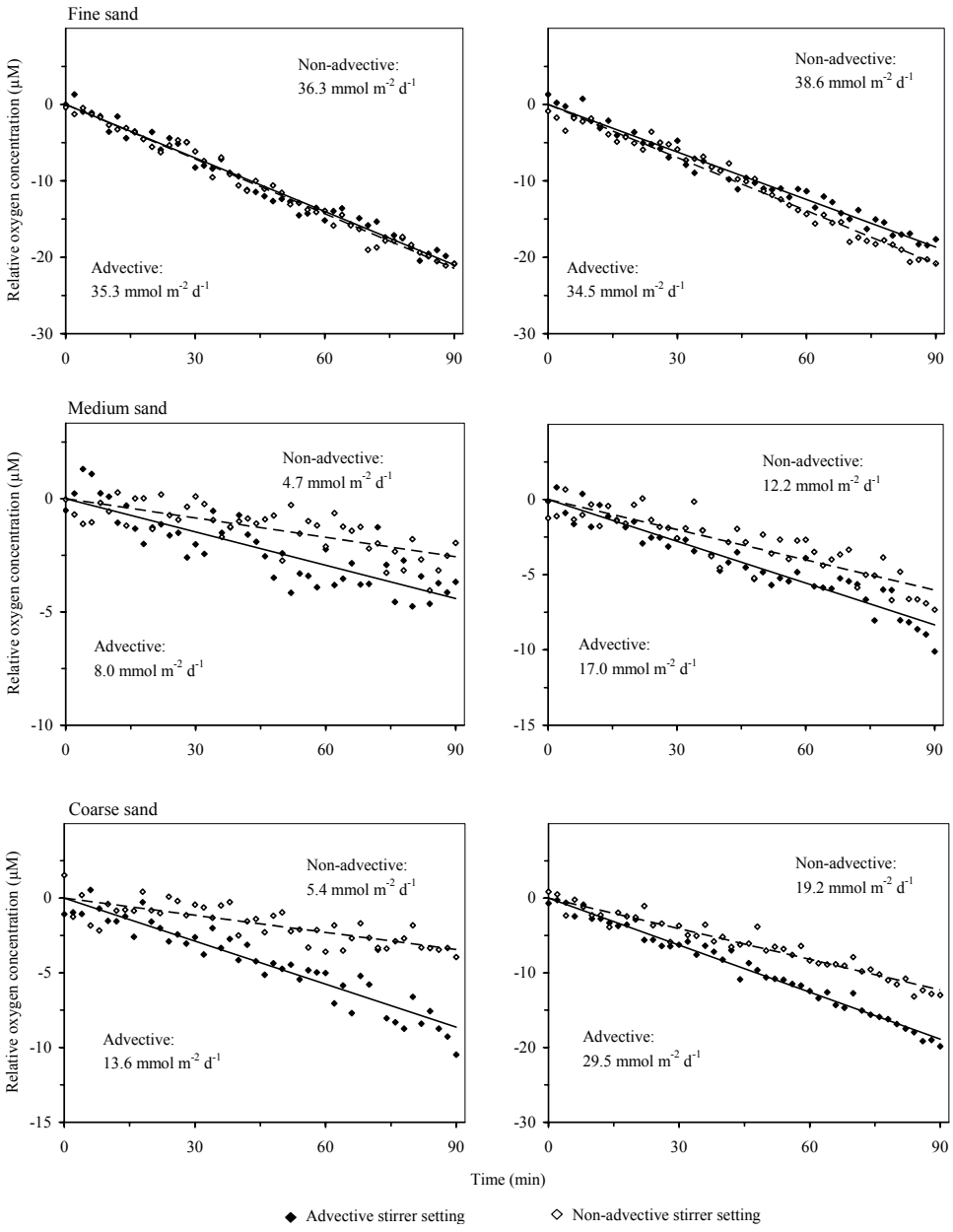

Fig. 5. Six examples of oxygen concentration time series (optode measurements) at the fine (upper two graphs), medium (central two graphs), and coarse sand station (lower two graphs). Oxygen concentrations are normalized to the same initial concentration and originate from the last 90 min of the advective (filled diamonds) and the first 90 min of the non-advective stirrer setting (open diamonds). The trendlines represent linear regressions to oxygen depletion during the advective (solid line) and non-advective stirrer setting (dashed line). The corresponding TOU values are indicated in the graphs.

A direct comparison of the respective slopes at all three stations shows that rates of TOU at the advective stirrer setting regularly exceeded those obtained in the absence of advection both at the medium and coarse sand station (central and lower panel of fig. 5). All in all, TOU at the fine, medium and coarse sand station was enhanced by a factor of 1.02, 1.38 and 1.91, respectively, at the advective as compared to the non-advective stirrer setting (geometric mean of factors calculated separately for each chamber incubation) (fig. 6).

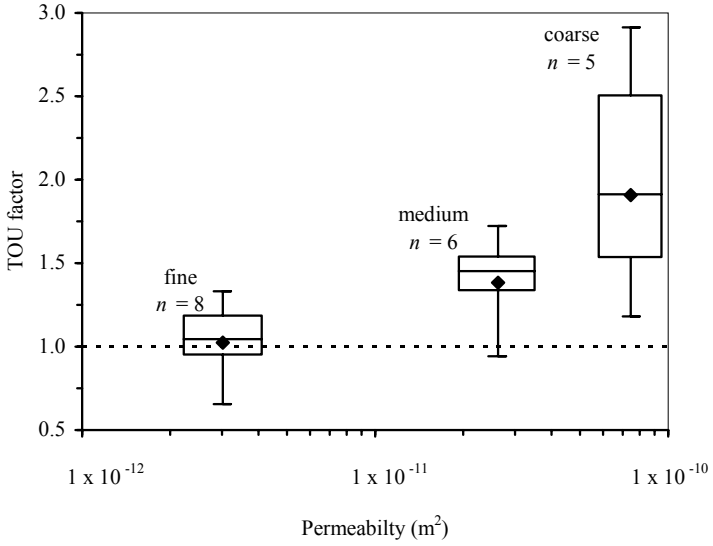

Fig. 6. Factor between total oxygen uptake rates (TOU) in the presence and absence of advection at the three stations (calculated separately for each chamber incubation). The diamond represents the geometric mean. The median is given by the horizontal line. The box marks the upper and lower quartile, the whiskers the total range of values.

Factors at the medium and coarse sand station were significantly higher ($p = 0.03$ and 0.01, respectively) than those at the fine sand station, where no effect of advection was observed. The disparity of TOU factors at the medium and coarse station, however, was statistically insignificant ($p = 0.17$). This is also reflected by the absolute differences of oxygen uptake in the presence and absence of advection (tab. 3), which are in the same range at the medium and coarse sand station (11.2 and 10.7 mmol m^{-2} d^{-1}).

Highest rates of TOU were found at the medium sand station (37.3 mmol m^{-2} d^{-1}) (tab. 3), but differences to TOU at the fine and coarse sand station (29.2 and

27.7 mmol m^{-2} d^{-1}, respectively) were statistically insignificant ($p > 0.05$ in pairwise and simultaneous comparisons).

Tab. 3: Rates of TOU (averages with standard deviations) as measured at the advective and non-advective stirrer setting, and differences between the respective rates.

		TOU (mmol m^{-2} d^{-1}), average ± s.d.		
Sediment type	Replicates	Advective setting	Non-advective setting	Difference
Fine	8	29.2 ± 12.2	28.8 ± 12.0	0.4 ± 4.8
Medium	6	37.3 ± 28.5	26.1 ± 18.3	11.2 ± 10.6
Coarse	5	27.7 ± 11.5	17.0 ± 12.8	10.7 ± 3.4
all sediments	19	31.3 ± 18.2	24.8 ± 14.5	6.5 ± 8.5

Nutrient fluxes

The nutrient fluxes varied considerably between deployments (fig. 7, tab. 4).

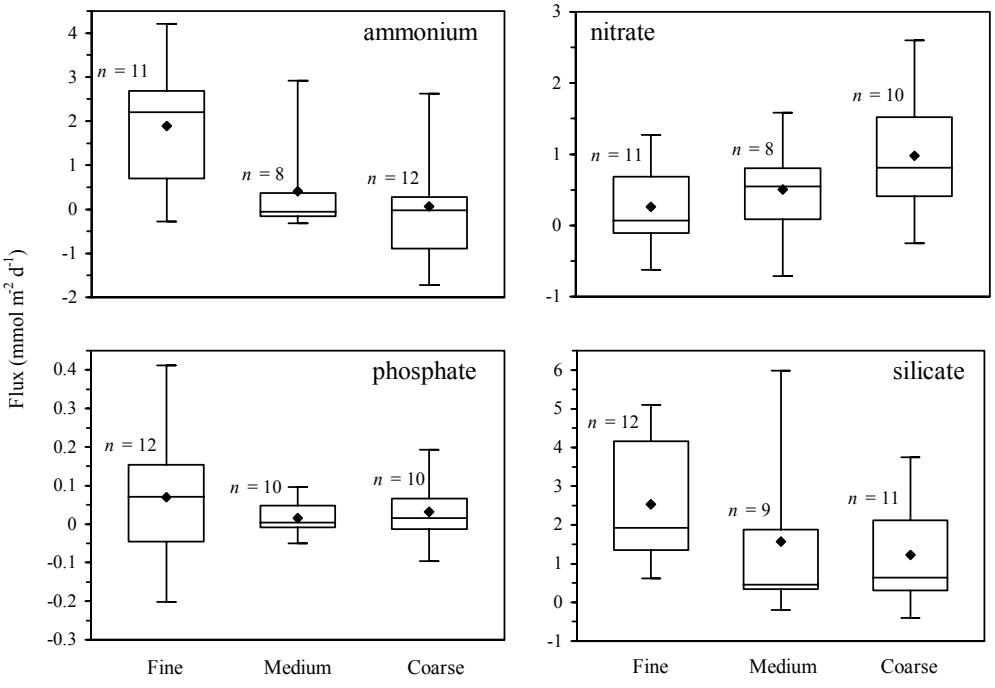

Fig. 7. Box plot of ammonium, nitrate, phosphate, and silicate fluxes. The diamond represents the mean, the median is given by the horizontal line. The box marks the upper and lower quartile, the whiskers the total range of values.

Nevertheless, some differences between stations could be identified. A pronounced release of ammonium was only found at the fine sand station with fluxes being significantly larger than those at the medium and coarse station (p = 0.04 and 0.01, respectively). The differences between ammonium fluxes at the medium and the coarse sand station were statistically insignificant (p = 0.46). Nitrate fluxes, on the contrary, were highest at the coarse sand station with averages being two and three times higher than those at the medium and fine sand station, respectively. These differences, however, proved to be statistically insignificant (p > 0.05 in pairwise and simultaneous comparisons). Nitrite concentrations of the chamber water were mostly close to or even below the detection limit of the method (0.6 µmol L^{-1}). Therefore, the nitrite fluxes (tab. 4) have to be treated with caution. Nevertheless it is obvious that they were of minor importance as compared to fluxes of the other N-compounds. Phosphate fluxes, being also very small, depicted no significant differences between stations. Silicate fluxes were highest at the fine sand station but significant differences were only detected between the fine and the coarse sediment (p = 0.04).

Tab. 4. Nutrient fluxes (averages with standard deviations) obtained at the three stations. Numbers of replicates are indicated in fig. 7.

	Nutrient fluxes (mmol m^{-2} d^{-1}), average ± s.d.				
Sediment type	Ammonium	Nitrate	Nitrite	Phosphate	Silicate
Fine	1.9 ± 1.49	0.26 ± 0.58	0.09 ± 0.14	0.07 ± 0.16	2.54 ± 1.67
Medium	0.41 ± 1.1	0.51 ± 0.74	0.06 ± 0.18	0.02 ± 0.05	1.57 ± 2.25
Coarse	0.07 ± 1.3	0.98 ± 0.89	0.06 ± 0.29	0.03 ± 0.09	1.22 ± 1.44

The nutrient and oxygen fluxes were used to calculate C : N : P flux ratios. Carbon equivalents were estimated from TOU at both stirrer settings assuming a respiratory quotient of 0.85. Ratios thus represent $J_{O_2} \times 0.85 : J_{NH_4^+ + NO_3^- + NO_2^-} : J_{PO_4^{3-}}$, where J_{O_2}, $J_{NH_4^+ + NO_3^- + NO_2^-}$, and $J_{PO_4^{3-}}$ are the measured fluxes of oxygen, dissolved inorganic nitrogen (DIN), and phosphate. Expressed as a fraction of "carbon fluxes", C : N : P ratios were 100 : 7.8 : 0.29 (fine), 100 : 2.7 : 0.06 (medium), and 100 : 4.4 : 0.17 (coarse sand station).

Discussion

Previous experiments indicated that advective pore-water exchange in permeable sediments may increase the volume of oxygenated sediment (Ziebis et al. 1996) as well as the oxygen consumption rate of the sediment (Booij et al. 1991; Forster et al. 1996). These findings have been restricted to laboratory systems because no instrument was available that allowed to assess the impact of advection on oxygen consumption rates in permeable shelf sediments in situ. The data presented here demonstrate for the first time the increase of sedimentary oxygen consumption due to advective pore-water exchange in the natural environment. Switching from the advective to the non-advective stirrer setting and thereby interrupting advective pore-water exchange, resulted in a clear drop of TOU in the incubations of both the medium and coarse sands. Oxygen consumption is an approved measure of the total organic matter mineralization including anaerobic heterotrophic processes through the re-oxidation of reduced electron acceptors (Rowe et al. 1988; Canfield et al. 1993; Thamdrup et al. 1994). The enhanced TOU is thus a strong indication of the potential of advection to promote the degradation of organic substrates in coarse grained deposits.

Incubation of the sediments at the seafloor ruled out sampling artifacts like the loss of pore-water or changes of the existing sediment stratification that would have affected the spatial distribution of solutes and sediment biota as well as the permeability. Progressive alterations of the biogeochemical zonation and community structure which sandy sediments may undergo in response to the specific conditions during enclosure (Booij et al. 1991; Berninger and Epstein 1995; Huettel et al. 1998; Heise and Gust 1999) are likewise minimized. Hence, it is assumed that general conditions of oxygen transport and consumption in the sediment, i.e., the factors that determined natural oxygen uptake rates, were maintained during the incubations.

In order to obtain reliable estimates of sediment oxygen consumption, it is crucial that the rates of advective pore-water exchange in the chambers match natural conditions. Advection in excess of natural rates could result in an artificially deep sediment oxygenation leading to re-oxidation of reduced solutes and, hence, an overestimation of natural oxygen fluxes. In the natural environment, pore-water exchange is controlled by bottom flow and sediment surface topography, while that in

the chamber depends on the stirring rate. Pressure gradients and the associated advective pore-water exchange increase exponentially both with bottom flow velocity and roughness element height (Huettel and Gust 1992a; Huettel et al. 1996). In theses studies a pressure gradient similar to that of the advective stirrer setting (2.9 Pa overall pressure difference, 0.044 Pa mm^{-1} maximum gradient) developed across mounds of 10 mm height that were exposed to unidirectional bottom flows < 20 cm s^{-1}. These values correspond to average roughness heights and flow conditions as they have been measured in the area. Maximum sediment elevations (35 mm) and peak tidal bottom flows (35 cm s^{-1}), however, proved to be much higher. Still, they are most likely well below maximum values as flow measurements and surface mapping took place at calm weather conditions and larger topographical features like dunes or ridges cannot be recognized in the 0.5 m long profiles. The pressure distributions as well as the rates of TOU that are obtained at the advective stirrer setting are therefore considered to represent "everyday conditions" while maximum pressures and fluxes in the area are expected to be much higher.

Huettel and Rusch (2000) emphasized that the radial pressure gradient and the resulting pore-water flow field within the enclosed sediment has strong similarities to what is produced by unidirectional flow interacting with sediment topography. Still, the concentric pressure distribution within the stirred chamber differs from patterns observed along current exposed topographical features (Huettel and Gust 1992a). Upon enclosure the natural pressure distribution is replaced by the stirrer-induced gradient which changes the pore-water circulation pattern. Initially, the oxygen concentration of the pore-water that is withdrawn from the sediment in the central low pressure region of the chamber therefore represents the remains of pre-enclosure oxygen supply and consumption. With ongoing deployment time, the oxygen distributions within the sediment gradually adjust to the new advective pattern as it has been observed in laboratory flumes and chambers (Booij et al. 1991; Ziebis et al. 1996; Precht et al. 2004). Pore-water emerging from the sediment then starts to reflect these changes. However, this transition in response to chamber conditions is not expected to introduce substantial artifacts to flux estimates. Shifting pore-water transport pathways can be expected to be common in natural permeable sands where direction and speed of tidal bottom flows permanently change (Antia et al. 1995), and alterations of sediment

topography take place due to currents and bioturbation (Wheatcroft 1994). Thus, changes in pore-water flow fields as they result from sediment enclosure, can be viewed as a normal scenario. In addition the flux determinations were restricted to deployments where oxygen decrease was linear i.e., where the effect of this transition on oxygen fluxes was negligible.

The drop in TOU after switching to the non-advective setting at the medium and coarse sand station showed that diffusion and bioirrigation alone were unable to supply the sediment community with enough oxygen to satisfy the sediment oxygen demand that was detected in the presence of advection. A significant contribution of the macrofauna to the drop in TOU, although unlikely, cannot be excluded. Such an effect would require a reduction in bioirrigation activity (Aller and Aller 1998; Forster et al. 1999) taking place in response to the stirring mode change. As the entire region is characterized by the same "*Tellina-fabula* macrofauna association" (Salzwedel et al. 1985), at least some drop in TOU would have been expected to occur at the fine sand station, too. It is therefore assumed that the respective factors between the oxygen uptake rates at both settings (1.38 and 1.91 at the medium and coarse sand station, respectively) are a measure for the proportion of oxygen supply that was provided by advection. An enhancement of oxygen uptake rates by means of an improved supply with oxygen is in agreement with the flume study of Forster et al. (1996) who reported rates of oxygen uptake to scale with the oxygenated sediment volume.

Several authors stressed that the flux estimates obtained with chambers on permeable sands are dependent on the actual pressure applied (Booij et al. 1991; Glud et al. 1996; Jahnke et al. 2000). The effect that the pressure gradient had on oxygen fluxes at the medium and coarse sand station confirms this view. Most available chamber designs include some kind of rotating stirrer to prevent stagnation of the chamber water (Malan and McLachlan 1991; Tengberg et al. 1995). As any rotation of the water column introduces a radial pressure gradient along the sediment surface (Glud et al. 1996; Tengberg et al. 2005) at least some advective pore-water exchange is most likely included in most existing chamber-derived solute flux estimates from highly permeable sandy sites. Aiming at an exact determination of natural solute fluxes, however, both a knowledge of natural pressure gradients within the area and stirrer-induced gradients within the chamber is needed to set up the chamber settings accordingly. Data on

natural pressure gradients are hard to obtain. In situ pressure gradient measurements are not available and model estimates (e.g., Rutherford et al. 1995) require the knowledge of topographies and currents. In order to facilitate the intercomparison of chamber-derived fluxes, a characterization of the pressure distribution in the chamber and information on the permeabilities should be considered as a minimum requirement for future investigations.

To further evaluate the effect of advection on TOU, it is useful to compare the oxygen flux to the rate of pore-water exchange. The latter has been quantified at the coarse sand station during the advective stirrer setting. Monitoring the progressive depletion of an inert tracer dye that was added to the chamber water revealed exchange rates of approximately 90 L m^{-2} d^{-1} (Janssen et al. 2005). According to Glud et al. (1996), the advective exchange at the medium sand station can be expected to be 40 % lower, i.e., 54 L m^{-2} d^{-1}. The net advective oxygen transport into the enclosed sediment equals the pore-water exchange rate multiplied by the difference in oxygen concentration between the chamber water that enters the sediment and the pore-water that is released. A minimum exchange rate of 50 L m^{-2} d^{-1} is needed to account for the average TOU enhancement of roughly 11 mmol m^{-2} d^{-1} at the medium and coarse sand station that was attributed to advection. Given the above pore-water exchange rates, this would mean that except for 7 % all oxygen was removed from the pore-water during the passage through the medium sand while, at the coarse sand station, 44 % of the chamber water oxygen was still present in the emerging pore-water. In contrast to muddy sediments, where supply with oxygen has been identified as a major limiting factor for the mineralization of organic matter (Froelich et al. 1979; Jørgensen and Sorensen 1985; Enoksson and Samuelsson 1987), the incomplete oxygen removal at the coarse sand station indicates that in the presence of advection, oxygen supply exceeded the demand of the ongoing biological and chemical processes. If, during typical summer conditions (T = 17 - 18° C and S = 33 psu) oxygen would be quantitatively removed from oxygen saturated seawater circulating through the sediment at a rate of 90 L d^{-1}, this would result in an advective oxygen supply of 22 mmol m^{-2} d^{-1}. Given the sediment topography is rough and flow velocities are high, pore-water exchange rates as well as maximum oxygen fluxes may even be much higher. This indicates that mineralization in highly permeable sands might take place at very high rates once highly reactive organic

matter is available. Such conditions can be expected during phytoplankton blooms when fresh organic particles are abundant in the water column and transported into the sediment by means of advection (Pilditch et al. 1998; Huettel and Rusch 2000; Rusch et al. 2001).

The potential of advection to contribute to oxygen supply and mineralization of organic matter proved to be restricted to the medium and coarse sand station. Oxygen consumption rates at the fine sand station were not affected by the change in stirrer setting. This suggests that permeability at this station was too low to allow for pore-water advection sufficiently strong to cause a significant transport of oxygen. With a permeability that is still orders of magnitude higher than those of muddy sediments, the sediment at the fine sand station is classified as permeable sand (Huettel and Gust 1992a). However, from the TOU measurements it can be expected that the transport of oxygen and other solutes at that station is largely restricted to diffusion and bioirrigation. This view agrees with results obtained in incubations of sieved sands in stirred cylindrical chambers (Glud et al. 1996), which showed no solute transport in excess of diffusion at permeabilities similar to that of the fine sand station.

If oxygen supply at the fine sand station was restricted to diffusion and bioirrigation, it can be expected that oxygen penetration was also low as compared to the other stations. This agrees to oxygen penetration depths (average ± s.d.) of 9.1 ± 2.5 and 25.7 ± 12.3 mm, at the fine and medium sand station, respectively, as they have been obtained from time series of in situ oxygen microprofiles (Janssen et al. in prep.). A reduced oxygen penetration in the fine sand also agrees with the release of ammonium at that station as it restricts nitrification to the uppermost sediment horizon. Furthermore, the reduced oxygen availability probably also favored an additional ammonium production through dissimilatory nitrate reduction in anoxic sediment regions. On the contrary, the release of nitrate at the medium and coarse sand station probably reflects the enhanced advective oxygen supply that allows a quantitative nitrification of ammonium within the sediment. This general pattern is in agreement with nutrient fluxes that were obtained in incubations of sands from the same three stations (Ehrenhauss et al. 2004).

While grain size, permeability, and oxygen penetration were lower at the fine sand station than at the other two stations, the TOC content was 4 to 5 times higher. Bacterial

biomass in the fine sand similarly exceeded that in the medium and coarse sand by a factor of 4 and 9, respectively, as estimated from concentrations of bacteria-specific fatty acids (Bühring et al. 2005). The fact that rates of TOU at all three stations nevertheless proved to be in the same range confirms that the mineralization activity was not limited by the standing stock of neither organic matter nor bacteria. Enhanced advection at the medium and coarse sand station probably creates favorable sedimentary environments that allow for microbial metabolism at rates that compensate for the lower biomass. In order to get an overview of organic matter mineralization on the continental shelf, Canfield and Teske (1996) provided a compilation of 60 studies on carbon oxidation at water depths < 200 m. The average organic carbon content of the sediments is given as 0.65 wt % (i.e., 5, 28 and 22 times that of the fine, medium, and coarse sand, respectively). Despite the fact that the sediments obviously included fine and organically rich deposits where bacterial numbers are typically orders of magnitudes higher than those in sands (Llobet-Brossa et al. 1998; Böttcher et al. 2000) the median oxygen uptake rate was calculated to be only 13.7 mmol m^{-2} d^{-1}. Rates obtained during this study were substantially higher, confirming that mineralization rates of sandy sediments are not necessarily small but can be in the same order than those of finer, organically rich deposits (Andersen and Helder 1987; Cammen 1991; Grant et al. 1991; Marinelli et al. 1998).

Compared to the rates of TOU, nutrient fluxes were relatively low at all three stations. The estimated C : N : P ratios deviated substantially from the Redfield ratio (100 : 15 : 0.9, if normalized to carbon). Assuming that the sediment TOC : TN ratio of approximately 100 : 12 (tab. 1) is representative of the organic matter that is mineralized, there is still a strong discrepancy between interfacial dissolved inorganic nitrogen (DIN) fluxes and the expected release during organic matter mineralization. Relative to TOU, nutrient fluxes where lower at the medium and coarse than at the fine sand station. A possible sink for DIN and phosphate is the uptake by growing bacteria (Van Duyl et al. 1993). The authors observed lowest nutrient fluxes in sandy sediments when bacterial production was highest. The low DIN fluxes, especially in the medium and coarse sand, suggest that bacterial populations in these sediments have the potential to grow if nutrients and organic matter becomes available. This may be a further indication for a high activity of bacteria at these stations. Other possible sinks for

nutrients include the uptake by benthic diatoms (Marinelli et al. 1998), the denitrification of nitrate, and the adsorption of phosphate to iron-rich particles (Gunnars and Blomqvist 1997). The latter process was found to be most pronounced in oxygenated sediments which may also explain that lowest phosphate fluxes were found at the medium and coarse sand station.

As highlighted in the introduction, advection-related enhancement of organic matter mineralization potentially involves a range of different processes. Several studies investigated the impact of permeability on such processes in sediments of different grain sizes. This included the quantification of the pore-water exchange (Huettel and Gust 1992a; Glud et al. 1996), the filtration of suspended tracer particles and microalgae (Huettel et al. 1996; Huettel and Rusch 2000), and the transport and consumption of oxygen as determined with enclosures and microsensors (Forster et al. 1996; Ziebis et al. 1996). In all investigations sediment permeability has been identified as the key factor that determines whether or not advection-related processes are significant relative to diffusive transport, bioturbation and bioirrigation. Despite the large diversity of the investigated processes and experimental approaches (flumes and chambers, in the laboratory and on tidal flats) all studies invariably reported that permeabilities between 10^{-11} to 10^{-12} m^2 were required for advection to significantly affect the processes in question. A permeability threshold between the respective permeabilities of the medium and fine station (i.e., between 0.3 and 2.6×10^{-11} m^2) as it was observed in this study with respect to the impact of advection on TOU is in agreement with the reported values. This confirms that the effect of advection on sedimentary processes does not necessarily apply to sandy sediments in general but may be restricted to sites of high permeability.

Approximately 98 % of the surficial sediments of the German Bight area are sands (all the colored area in fig. 8). While permeability measurements in the area are largely missing, rough estimates may be obtained based on granulometric data according to Krumbein and Monk (1943). Rusch et al. (2001) found that results calculated in that manner overestimated the measured permeabilities of intertidal sands by a factor of 3.87 ± 2.21 (s.d.). This is most likely because the approach does not account for grain size distribution skewness and kurtosis, and biological clogging of the pores. An

overestimation by a factor of 2.03 ± 0.94 was also observed at the three sites of this study. Fig. 8 shows permeabilities of the entire German Bight as calculated from median grain size and sorting of a total of approximately 16,000 surface sediment samples (MUNDAB database, Federal Maritime and Hydrographic Agency of Germany). The values were reduced by a factor of 3 to account for the effects mentioned above. Fig. 9 presents the areal coverage of the sediment permeabilities as a cumulative frequency plot.

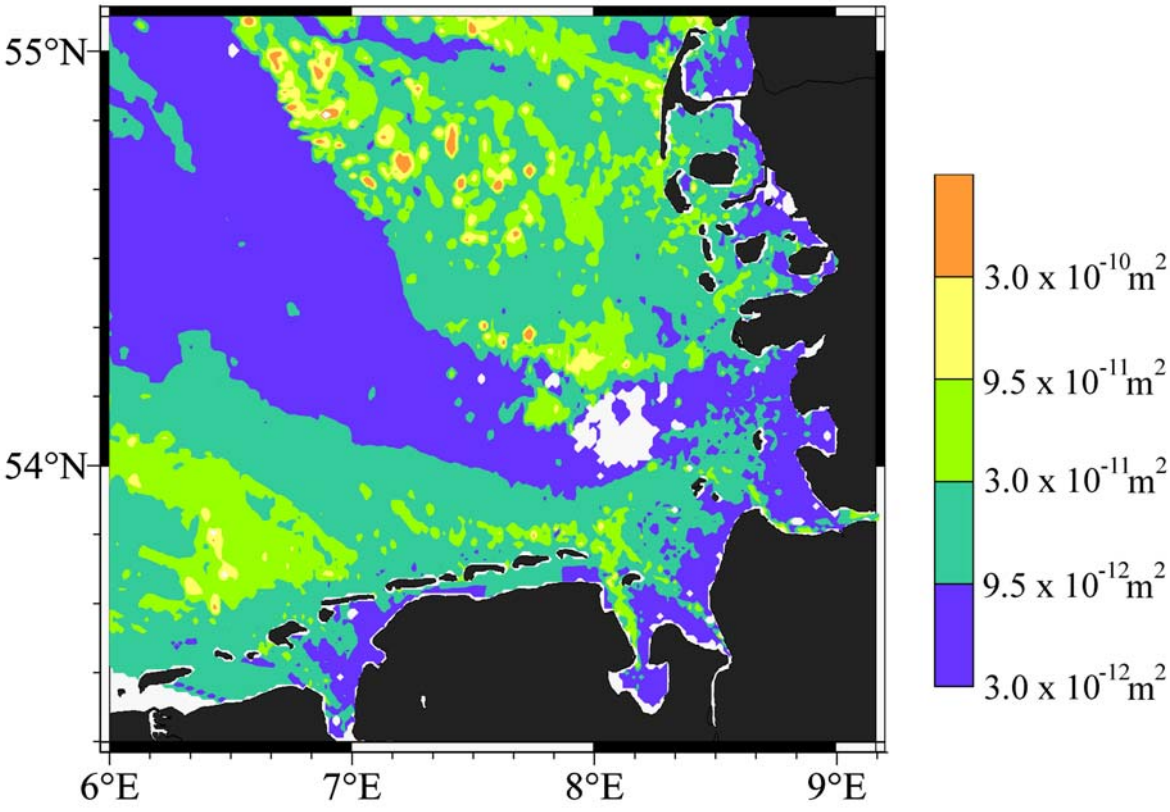

Fig. 8. Contour plot of the permeabilities of the German Bight as calculated based on grain size measures according to Krumbein and Monk (1943) using the median grain sizes and standard deviation in phi units. The standard deviation was inferred from the reported 25th and 75th percentile. The permeablities of the indvidual samples were transferred to an approximately 1×1 km^2 grid by triangulation with linear interpolation. Gridding and contour plotting were done with the software Surfer© 6.01 (Golden Software Inc.). Blank parts in the plot mark areas that were not covered by samples (lower left corner) or where median grain sizes were below the sand size range (e.g., large mud patch around 54° N, 8° E)

Sediments with permeabilities below that of the fine sand station (i.e., all blue areas in fig. 8) are estimated to cover roughly 40 % of the total surface area. Based on the chamber results an impact of advection on oxygen fluxes can be largely excluded in these areas. In the remaining 60 % of the German Bight permeabilities are within a range where significant advective pore-water exchange is expected to occur (Huettel and Gust 1992b; Glud et al. 1996). It is thus likely that in these regions advection contributes to oxygen uptake and organic matter mineralization to an extent that gradually increases with increasing permeability. Direct evidence for such an effect was restricted to the medium and coarse sand station. Sands with such high permeabilities (i.e., 2.6×10^{-11} m^2 or higher), however, are only expected to occur in 3 % of the German Bight seafloor (fig. 9).

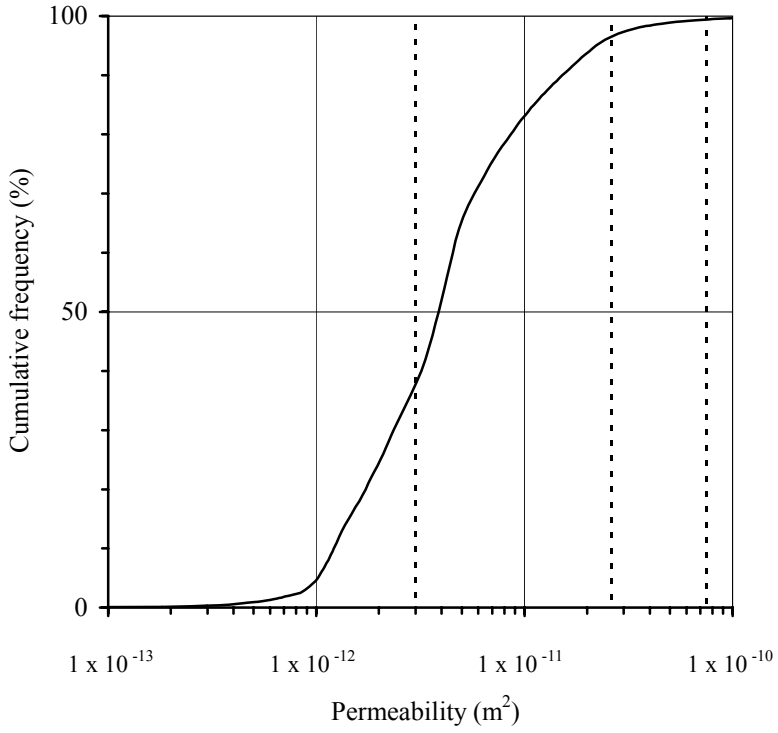

Fig. 9. Cumulative frequencies of the permeabilities of the German Bight according to the 1 × 1 km^2 grid (see caption of fig. 9). Apart from small errors that might result from the simplifying equidistant cylindrical projection, the frequencies equal the proportion of the total seafloor area of fig. 8 (approximately 29.000 km^2) that is covered by sands of the respective permeabilities.

The areal coverage of sediments where advection is strong enough to significantly enhance organic matter mineralization thus remains largely unresolved. More detailed studies are needed to increase our knowledge of advection-related processes in natural environments in order to gain insight into the relevance of permeable sediments for carbon cycling on the shelf. Main topics to be addressed include both the essentials of advective pore-water flow and solute exchange in natural environments (i.e., permeabilities, topographies, and hydrodynamics) as well as the impact that advective exchange has on oxygen uptake and organic matter mineralization in these beds.

References

Aller, R.C. 1994. Bioturbation and remineralization of sedimentary organic matter: effects of redox oscillation. Chem. Geol. **114**: 331-345.

Aller, R.C., and J.Y. Aller. 1998. The effect of biogenic irrigation intensity and solute exchange on diagenetic reaction rates in marine sediments. J. Mar. Res. **56**: 905-936.

Andersen, F.O., and W. Helder. 1987. Comparison of oxygen microgradients, oxygen flux rates and electron-transport system activity in coastal marine sediments. Mar. Ecol. Prog. Ser. **37**: 259-264.

Antia, E.E. 1993. Sedimentology, morphodynamics and facies association of a mesotidal barrier island shoreface (Spiekeroog, southern North Sea). In *Berichte aus dem Fachbereich Geowissenschaften*. Bremen: Univ. Bremen, Geowissenschaften.

Antia, E.E., B.W. Flemming, and G. Wefer. 1995. Calm-weather spring and neap tidal current characteristics at a shoreface connected ridge complex in the German Bight (southern North-Sea). Geo-Mar. Lett. **15**: 30-36.

Bacon, M.P., R.A. Belastock, and M.H. Bothner. 1994. ^{210}Pb balance and implications for particle transport on the continental shelf, U.S. Middle Atlantic Bight. Deep-Sea Res. Part II **41**: 511-535.

Basu, A.J., and A. Khalili. 1999. Computation of flow through a fluid-sediment interface in a benthic chamber. Phys. Fluids **11**: 1395-1405.

Berninger, U.G., and S.S. Epstein. 1995. Vertical distribution of benthic ciliates in response to the oxygen concentration in an intertidal North Sea sediment. Aquat. Microb. Ecol. **9**: 229-236.

Booij, K., W. Helder, and B. Sundby. 1991. Rapid redistribution of oxygen in a sandy sediment induced by changes in the flow velocity of the overlying water. Neth. J. Sea Res. **28**: 149-165.

Böttcher, M.E., B. Hespenheide, E. Llobet-Brossa, C. Beardsley, O. Larsen, A. Schramm, A. Wieland, G. Böttcher, U.G. Berninger, and R. Amann. 2000. The biogeochemistry, stable isotope geochemistry, and microbial community structure of a temperate intertidal mudflat: an integrated study. Cont. Shelf Res. **20**: 1749-1769.

Boudreau, B.P., M. Huettel, S. Forster, R.A. Jahnke, A. McLachlan, J.J. Middelburg, P. Nielsen, F. Sansone, G. Taghon, W.R. Van Raaphorst, I. Webster, J.M. Weslawski, P. Wiberg, and B. Sundby. 2001. Permeable marine sediments: overturning an old paradigm. EOS Trans. Am. Geophys. Union **82**: 133-136.

Bühring, S.I., M. Elvert, and U. Witte. 2005. The microbial community structure of different permeable sandy sediments characterized by the investigation of bacterial fatty acids and fluorescence *in situ* hybridization. Environ. Microbiol. **7:** 281-293.

Burnett, W.C., M. Taniguchi, and J. Oberdorfer. 2001. Measurement and significance of the direct discharge of groundwater into the coastal zone. J. Sea Res. **46**: 109-116.

Cahoon, L.B. 1999. The role of benthic microalgae in neritic ecosystems, p. 47-86. *In* A. Ansell, R. N. Gibson and M. Barnes, [eds.]. Oceanography and Marine Biology. An Annual Review. Taylor & Francis.

Cammen, L.M. 1991. Annual bacterial production in relation to benthic microalgal production and sediment oxygen uptake in an intertidal sandflat and an intertidal mudflat. Mar. Ecol. Prog. Ser. **71**: 13-25.

Canfield, D.E., B.B. Jørgensen, H. Fossing, R.N. Glud, J. Gundersen, N.B. Ramsing, B. Thamdrup, J.W. Hansen, L.P. Nielsen, and P.O.J. Hall. 1993. Pathways of organic carbon oxidation in three continental margin sediments. Mar. Geol. **113**: 27-40.

Canfield, D.E., and A. Teske. 1996. Late Proterozoic rise in atmospheric oxygen concentration inferred from phylogenetic and sulphur-isotope studies. Nature **382**: 127-132.

Clesceri, L.S., A.E. Greenberg, and R.R. Trusall, eds. 1989. *Standard methods for the examination of water and wastewater*. 17 ed. Washington, D.C.: American Public Health Association.

Dando, P.R., S. Aliani, H. Arab, C.N. Bianchi, M. Brehmer, S. Cocito, S.W. Fowler, J. Gundersen, L.E. Hooper, R. Kolbl, J. Kuever, P. Linke, K.C. Makropoulos, R. Meloni, J.C. Miquel, C. Morri, S. Muller, C. Robinson, H. Schlesner, S. Sievert, R. Stohr, D. Stuben, M. Thomm, S.P. Varnavas, and W. Ziebis. 2000. Hydrothermal studies in the Aegean Sea. Phys. Chem. Earth B: Hydrol. Oceans Atmos. **25**: 1-8.

Dando, P.R., M.C. Austen, R.A. Burke, M.A. Kendall, M.C. Kennicutt, A.G. Judd, D.C. Moore, S.C.M. Ohara, R. Schmaljohann, and A.J. Southward. 1991. Ecology of a North-Sea pockmark with an active methane seep. Mar. Ecol. Prog. Ser. **70**: 49-63.

DeFlaun, M.F., and L.M. Mayer. 1983. Relationships between bacteria and grain surfaces in intertidal sediments. Limnol. Oceanogr. **28**: 873-881.

Dette, H.H. 1977. Ein Vorschlag zur Analyse eines Wellenklimas. Die Küste **31**: 166-180.

Ehrenhauss, S., U. Witte, F. Janssen, and M. Huettel. 2004. Decomposition of diatoms and nutrient dynamics in permeable North Sea sediments. Cont. Shelf Res. **24:** 721-737.

Emery, K.O. 1968. Relict sediments on continental shelves of the world. Am. Assoc. Pet. Geol. Bull. **52**: 445-464.

Emery, K.O., and E. Uchupi. 1972. Western North Atlantic Ocean: topography, rocks, structures, water, life, and sediments. Vol. 17, *Am. Assoc. Pet. Geol. Mem.* The American Association of Petroleum Geologists.

Enoksson, V., and M.O. Samuelsson. 1987. Nitrification and dissimilatory ammonium production and their effects on nitrogen flux over the sediment-water interface in bioturbated coastal sediments. Mar. Ecol. Prog. Ser. **36**: 181-189.

Figge, K. 1981. Sedimentverteilung in der Deutschen Bucht. Hamburg: Deutsches Hydrographisches Institut.

Forster, S., R.N. Glud, J.K. Gundersen, and M. Huettel. 1999. In situ study of bromide tracer and oxygen flux in coastal sediments. Est. Coast. Shelf Sci. **49**: 813-827.

Forster, S., M. Huettel, and W. Ziebis. 1996. Impact of boundary layer flow velocity on oxygen utilization in coastal sediments. Mar. Ecol. Prog. Ser. **143**: 173-185.

Fries, J.S., and J.H. Trowbridge. 2003. Flume observations of enhanced fine-particle deposition to permeable sediment beds. Limnol. Oceanogr. **48**: 802-812.

Froelich, P.N., G.P. Klinkhammer, M.L. Bender, N.A. Luedtke, G.R. Heath, D. Cullen, P. Dauphin, D. Hammond, B. Hartman, and V. Maynard. 1979. Early oxidation of organic matter in pelagic sediments of the eastern equatorial Atlantic: suboxic diagenesis. Geochim. Cosmochim. Acta **43**: 1075-1090.

Gehlen, M., H. Malschaert, and W.R. Van Raaphorst. 1995. Spatial and temporal variability of benthic silica fluxes in the southeastern North-Sea. Cont. Shelf Res. **15**: 1675-1696.

Glud, R.N., S. Forster, and M. Huettel. 1996. Influence of radial pressure gradients on solute exchange in stirred benthic chambers. Mar. Ecol. Prog. Ser. **141**: 303-311.

Grant, J., C.W. Emerson, B.T. Hargrave, and J.L. Shortle. 1991. Benthic oxygen consumption on continental shelves off Eastern Canada. Cont. Shelf Res. **11**: 1083-1097.

Gunnars, A., and S. Blomqvist. 1997. Phosphate exchange across the sediment-water interface when shifting from anoxic to oxic conditions - an experimental comparison of freshwater and brackish-marine systems. Biogeochemistry **37**: 203-226.

Heise, S., and G. Gust. 1999. Influence of the physiological status of bacteria on their transport into permeable sediments. Mar. Ecol. Prog. Ser. **190**: 141-153.

Holst, G., R.N. Glud, M. Kuhl, and I. Klimant. 1997. A microoptode array for fine-scale measurement of oxygen distribution. Sens. Actuat. B **38**: 122-129.

Huettel, M., and G. Gust. 1992a. Impact of bioroughness on interfacial solute exchange in permeable sediments. Mar. Ecol. Prog. Ser. **89**: 253-267.

Huettel, M., and G. Gust. 1992b. Solute release mechanisms from confined sediment cores in stirred benthic chambers and flume flows. Mar. Ecol. Prog. Ser. **82**: 187-197.

Huettel, M., H. Røy, E. Precht, and S. Ehrenhauss. 2003. Hydrodynamical impact on biogeochemical processes in aquatic sediments. Hydrobiologia **494**: 231-236.

Huettel, M., and A. Rusch. 2000. Transport and degradation of phytoplankton in permeable sediment. Limnol. Oceanogr. **45**: 534-549.

Huettel, M., and I.T. Webster. 2001. Porewater flow in permeable sediments, p. 144-179. *In* B. P. Boudreau and B. B. Jørgensen, [eds.]. The benthic boundary layer: transport processes and biogeochemistry. Oxford Univ. Press.

Huettel, M., W. Ziebis, and S. Forster. 1996. Flow-induced uptake of particulate matter in permeable sediments. Limnol. Oceanogr. **41**: 309-322.

Huettel, M., W. Ziebis, S. Forster, and G.W. Luther III. 1998. Advective transport affecting metal and nutrient distribution and interfacial fluxes in permeable sediments. Geochim. Cosmochim. Acta **62**: 613-631.

Jahnke, R.A., J.R. Nelson, R.L. Marinelli, and J.E. Eckman. 2000. Benthic flux of biogenic elements on the Southeastern US continental shelf: influence of pore water advective transport and benthic microalgae. Cont. Shelf Res. **20**: 109-127.

Janssen, F., P. Faerber, M. Huettel, V. Meyer, and U. Witte. 2005. Pore-water advection and solute fluxes in permeable marine sediments (I): calibration and performance of the novel benthic chamber system *Sandy*. Limnol. Oceanogr. **50:** 768-778.

Janssen, F., H. Røy, U. Werner, and U. Witte, in prep. Sediment surface topographies and bottom water flow: an in situ case-study on the fundamentals of porewater advection.

Jørgensen, B.B. 1996. Material flux in the sediment, p. 115-135. *In* B. B. Jørgensen and K. Richardson, [eds.]. Eutrophication in coastal marine ecosystems. American Geophysical Union.

Jørgensen, B.B., and J. Sorensen. 1985. Seasonal cycles of O_2, NO_3^- and SO_4^{2-} reduction in estuarine sediments - the significance of a NO_3^- reduction maximum in spring. Mar. Ecol. Prog. Ser. **24**: 65-74.

Khalili, A., A.J. Basu, and M. Huettel. 1997. A non-Darcy model for recirculating flow through a fluid-sediment interface in a cylindrical container. Acta Mech. **123**: 75-87.

Klimant, I., V. Meyer, and M. Kuhl. 1995. Fiberoptic oxygen microsensors, a new tool in aquatic biology. Limnol. Oceanogr. **40**: 1159-1165.

Klute, A., and C. Dirksen. 1986. Hydraulic conductivity and diffusivity: laboratory methods, p. 687ff. *In* A. Klute, [eds.]. Methods of soil analysis - part 1 - physical and mineralogical methods. American Society of Agronomy.

Krumbein, W.C., and G.D. Monk. 1943. Permeability as a function of the size parameters of unconsolidated sand. Trans. Am. Inst. Min. Metall. Eng. **151**: 153-163.

Lindholm, R. 1987. A practical approach to sedimentology. Allen & Unwin.

Llobet-Brossa, E., R. Rosselló-Mora, and R. Amann. 1998. Microbial community composition of wadden sea sediments as revealed by flourescence *in situ* hybridization. Appl. Environ. Microbiol. **64**: 2691-2696.

Malan, D.E., and A. McLachlan. 1991. In situ benthic oxygen fluxes in a nearshore coastal marine system: a new approach to quantify the effect of wave action. Mar. Ecol. Prog. Ser. **73**: 69-81.

Malone, T.C., T.S. Hopkins, P.G. Falkowski, and T.E. Whitledge. 1983. Production and transport of phytoplankton biomass over the continental shelf of the New York Bight. Cont. Shelf Res. **1**: 305-337.

Marinelli, R.L., R.A. Jahnke, D.B. Craven, J.R. Nelson, and J.E. Eckman. 1998. Sediment nutrient dynamics on the South Atlantic Bight continental shelf. Limnol. Oceanogr. **43**: 1305-1320.

McLachlan, A., I.G. Eliot, and D.J. Clarke. 1985. Water filtration through reflective microtidal beaches and shallow sublittoral sands and its implications for an inshore ecosystem in western Australia. Est. Coast. Shelf Sci. **21**: 91-104.

Nelson, J.R., J.E. Eckman, C.Y. Robertson, R.L. Marinelli, and R.A. Jahnke. 1999. Benthic microalgal biomass and irradiance at the sea floor on the continental shelf of the South Atlantic Bight. Cont. Shelf Res. **19**: 477-505.

Niemeyer, H.D. 1979. Untersuchungen zum Seegangsklima im Bereich der Ostfriesischen Inseln und Küste. Die Küste **34**: 53-70.

Pilditch, C.A., C.W. Emerson, and J. Grant. 1998. Effect of scallop shells and sediment grain size on phytoplankton flux to the bed. Cont. Shelf Res. **17**: 1869-1885.

Precht, E., and M. Huettel. 2003. Advective pore-water exchange driven by surface gravity waves and its ecological implications. Limnol. Oceanogr. **48**: 1674-1684.

Precht, E., U. Franke, L. Polerecky, and M. Huettel. 2004. Oxygen dynamics in permeable sediments with wave-driven pore water exchange. Limnol. Oceanogr. **49:** 693-705.

Riedl, R.J., N. Huang, and R. Machan. 1972. The subtidal pump, a mechanism of intertidal water exchange by wave action. Mar. Biol. **13**: 210-221.

Rocha, C. 1998. Rhythmic ammonium regeneration and flushing in intertidal sediments of the Sado estuary. Limnol. Oceanogr. **43**: 823-831.

Rocha, C. 2000. Density-driven convection during flooding of warm, permeable intertidal sediments: the ecological importance of the convective turnover pump. J. Sea Res. **43**: 1-14.

Rowe, G.T., S. Smith, P. Falkowski, T. Whitledge, R. Theroux, W. Phoel, and H. Ducklow. 1986. Do continental shelves export organic matter? Nature **324**: 559-561.

Rowe, G.T., R. Theroux, W. Phoel, H. Quinby, R. Wilke, D. Koschoreck, T.E. Whitledge, P.G. Falowski, and C. Fray. 1988. Benthic carbon budgets for the continental shelf south of New England. Cont. Shelf Res. **8**: 511-527.

Rusch, A., S. Forster, and M. Huettel. 2001. Bacteria, diatoms and detritus in an intertidal sandflat subject to advective transport across the water-sediment interface. Biogeochemistry **55**: 1-27.

Rutgers van der Loeff, M.M. 1981. Wave effects on sediment water exchange in a submerged sand bed. Neth. J. Sea Res. **15**: 100-112.

Rutherford, J.C., J.D. Boyle, A.H. Elliott, T.V.J. Hatherell, and T.W. Chiu. 1995. Modeling benthic oxygen uptake by pumping. J. Environ. Eng. **121**: 84-95.

Salzwedel, H., E. Rachor, and D. Gerdes. 1985. Benthic macrofauna communities in the German Bight. Veröff. Inst. Meeresforsch. Bremerhav. **20**: 199-267.

Savant, S.A., D.D. Reible, and L.J. Thibodeaux. 1987. Convective transport within stable river sediments. Water Resour. Res. **23**: 1763-1768.

Shum, K.T., and B. Sundby. 1996. Organic matter processing in continental shelf sediments - the subtidal pump revisited. Mar. Chem. **53**: 81-87.

Strickland, J.D.H., and T.R. Parsons. 1968. A practical handbook of seawater analysis. Vol. 167, *Bull. Fish. Res. Board Can.* Fisheries Research Board of Canada.

Tengberg, A., F. De Bovee, P. Hall, W. Berelson, D. Chadwick, G. Cicer, P. Crassous, A. Devol, S. Emerson, J. Gage, R.N. Glud, F. Graziottini, J. Gundersen, D. Hammond, W. Helder, K. Hinga, O. Holby, R. Jahnke, A. Khripounoff, S. Lieberman, V. Nuppenau, D. Smallman, B. Wehrli, and P. De Wilde. 1995. Benthic chamber and profiling landers in oceanography - a review of design, technical solutions and functioning. Prog. Oceanog. **35**: 253-294.

Tengberg, A., P.O.J. Hall, U. Andersson, B. Lindén, O. Styrenius, G. Boland, F. de Bovee, B. Carlsson, S. Ceradini, A. Devol, G. Duineveld, J.-U. Friemann, R.N. Glud, A. Khripounoff, J. Leather, P. Linke, L. Lund-Hansen, G. Rowe, P. Santschi, P. De Wilde, and U. Witte. 2005. Intercalibration of benthic flux chambers II. Hydrodynamic characterization and flux comparisons of 14 different designs. Mar. Chem. **94:** 147–173.

Thamdrup, B., H. Fossing, and B.B. Jørgensen. 1994. Manganese, iron, and sulfur cycling in a coastal marine sediment, Aarhus Bay, Denmark. Geochim. Cosmochim. Acta **58**: 5115-5129.

Thibodeaux, L.J., and J.D. Boyle. 1987. Bedform-generated convective transport in bottom sediment. Nature **325**: 341-343.

Van Duyl, F.C., W. Van Raaphorst, and A.J. Kop. 1993. Benthic bacterial production and nutrient sediment-water exchange in sandy North Sea sediments. Mar. Ecol. Prog. Ser. **100**: 85-95.

Walsh, J.J. 1988. On the nature of continental shelves. Academic Press.

Walsh, J.J., G.T. Rowe, R. Iverson, and C.P. McRoy. 1981. Biological export of shelf carbon is a sink of the global CO_2 cycle. Nature **291**: 196-201.

Webster, I.T., S.J. Norquay, F.C. Ross, and R.A. Wooding. 1996. Solute exchange by convection within estuarine sediments. Est. Coast. Shelf Sci. **42**: 171-183.

Wentworth, C.K. 1922. A scale of grade and class terms for clastic sediments. J. Geol. **30**: 377-392.

Wheatcroft, R.A. 1994. Temporal variation in bed configuration and one-dimensional bottom roughness at the mid shelf STRESS site. Cont. Shelf Res. **14**: 1167-1190.

Witte, U., and O. Pfannkuche. 2000. High rates of benthic carbon remineralisation in the abyssal Arabian Sea. Deep-Sea Res. Part II **47**: 2785-2804.

Ziebis, W., M. Huettel, and S. Forster. 1996. Impact of biogenic sediment topography on oxygen fluxes in permeable seabeds. Mar. Ecol. Prog. Ser. **140**: 227-23

Sediment surface topographies and bottom water flow: an in situ case-study on the fundamentals of pore-water advection

Felix Janssen[1], Hans Røy[1], Ursula Werner[1] & Ursula Witte[1,2]

[1] Max Planck Institute for Marine Microbiology, Celsiusstrasse 1, D-28359 Bremen, Germany

[2] Present address: University of Aberdeen, Oceanlab, Newburgh, Aberdeen AB41 6AA, Scotland, UK

Acknowledgements

B. B. Jørgensen is acknowledged for the support of this work. We are indepted to the following technicians who constructed and set up the system: V. Meyer, P. Färber, J. Langreder, A. Nordhausen, E. Labahn, and T. Kumbier. Special thanks go to the crews of RV HEINCKE and UTHOERN for their great support during cruises. S. Bühring, S. Ehrenhauss, A. Kamp, M. Keller, H. Woyt, and A. M. Alraei are gratefully acknowledged for their help during cruise preparation as well as on board. M. Schlösser is thanked for his assistance in video processing. S. Dick from the Federal Maritime and Hydrographic Agency of Germany is gratefully acknowledged for providing current model data for the German Bight. This study was funded by the Max Planck Society.

Abstract

Advective pore-water exchange along horizontal pressure gradients substantially affects benthic solute and particle fluxes in permeable sands and has strong implications for biogeochemical zonation and organic matter mineralization. The pressure gradients, and hence the rates of pore-water exchange, scale with the size of the current exposed topographical features at the sediment surface. This study presents small-scale surface topographies that were obtained at a fine-, medium-, and coarse sand site by means of laser-based surface scanning and acoustic altimetry. Seafloor topographies were highly variable with a more than 6 fold range in average roughness element height between the respective stations and cruises (3.1 to 20.1 mm). Ripples generally provided the most prominent roughness elements. Highest ripples were observed at the medium sand station while ripples were smaller and less common at the coarse sand site. Here, bioroughness prevailed, indicating that ripple formation may have been hampered due to the large grain size. Based on ripple dimensions and measurements of near-bottom flow, advection at the medium sand station is expected to result in pore-water exchange at a rate of 45.4 L m^{-2} d^{-1}. The presence of pore-water advection at that site was confirmed by a time series of in situ oxygen microprofiles. These measurements clearly indicated an intensive advective oxygen supply which is expected to substantially affect oxygen uptake and sediment biogeochemistry. This may be even more pronounced at the coarse sand site where similar pressure gradients would result in 2.8 times higher rates of pore-water advection. However, an assessment of the effect of advection at that site is limited by the lack of appropriate modeling approaches that allow a quantification of pore-water exchange as it is induced by irregularly spaced biogenic roughness elements.

Introduction

"The seafloor rarely is smooth" (Yager et al. 1993). Surface roughness is an intrinsic characteristic of marine sediments throughout the ocean at any depth and location (Heezen and Hollister 1971). Sediment topographies in shelf areas include sandwaves, ripples, bioroughness like mounds, pits, and burrows but also roughness elements in the size range of individual sediment particles and microorganisms (Langhorne 1982; Briggs 1989; Wheatcroft 1994; Li and Amos 1999; Paterson 2001). Roughness elements may significantly affect the rates of solute exchange across the sediment-water interface. In fine grained, diffusion dominated sediments, roughness may enhance diffusive fluxes as compared to smooth surfaces by increasing the effective exchange area (Gundersen and Jørgensen 1990; Røy et al. 2002). Near bed turbulences as introduced by minute roughness elements in the presence of bottom flows locally reduce the thickness of the diffusive boundary layer thereby enhancing diffusive exchange (Jørgensen and Des Marais 1990; Dade 1993).

Sandy sediments, that cover large sections of the continental shelves (Emery 1968), have relatively high permeabilities that permit solute exchange by means of advective transport of water across the sediment water interface. Solute distributions in sands suggest that this pore-water advection can reach down to several centimeters sediment depth (Rutgers van der Loeff 1981; Lohse et al. 1996; Marinelli et al. 1998). Advective pore-water flows are driven by pressure gradients that develop when unidirectional or oscillating bottom water flows are deflected by topographical features of the sediment surface (e.g., Savant et al. 1987; Huettel and Gust 1992; Precht and Huettel 2003). As a result, bottom water percolates through the pore space along curved paths from high pressure areas, located up- and downstream- from the center of the roughness element, towards a central low pressure area close to its top (Huettel and Gust 1992; Huettel et al. 1996). Exposing sands with stained pore-water to unidirectional flow, Huettel and Gust (1992) demonstrated that advection takes place already at minute roughness elements. In the presence of 1 mm high elevations (areal density 17 m^{-2}) the dye flux was almost doubled as compared to molecular diffusion. Mounds of 1-2 cm height caused advective solute release that exceeded diffusion by a factor of 3 - 6.

Several flume investigations demonstrated the effect of current-induced pore-water advection on biogeochemical zonation and processes in sandy sediments. Advective supply with oxygen can increase oxygen penetration into the sediment and enhance oxygen uptake rates (Forster et al. 1996; Ziebis et al. 1996b; Precht et al. 2004). Suspended organic particles (e.g., unicellular algae, bacteria, and organic detritus) may be transported several centimeters into the sand by means of advection and potentially provide the sediment biota with fresh particulate organic matter (Pilditch et al. 1998; Huettel and Rusch 2000; Fries and Trowbridge 2003). Waste products, such as reduced electron acceptors and remnants of organic matter mineralization (e.g., nutrients and heavy metals), are efficiently removed by upwards directed pore-water flows (Huettel et al. 1998). Pore-water advection can thus be expected to increase the metabolic activity of sands leading to rapid mineralization of organic matter in these sediments (Boudreau et al. 2001).

The significance of advection at a specific site will largely depend on the prevailing conditions with respect to current velocity, roughness element height, and permeability (Fehlman 1985; Huettel and Gust 1992; Rutherford et al. 1995). In situ measurements of these parameters are needed in order to assess the potential effects of pore-water exchange in natural environments, to set up future experimentation (e.g., in situ chamber incubations) according to typical natural settings, and to provide information that is crucial for modeling of transport and biogeochemical reactions in sands. So far, in situ topography measurements with a vertical resolution in the millimeter range, have been largely restricted to silty and muddy sediments (e.g., Swift et al. 1985; Smith et al. 1986; Wheatcroft 1994; Glud et al. 2003; Røy et al. 2005). Studies on topographies at sandy sites, aiming mostly at the quantification of sediment transport, focused on larger structures of physical origin and neglected biogenic roughness elements (e.g., Langhorne 1982; Amos et al. 1999; Li and Amos 1999). In order to quantify advective transport, however, bioroughness has to be included in the measurements, as it is an ubiquitous element of sea bed topography that can result in significant pore-water advection (e.g., Cadée 1976; Grant 1983; Huettel 1990; Ziebis et al. 1996b).

The present study focuses on small scale roughness elements of permeable sands with heights ≥ 1 mm and maximum horizontal dimensions in the small decimeter range.

Two different methods were used to measure topographies at three sublittoral sites with different permeabilities. In combination with concurrent flow recordings the topography data are used to assess of the rates of pore-water advection and solute transport at the respective sites.

Material and Methods

Investigations were carried out during four cruises in June, September, October, and November 2001, seawards of the barrier island of Spiekeroog in the southeastern North Sea (fig. 1, exact cruise dates are found in tab. 2).

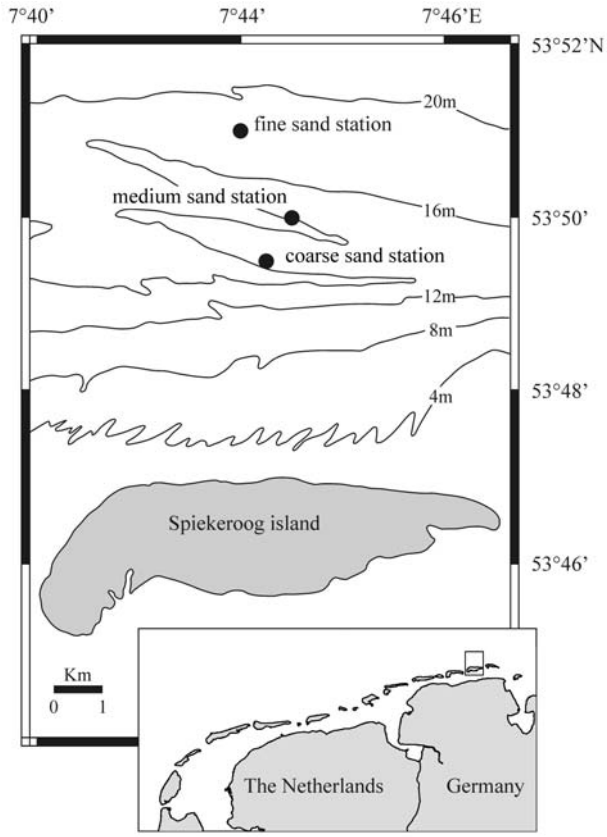

Fig. 1. Upper graph: location of the three stations and the bathymetry of the area (redrawn after Antia 1993). Lower right graph: The chain of West and East Frisian Islands. The box marks the area around the Island of Spiekeroog.

The study area is located in a mesotidal high-energy environment with a mean tidal range of 2.5 m (Postma 1982), resulting in strong along-shore tidal currents reversing direction every 6 h (Antia et al. 1995). Topography mapping and current measurements took place at three stations located within a radius of 1.4 km. Despite their close proximity, the sediments at the three stations differed considerably with respect to grain size and permeability (tab. 1). Following the classification of Wentworth (1922) the stations are subsequently referred to as fine-, medium-, and coarse sand station (fig. 1).

Water temperature in June, September, October, and November was 13, 16, 14, and 11° C, respectively. Salinity was ~ 33 psu at all cruises. For more detailed information on site characteristics see Janssen et al. (2005) and Ehrenhauss et al. (2004).

Tab. 1. General station data.

			Bulk sediment characteristics [1)]				
Sediment type	Position	Water depth (m)	Permeability (10^{-11} m^2)	Median grain size (μm)	Sorting[2)]	Porosity	TOC (% DW)
Fine	53° 51.0' N 7° 44.0' E	19	0.30 ± 0.17 (14)	163 ± 20 (3)	0.58 ± 0.03 (3)	0.37 ± 0.01 (3)	0.12 ± 0.02 (6)
Medium	53° 50.0' N 7° 45.0' E	16	2.63 ± 0.33 (7)	299 ± 8 (3)	0.46 ± 0.02 (3)	0.34 ± 0.01 (3)	0.02 ± 0.002 (6)
Coarse	53° 49.5' N 7° 44.5' E	16	7.46 ± 1.34 (13)	672 ± 78 (3)	0.80 ± 0.11 (3)	0.33 ± 0.01 (3)	0.03 ± 0.01 (6)

[1)] Averages ± s.d. and number of replicate cores (in parentheses)

[2)] Sorting (i.e. the graphic s.d.) in Φ notation

Topography mapping methods

Sediment surface mapping took place by acoustic altimetry and, in September and October, additionally by laser scanning. The acoustic altimetry yielded height measurements at a single spot while the laser scanning determined heights along a line of up to 300 mm length. Both measuring devices were attached to a programmable horizontal drive, similar to the profiling unit described by Wenzhöfer et al. (2001). All instruments were mounted to a triangular frame as shown in fig. 2. At the seafloor, the horizontal drive moved the devices in 5 mm steps along a distance of 500 mm. Each deployment thus resulted in 500 mm long, acoustically determined profiles and in equally long and up to 300 mm wide surface scans. The instrument was lowered to different spots at the seafloor of the respective stations. Upon lowering, a current vane aligned the frame (i.e., the profiling direction) to the main current. Average deviation of the profiling direction and the direction of the near-bottom flow (recorded previous to topography mapping; see below) was 8.0 ± 17.3 ° (n = 58).

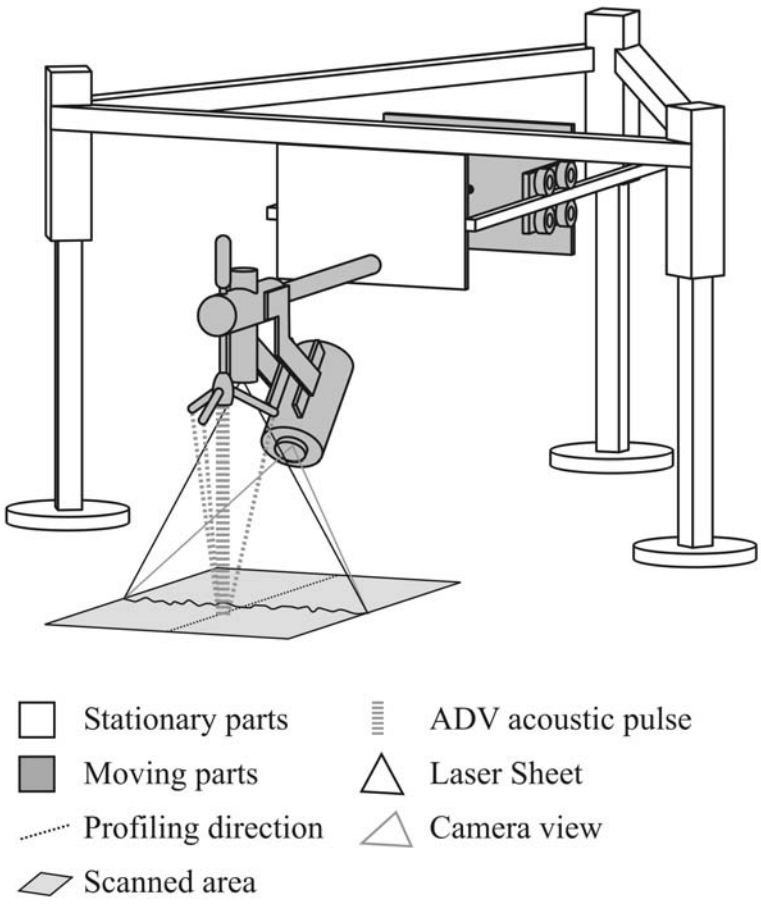

Fig. 2. Schematic drawing of the instrument used for topography mapping and current velocity measurements. The motor and the threaded rod used to move the linear drive are hidden behind the front plate.

Acoustic altimetry was performed with a 10 MHz Acoustic Doppler Velocimeter (ADV; 'Ocean Probe' ADVfield, Nortek AS), that measures current velocities in three dimensions within a small cylindrical sampling volume (~ 6 mm ø × 6 mm), located 100 mm below the probe. When operating in the "distance to boundary" mode the ADV infers distance information from the time acoustic pulses need to travel from the central transducer to the seafloor and back to the three surrounding receivers. The acoustic "footprint" of the method is at least equal to the transducer size (ø 6 mm). The ADV was connected to a computer on board of the ship via RS232 interface. Distance to boundary readings were initiated at each position of the horizontal drive by means of a

LabVIEW routine (National Instruments Corp.). Blank readings due to measurement failure (< 3 % of all readings) were interpolated from the neighboring heights. In order to evaluate the suitability of the ADV to resolve sediment surface topographies, test mapping was performed with a submerged cast of natural sand ripples of known dimensions.

The laser scanning technique was based on the principle described by Røy et al. (2002) and Glud et al. (2003). A < 1 mm wide laser line (1 mW, 635 nm line-generating diode laser) was projected vertically onto the seafloor. In video images, taken at an angle of 45° relative to the laser sheet, seafloor elevations were represented by upward shifts in the location of the laser line. The analog video camera (Mariscope Micro monochrome 1/3" CCD, 4.5 mm lens) was connected to a S-VHS video recorder on board of the ship. On-shore processing of the video images taken at each position of the horizontal drive included the following steps: (1) digitizing and conversion to 720 × 576 Pixel 8-bit bitmaps via a MiniDV recorder and video editing software iMovie™ 2.0.1 and QuickTime™ 5.0.2 (Apple Computer Inc.); (2) averaging of sequences of 10 images; (3) image rectification using the "spherize" and "perspective" tools of the software PhotoShop® (Adobe Systems Inc.); (4) determination of the laser line position for each column at subpixel accuracy by the use of a three point estimator based on the known gaussian intensity distribution across the line (Raffel et al. 1998) with a LabVIEW routine. For calibration, images of a submerged line grid (5 × 5 mm spacing), mounted in the plane of the laser sheet were taken and processed similarly. In the part of the original picture where the laser line was located, one pixel represented a width and elevation height of 0.43 mm × 0.49 mm (uppermost, central pixels) to 0.61 mm × 0.77 mm (lowermost, distant pixels). After image rectification these differences in pixel sizes were reduced to < 3 % (2.49 mm × 0.43 mm and 2.56 mm × 0.44 mm, respectively). A slight persisting curvature of horizontal gridlines (~ 3 pixels or 1.5 mm across the image width) was removed by subtracting the respective vertical position of the gridline from the laser line position. Laser line pixel coordinates were then transformed into sediment surface coordinates by means of vertical and horizontal scaling factors (0.433 mm pixel^{-1} and 2.5 mm pixel^{-1}, respectively). In several of the topography scans that were assembled from the resulting laser line profiles, outliers

(i.e., singular data points that differed by more than 10 mm from the neighboring heights) were observed in the distant regions where the laser line intensity was reduced. These regions were cropped, reducing the surface width of the scans. Remaining outliers in the inner region (< 1 % of all data points) were replaced by their nearest neighbors.

Roughness element descriptors

Heights and widths of roughness elements or peaks were determined in profiles that were measured with the ADV or, if available, in 3 parallel, 65 mm spaced profiles that were extracted from each laser surface scan. The central profile was located at the same position where the ADV measurements took place. To account for a possible pitch of the frame position and a general slope of the terrain, the raw profiles were adjusted by subtracting the slope of a linear regression that was fitted to the entire profile. To prevent misinterpretation of measurement noise as roughness elements, the topographies were smoothed by calculating running averages from 5 adjacent data points before peak determination. The peak height was defined as $(h_1 + h_2) \times 0.5$, with h_1 and h_2 being the average vertical distances between the local maximum and both adjacent local minima (fig. 3). The horizontal distance between the adjacent local minima represented the peak width. To avoid that minute peaks obscure underlying larger roughness elements, local maxima were rejected if they protruded less than 1 mm from the adjacent minima. A local maximum – or minimum – was only considered if it represented the highest – lowest – observation in 5 consecutive data points, respectively, and if it was separated by a horizontal distance of more than 5 mm from the previous minimum – or maximum. Finally intermediate maxima – or minima – were rejected if they were surpassed by their neighboring maximum – or minimum, respectively. In cases where pronounced ripples represented the dominant roughness elements, the orientation of the crests relative to the bottom flow was determined visually in contour plots of the surface scans and related to current measurements.

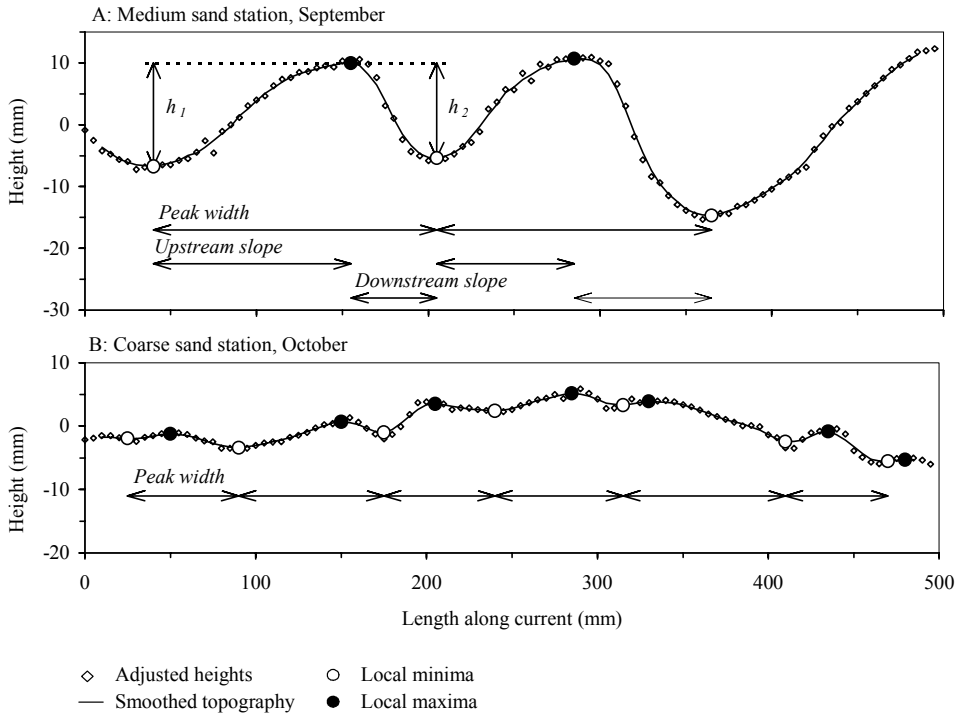

Fig. 3. Two examples of peak detection in the presence (upper graph) and absence of ripples (lower graph). Note the asymmetry of the ripple cross-sections.

Current measurements

In order to describe the current regime in the working area, recordings of near-bottom flow and free flow velocity 4 meters above bottom have been performed with the ADV. Near-bottom flows were recorded for 1 - 7 min at 25 Hz right before mapping the seafloor topographies (n = 58; 3 h total recording time). The average distance of the ADV sampling volume to the sediment surface (± s.d.) was 15.1 ± 4.3 cm. The horizontal component of these measurements is subsequently referred to as $U_{15,}$ with $\overline{U}_{15}$ denoting the time averaged horizontal flow over the time course of the respective deployments. Free flow velocities were measured with the same frame, hanging at a distance of ~ 4 m above the seafloor and are subsequently referred to as U_{400}. Four time series of U_{400} were recorded in June and September at 1 Hz covering a total time of 24 h.

To obtain "typical" current velocities for the working area, measurements of $\overline{U}_{15}$ and U_{400} were related to currents that were modeled for the periods of the respective cruises by an established North Sea current model (Federal Maritime and Hydrographic Agency of Germany) for the same area (53° 50' N, 7° 45' E). These are calculated routinely one day in advance at 15 min temporal resolution for three layers representing surface- (0 m), midwater- (10 m) and near-bottom flows (19m) and account for wind driven currents based on the latest wind forecast of the German Meteorological Service.

Estimates of the shear velocity (u_*) were calculated from the absolute intensity of vertical velocity fluctuations in the near-bottom flow recordings according to Kim et al. (2000). This close to the bed, the shear stress within the water column only varies slightly from bottom stress. The stress (τ) can be estimated from $\tau = 0.9 \times \overline{w'^2}$, where $\overline{w'^2}$ is the variance of the vertical velocity fluctuations. From τ, u_* can be calculated as $u_* = \sqrt{\tau/\rho}$ with ρ being the water density.

Results

Validation and comparison of ADV topography profiling and laser surface scanning

The ADV distance to boundary readings were able to resolve the main features of the ripple cast (fig. 4, upper left graph) but a considerable scatter existed between replicate measurements. The relation between ADV measurements and heights obtained with the measuring machine revealed that the ADV slightly underestimated the vertical dimension of the ripples by ~ 5 % (see trendline in upper right graph of fig. 4).

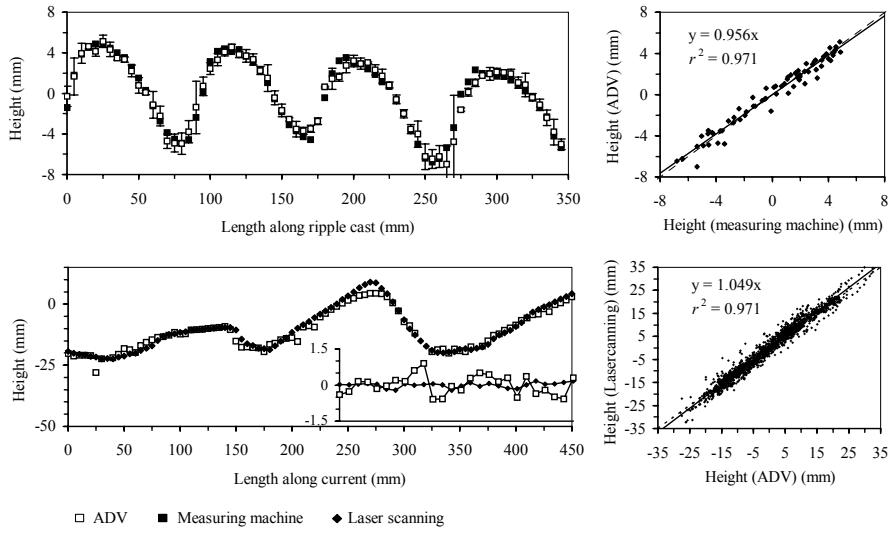

Fig. 4. The upper left graph shows the surface profile obtained with the ADV (average ± s.d. of three measurements) along a cast of an intertidal ripple field (glass-fiber reinforced resin with sand coating) compared to heights as measured mechanically with a coordinate measuring machine at < 0.1 mm accuracy (filled squares). The lower left graph gives an example of a sediment surface profile at the medium sand station obtained with the ADV (open squares) and the laser scanner (filled diamonds; profile extracted from the center line of the surface). The small insert shows the variability of 26 replicate measurements of the respective instruments obtained at the fine sand station without moving the sensors. The upper and lower right graph compare ADV heights to mechanically measured heights (n = 70), and in situ heights as determined with the laser scanner and the ADV (n = 1733 from 21 profiles). The equations of the linear regressions are given in the graphs (solid line), the dotted line marks a slope of 1.

A comparison of all in situ height measurements of the ADV and the laser-scanner is shown in the lower panel of fig. 4. ADV height measurements covered a ~ 5 % smaller

range than laser measurements (see trendline in the lower right graph of fig. 4). This confirms the tendency of the ADV to underestimate the vertical dimensions of roughness elements and indicates that the laser scanning yielded accurate results. In addition, laser measurements were less noisy (lower left graph of fig. 4). This is confirmed by replicate measurements of a single sediment patch obtained by both methods (insert in the lower left graph of fig. 4). The total range of replicate measurements (and their standard deviation) amounted to ± 0.19 (± 0.10) mm and ± 0.75 (± 0.41) mm for the laser scan and the ADV, respectively (n = 26).

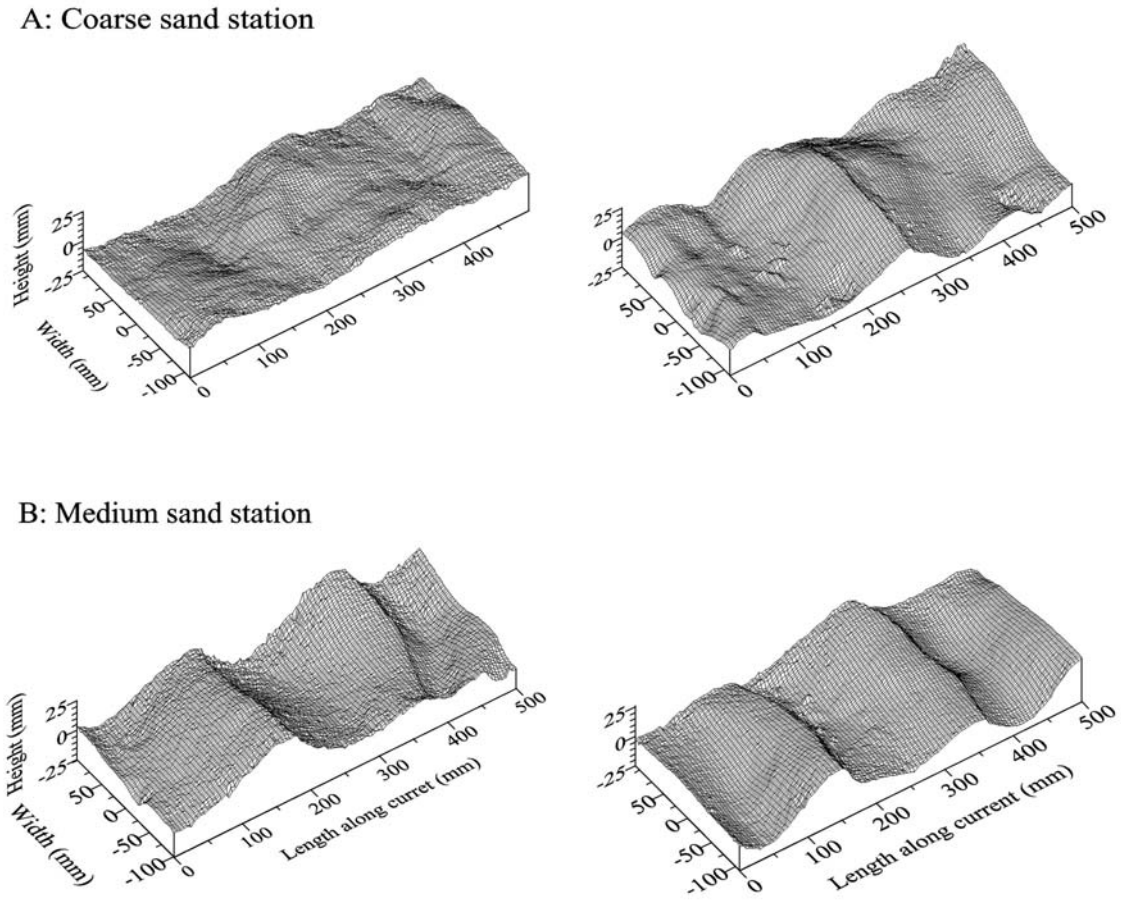

Fig. 5. Sediment surface scans obtained during in September 2001. All surfaces with 2 × vertical exaggeration.

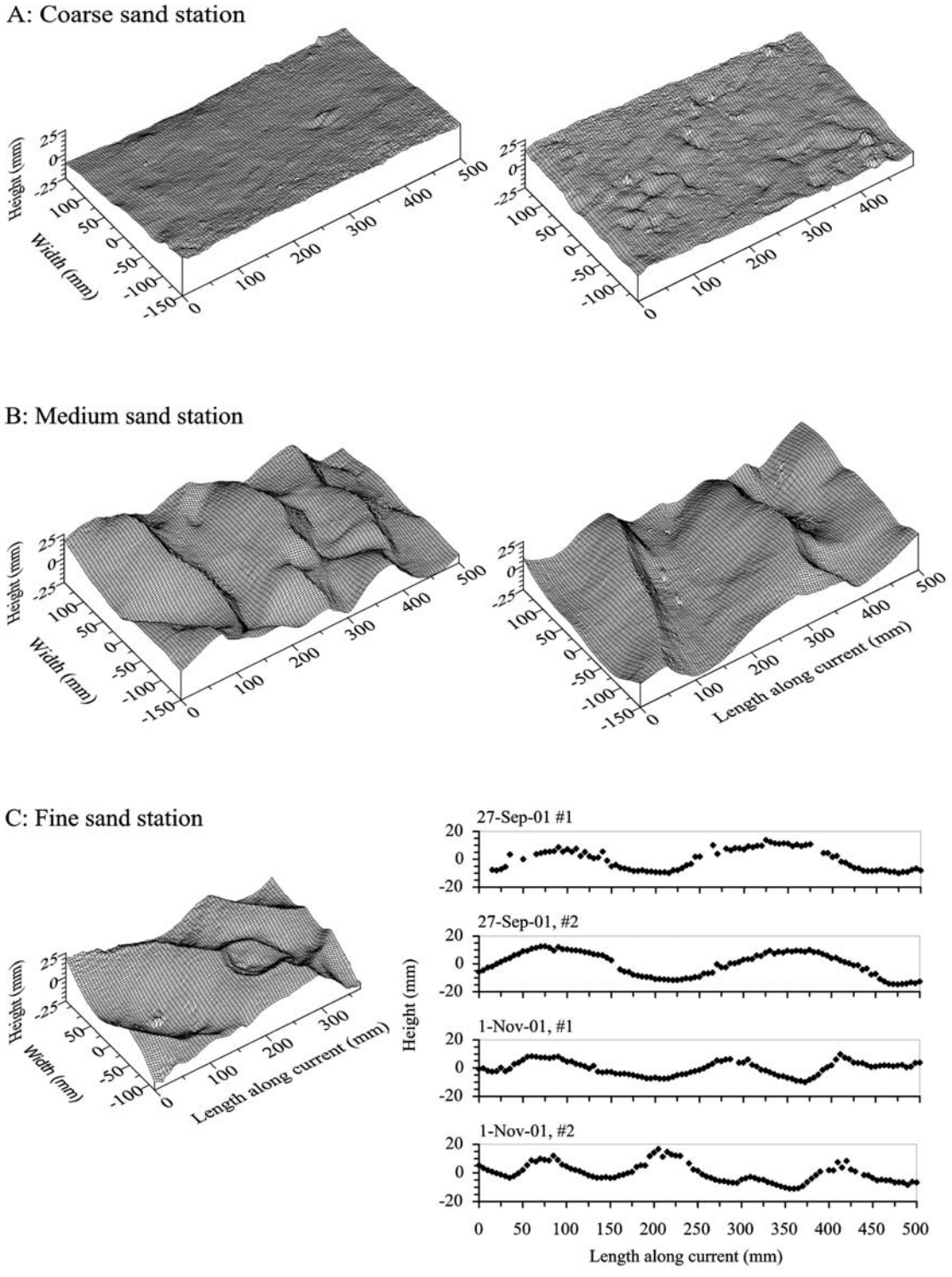

Fig. 6. Sediment surface scans obtained in October 2001. All surfaces with 2 × vertical exaggeration. Four ADV obtained sediment surface profiles obtained in September and November 2001 on the fine sand station are shown in the lower panel.

Natural sediment surface topographies

Examples of sediment surface topographies obtained during the cruises in September and October are shown in fig. 5 and 6. Conspicuous roughness elements were present in all scanned surfaces but differed between stations. On the medium sand station, distinct ripples were always present (panel B in fig. 5 and 6) while they were less obvious or even absent in the scans obtained at the coarse sand station (panel A in fig. 5 and 6, respectively). On this station, on the other hand, small individual and irregularly arranged roughness elements seemed to be particularly abundant. Especially in October, the entire surface roughness at the coarse sand station was provided by discrete elevations and depressions (panel A in fig. 6).

A single surface scan was obtained at the fine sand station confirming the presence of ripples for this site, too (left graph of panel C in fig. 6). Further topographical information was restricted to ADV profiles. Regularly spaced roughness elements, however, were frequently observed in the profiles (see examples in upper panel of fig. 6), which may indicate that ripples were common at this station.

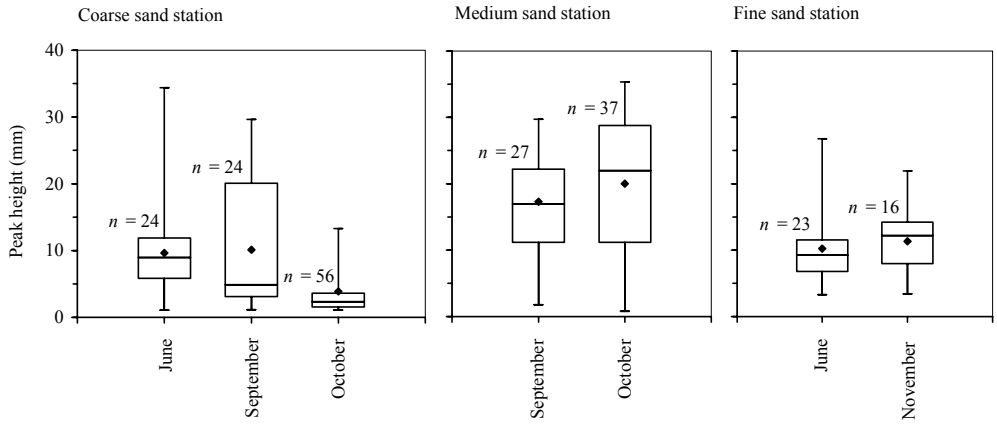

Fig. 7. Roughness element heights at the respective stations and months as detected in profiles obtained with the ADV or extracted from surface scans. The diamond represents the mean, the median is given by the horizontal line. The box marks the upper and lower quartile, the whiskers the total range of values. The total numbers of detected peaks are given in the graphs.

The peak heights at the three stations are shown in fig. 7. Particularly large peaks with heights of up to ~ 35 mm were occasionally observed at the coarse and medium sand station. On average, the most prominent peaks were detected at the medium sand

station with typical heights of 17 - 20 mm (tab. 2). Peak height and width at that station corresponded to ripple height and spacing as virtually all local maxima and minima were located at ripple crests and troughs, respectively. Smallest peak heights with an average of 3.1 mm occurred at the coarse sand station in October, when ripples were absent and discrete roughness elements prevailed.

Tab. 2. Roughness element measures as obtained in profiles from the three stations at the respective cruises.

	Roughness element measures (mm; average ± s.d.)								
	Fine sand station			Medium sand station			Coarse sand station		
Date (Vessel)	Height	Width	Profiles [1] (*n*)	Height	Width	Profiles [1] (*n*)	Height	Width	Profiles [1] (*n*)
07 - 15 June (HEINCKE)	10.4 ± 5.8 (*n*=23)	128 ± 45 (*n*=23)	9 + 0				9.7 ± 6.8 (*n*=24)	130 ± 45 (*n*=24)	10 + 0
24 - 30 September (HEINCKE)				16.8 ± 7.9 (*n*=27)	154 ± 40 (*n*=27)	3 + 12	10.7 ± 9.9 (*n*=24)	149 ± 75 (*n*=24)	1 + 12
22 - 27 October (UTHOERN)				20.1 ± 10.9 (*n*=37)	157 ± 67 (*n*=37)	0 + 18	3.1 ± 2.4 (*n*=56)	111 ± 53 (*n*=56)	0 + 21
10 - 13 November (UTHOERN)	11.5 ± 5.5 (*n*=16)	123 ± 34 (*n*=16)	6 + 0						
All cruises	11.0	125		18.4	155		7.8 ± 4.1	130 ± 19	

[1] The number of profiles obtained at the respective cruises with the ADV (first number) and with the surface scanner (second number). 3 Profiles have been extracted from each scanned surface (refer to text for details).

Surface scans at the medium sand station were all obtained around maximum flood tide. The average direction of the ripple crests at the medium sand station was close to perpendicular to the measured main near-bottom flow directions with a deviation of 15.4 ± 17.3 ° (average ± s.d. of all ripples scanned in September and October; $n = 28$). The cross-section of the ripples often showed a slightly asymmetric, tooth-shaped form with a relatively steep downstream slope (fig. 5, 6, and 3 A). This corresponds to upstream slopes of the ripples being longer than the downstream slopes (84 ± 32 and 71 ± 32 mm, respectively; $n = 64$).

Current regime

Free-flow recordings (U_{400}) show a clear tidal periodicity and are in good agreement with model results (fig. 8).

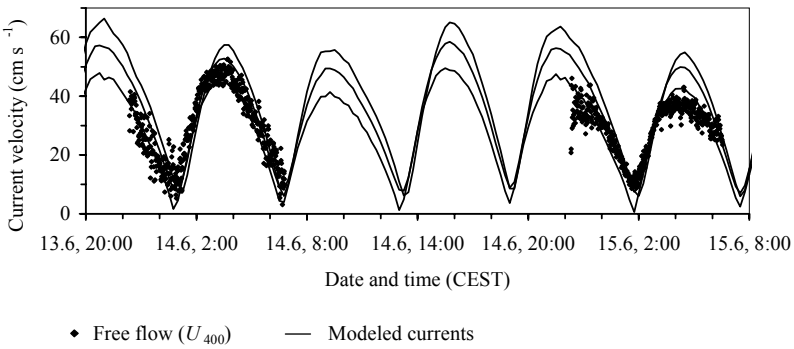

Fig. 8. Two examples of free flow velocities (U_{400}) recorded with the ADV 4 m above the sea bed at 1 Hz (diamonds) in comparison to modeled currents (lines) (Federal Maritime and Hydrographic Agency of Germany). The upper, medium, and lower line represent surface (0 m), midwater (10 m), and near-bottom flows (19m water depth).

A close relation between all measured currents and model results for the same points in time confirms that the current regime is properly described by the model (graph A of fig. 9). Transformation of the modeled current velocities by means of the linear regression equation as given in the graph results in an average free-flow velocity of 32.2 cm s^{-1} for all cruises (tab. 3).

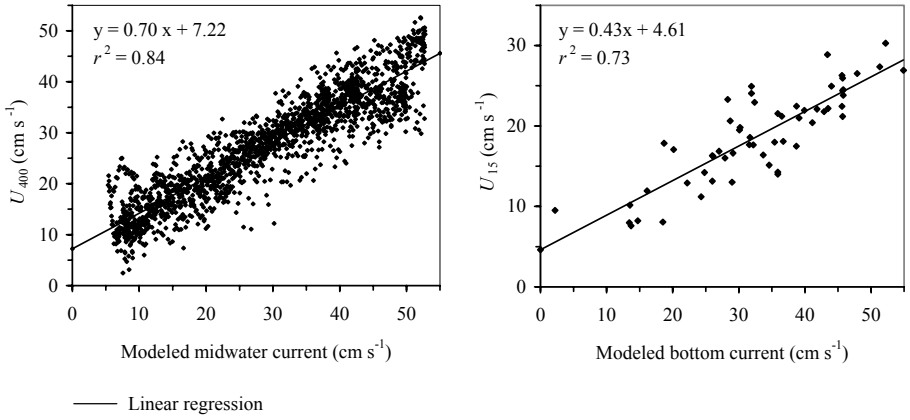

Fig. 9. ADV obtained free-flow- (U_{400}) (left graph) and near-bottom flows ($\overline{U}_{15}$) (right graph) vs. currents modeled for the midwater layer (left graph) and the bottom water layer (right graph). The equations of the linear regression lines are given in the graphs. The U400 values represent 1 min moving averages, $\overline{U}_{15}$ values are averaged over the time course of the respective recordings.

Tab. 3. Typical hydrodynamic conditions estimated from a combination of ADV measurements and model-obtained midwater- and bottom flow velocities.

Month (Vessel)	Free-flow [1] (cm s^{-1})	Near-bottom flow [1] (cm s-1)	Shear velocity [2] (cm s^{-1})
June (HEINCKE)	35.2	19.1	1.65
September (HEINCKE)	30.4	16.4	1.46
October (UTHOERN)	31	16.7	1.48
November (UTHOERN)	32.4	17.6	1.54
All cruises [3]	32.2 ± 2.2 (s.d.)	17.4 ± 1.2 (s.d.)	1.53 ± 0.09 (s.d.)

[1] Average velocities calculated from current model results adjusted according to ADV measurements (U_{400} and $\bar{U}_{15}$; refer to text for details)

2) Expected shear at average near-bottom flow velocity

3) Averages of all cruises (± s.d.)

Recordings of near-bottom flow (U_{15}) regularly depicted an oscillating component with periodicities of a few seconds that was superimposed on the steady, tidal current, (fig. 10).

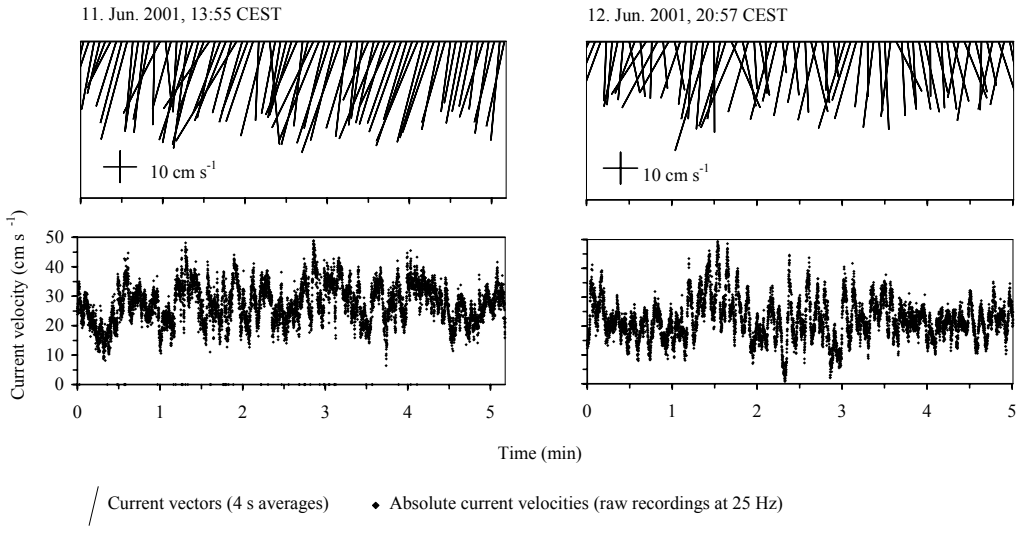

Fig. 10. Two examples of near-bottom flow recorded with the ADV at 25 Hz at the fine and medium sand station (left and right graphs, respectively). The stick plots (upper graphs) give 4 second averages of current heading and speed relative to the instrument (vertical lines represent currents that are aligned with the surface profiling direction). The diamonds in the lower graphs represent the absolute values of the individual readings.

The average absolute bottom flow velocities ($\overline{U}_{15}$) ranged between 7.6 and 30.3 cm s^{-1} and correlated well to the modeled current velocity (right graph of fig. 9). Transformation of the modeled current velocities as described above resulted in an estimated average bottom flow of 17.4 cm s^{-1} for all cruises (tab. 3) with peak current velocities of up to 35 cm s^{-1} at half tide.

The shear velocity (u_*) as obtained by the TKE method was found to generally scale with the near-bottom flow (fig. 11). In some cases shear velocities that are based on current recordings obtained within the same series of deployments appear to be grouped (e.g., 12th of June, 25th of October, 26th of October). This indicates that shear depends not only on the average near bottom flow velocity. Additional factors could be differences in wave action (orbital motion increasing the variability of W and hence u_*) and differences in roughness (increasing the hydraulic roughness, z_0 and thereby u_*). The latter effect could explain differences between u_* obtained from the recordings at the 25th of October on the coarse sand station and those of the next day that originate from the fine sand station. Based on the linear regression in fig. 11 (excluding the values in parentheses), the estimated average near-bottom flow of 17.4 cm s^{-1} resulted in a shear velocity of approximately 1.53 cm s^{-1} (grey line).

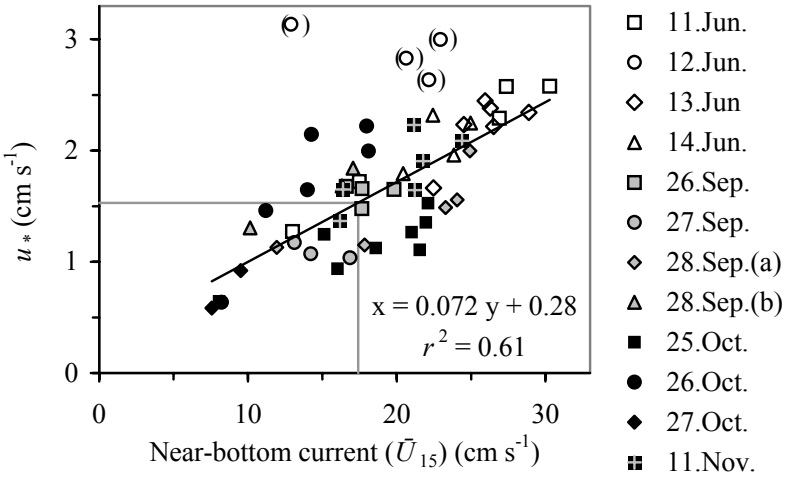

Fig. 11. Comparison of shear velocities calculated from the fluctuations of the vertical current component to the average horizontal component of near-bottom flows ($\overline{U}_{15}$). The different markers tag data that were obtained within the same series of measurements.

Discussion

Evaluation of the topography mapping methods

Both the acoustic altimetry with the ADV and the laser scanning were successfully deployed on the North Sea Shelf and proved to be suited for in situ topography mapping in sandy areas. The instrumentation needed for both methods is either commercially available (ADV, video camera, line laser) or easy to construct (frame, horizontal drive).

Despite the fact that the ADV is optimized for measurements of current velocities it was able to resolve roughness elements with amplitudes in the millimeter to centimeter range. A strong advantage of the ADV is that measurements of currents and topographies may readily be obtained at the same site. Additionally, ADVs are standard instruments that already exist in many places. The main purpose of the distance to boundary mode is to avoid sensor positions where acoustic backscatter of the boundary reduces the current measurement quality ("weak spots"). The slight tendency to underestimate the roughness element height might result from the configuration with a central transducer and three surrounding receivers. If acoustic backscatter from adjacent areas of sloping surfaces, especially in troughs, arrives earlier at one of the distant receivers than the backscatter of the targeted spot this would lead to distance underestimations. A limitation of all acoustic altimeters is that they provide only single spot measurements and that they average over a relatively large surface area.

The maximum spatial resolution obtained by laser scanning is only limited by the thickness of the laser line. At an appropriate camera resolution and viewing distance the horizontal resolution can reach down to 500 micrometers, while the vertical resolution may be even smaller (Røy et al. 2002). The configuration used in this study, with pixel heights corresponding to vertical distances of well below 1 mm and subpixel accuracy for the determination of the laser line position, results in a vertical resolution of better than one millimeter. This was confirmed by the replicate measurements at a single sediment patch.

Processing of the laser scanning data is user friendly. Unlike photogrammetry, an optical approach that has also been used to obtain seafloor topographies (e.g., Swift et al. 1985; Smith et al. 1986), the laser scanning requires no sophisticated orientation and

triangulation operations. Calibration and the transformation of pixel coordinates to absolute heights are straightforward, and image rectification is readily performed at adequate accuracy by standard image processing tools. Another advantage as compared to photogrammetry is that laser scanning still works at relatively low visibilities, which is crucial in turbid shelf environments.

Topographies at the three sites

Sediment topographies obtained at the medium and at the fine sand station were dominated by ripples, i.e., roughness elements of physical origin. As indicated by their cross-current orientation and the asymmetry of the ripple cross-sections, the ripples are formed by tidal currents rather than waves (Tanner 1967). This indicates that tidal currents are sufficiently strong to permanently maintain ripples at the medium sand station. Ripples are therefore expected to be permanently present at that site, except when eroded during storm events (Arnott and Southard 1990). Unfortunately no scans have been obtained at ebb currents. Therefore it remains unclear if the ripple asymmetry in direction of the flood tide persists during ebb current or if the crests change shape during each tidal cycle.

The irregularly arranged surface elevations and depressions that were characteristic for the coarse sand station are attributed to the sediment reworking activity of macrofauna. This process is well-known to produce distinct topographical features (Grant 1983; Smith et al. 1986; Ziebis et al. 1996a). Peak heights associated with these bioturbated beds were much smaller than those of the rippled surfaces in this study. This agrees to results obtained in a variety of shelf environments showing that roughness of rippled surfaces usually is higher than that of isotropic sediment topographies of presumably biological origin (Briggs 1989). Such a tendency, however, should not be generalized as the roughness introduced by bioturbation may differ largely even at a single sediment patch (Wheatcroft 1994) and certain benthic organisms such as lugworms or calianassoid shrimp produce topographical features of similar or even higher amplitudes than the ripples observed in this study (Huettel 1990; Ziebis et al. 1996a).

A possible explanation for the reduced abundance of ripples at the coarse sand station would be that tidal currents remain subcritical, i.e., that the large sand grains at that site are not transported on a daily basis. Based on the empirical relationship between Shields erosion threshold θ_t (representing a measure of critical shear stress) and the Yalin parameter Ξ (a grain size dependent measure of particle inertia), grains of up to 380 µm are expected to be moved at a u_* of 1.53 cm s^{-1}. Grains of a size similar to the median grain size at the coarse sand station, on the other hand, would require shear velocities > 1.8 cm s^{-1} (Miller et al. 1977). It is thus possible that under calm conditions bottom shear is not strong enough (or the period with strong currents is too short) to lead to significant sediment transport and ripple formation. However, the presence of ripples in September shows that they develop at least occasionally at the coarse sand station, probably as a result of a combination of currents and waves as it has also been observed elsewhere (e.g., Amos et al. 1988).

Other than in September not a single ripple was observed in the topographies that were obtained at the coarse sand station in October. While the observed difference between the two cruises may also reflect small scale spatial variability it is nevertheless a strong indication that the topographies were temporally dynamic. This involves not only quantitative differences (like the average roughness element height that was smaller in October) but also the origin of the predominant roughness elements (physical vs. biogenic). It has been previously reported that physically induced topographies vanish in the presence of bioturbating benthic infauna in a matter of days to weeks (Clifton and Hunter 1973; Grant 1983; Wheatcroft 1994). The presence of biogenic structures on the other hand, was also observed to facilitate the (re-) formation of ripples (Fries et al. 1999). While an investigation of temporal dynamic is beyond the scope of this study it is clear that the identification of characteristic topographies requires time series of surface topography measurements.

Scale considerations

The fraction of the existing roughness that is resolved by a given method depends on the resolution and the length scale at which the measurements take place (Thomas 1982). Minute roughness elements with heights of ~ 1 mm, while principally resolved with the

laser scanning, were disregarded by averaging of the raw heights and introduction of size thresholds to the peak definition. This was necessary to exclude misinterpretations of the ADV-scatter as peaks. The limited profiling distance, on the other hand, excluded topographies of larger horizontal scales like dunes or ridges that may only show up as a general slope or curvature of the profiles (compare fig. 3 B). Shoreface-connected ridges in the same area with vertical amplitudes of a few meters and wavelengths of around 1 km (Antia 1994), represent an extreme example of such large scale roughness elements.

Topographical features as they are resolved by this study, fit the size range of roughness elements that may result in significant pore-water advection with strong effects on solute exchange and biogeochemical processes (Huettel and Gust 1992; Forster et al. 1996; Huettel et al. 1996; Ziebis et al. 1996b; Huettel et al. 1998; Precht and Huettel 2003; Precht et al. 2004). Nevertheless, it cannot be ruled out that roughness elements with wavelengths beyond the profiling length contributed significantly to advective pore-water transport. Estimates of pore-water exchange rates based on the mapped roughness elements will thus most likely be conservative representations of the actual field rates.

Advective exchange across irregular topographies

Pressure differences at distinct roughness elements as they prevailed at the coarse sand station have been investigated by Huettel et al. (1996) in a recirculating flume. Under unidirectional currents at velocities similar to the average near-bottom flow of the working area a difference of ~ 1.6 Pa developed across mounds of 5 mm height. Pressure differences at typical roughness elements at the coarse sand station in October (3.2 mm) thus are expected to be somewhat lower, while differences of > 2 Pa can be expected for the highest roughness elements (13 mm).

An order of magnitude estimate of the corresponding advective exchange rates may be obtained based on the flume study of Huettel and Gust (1992). They determined how an array of 10 mounds (areal density: 17 m^{-2}) intensified the efflux of tracer dye from a sandy sediment with stained pore-waters in the presence of unidirectional flow. From the exponential relationship observed between excess dye fluxes and the height of the

mounds (1, 5, 10, and 20 mm) an advective pore-water exchange of 0.79 L m^{-2} d^{-1} is expected for 3.2 mm high roughness elements. Tab. 4 compiles the experimental settings of Huettel and Gust (1992) and the estimated parameters at the coarse sand station. Multiplication of the above rate with the combined scaling factor results in an estimated pore-water exchange of 58 L m^{-2} d^{-1}.

Tab. 4. Comparison of experimental settings used by (Huettel and Gust 1992) to characteristics at the coarse sand station.

Parameter	Huettel and Gust (1992)	This study	Scaling-factor
Roughness element density	17	81[1)]	4.8
Shear velocity u_* (cm s^{-1})	0.5	1.53	3.1
Permeability (10^{-11} m^2)	1.48	7.46	5.0
All parameters combined			73.5

[1)] Assuming a density of 1 / (average width) ≈ 9 roughness elements per meter in both directions

This approach clearly comprises a number of uncertainties. First it is unknown how the pronounced conical mounds, protruding from a smoothed sandy surface, compare to irregular natural roughness elements. Furthermore the approach assumes that advective exchange scales linearly with both shear velocity and the abundance of roughness elements. This is most likely not valid. Exchange rates have been found to scale exponentially with u_* (Huettel and Gust 1992). Closely arranged roughness elements, on the other hand, may reduce pressure gradients and hence the exchange rates per mound as they can result in “skimming flow” (Nowell and Church 1979) that leads to quiescent areas between obstructions. To be able to estimate exchange rates across the irregularly sculptured surfaces of sands, there thus is a strong need for descriptors of roughness that are meaningful in the context of advection and for model approaches that account not only for height but also for aspect ratios and the abundance of roughness elements.

Advective exchange across rippled surfaces

Advection across rippled surfaces may be estimated by models that were developed for permeable river beds in the presence of dunes (Savant et al. 1987; Rutherford et al. 1995). The two-dimensional analytical model provided by Rutherford et al. (1995) allows an estimate on pore-water velocities, -exchange rates, and -residence times. It applies a sinusoidal pressure distribution with a wavelength similar to the dune spacing and an amplitude that is inferred from ripple height, mean flow velocity and the vertical dimension of the moving water (Fehlman 1985). It is assumed, that roughness elements are aligned perpendicular to the current. This requirement was met by the ripples at the medium sand station for most of the time as ebb- and flood currents are virtually reversed in the area (Antia et al. 1995).

Assuming the presence of a stationary log layer for the near-bottom flow, the mean flow velocities for each distance z to the sediment can be estimated from the typical near-bottom velocity at z = 15 cm (17.4 cm s^{-1}), the typical u_* (1.53 cm s^{-1}) and the von Kármán constant (5.75) (Monin and Yaglom 1971). Averaging over the height of the lowermost 15 cm results in a mean velocity 13.7 cm s^{-1} for this layer. Passing over 18.4 mm high ripples as observed at the medium sand station, this flow would result in a pressure distribution with a half amplitude (p_{max}) of 1.83 Pa (Fehlman 1985), or a pressure gradient of 0.047 Pa mm^{-1} between the 77.5 mm spaced crests and troughs at that station. These pressure gradients, in turn, lead to pore-water circulation at maximum velocities of ~ 6 mm h^{-1} (eq. 9 d in Rutherford et al. 1995).

Strong evidence for the presence of pore-water advection at the medium sand station is provided by an 18 h oxygen distribution time series (fig. 12 B). The series consists of 55 consecutive vertical oxygen profiles obtained with an oxygen microelectrode mounted to a pre-programmed profiler unit as described by Reimers (1987). The profiler was attached to a frame similar to the one used for topography mapping (fig. 2) and was lowered and recovered by means of a rope with an attached surface marker buoy. Oxygen concentrations are given relative to the oxygen content of the overlying water. The location of the sediment surface in the central panel in fig. 12 as shown by the black line corresponds to the vertical position in the profile where

oxygen concentration started to decrease. The white line marks the oxygen penetration depth, the sediment depth where oxygen reached 1 %. In cases where profiling failed to reach the oxygen penetration depth (between 80 and 320 min) the penetration depth was assumed to equal the maximum profiling depth.

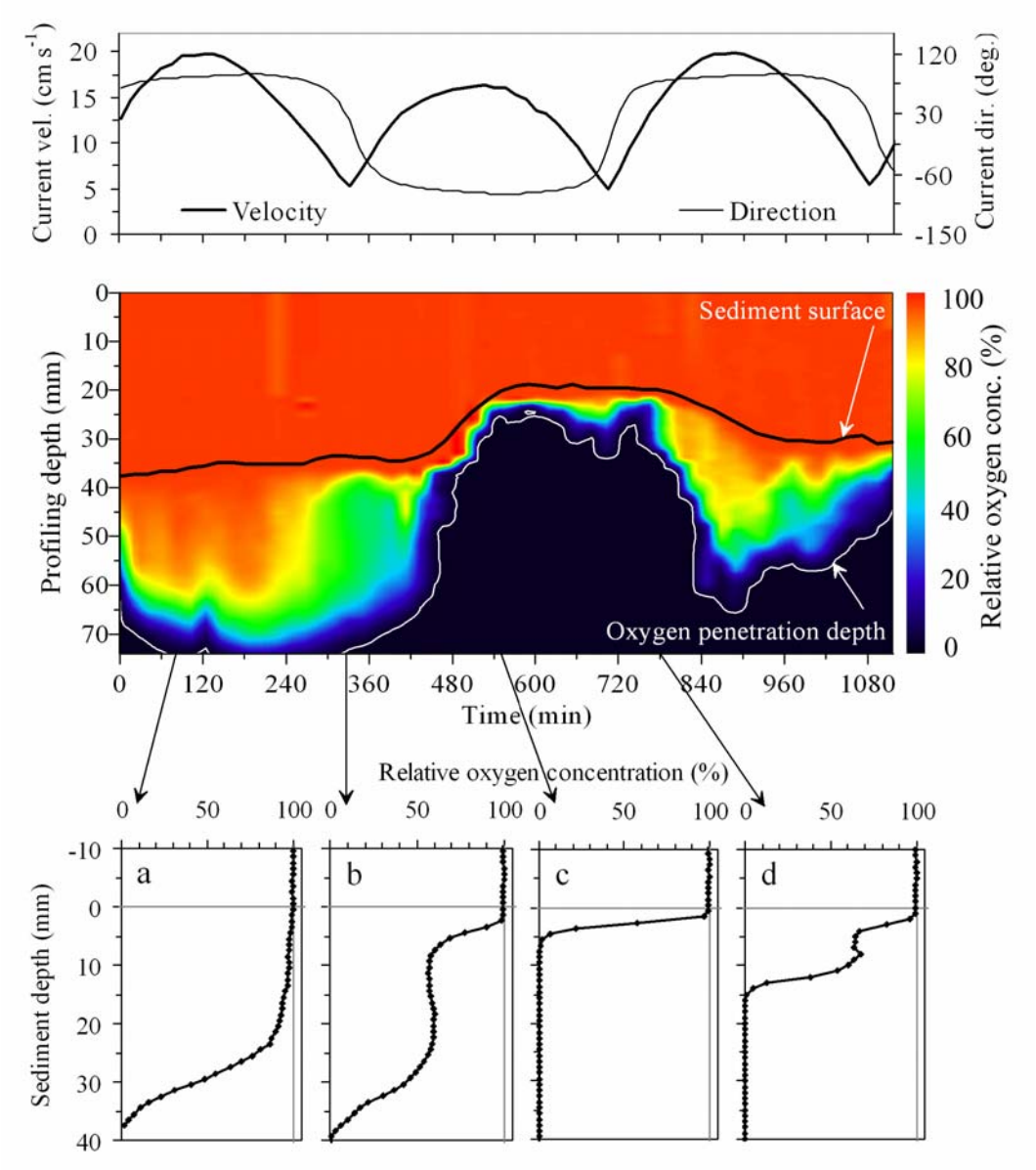

Fig. 12. 18 h time series of sediment oxygenation at the medium sand station (55 consecutive in situ oxygen microsensor profiles). Four characteristic profiles are shown in the lower panel. The arrows refer to the time at which the profiles have been measured. The upper graph shows the velocity and heading (black and grey line) of modeled near-bottom flows (velocity corrected according to right graph of fig. 9).

The vertical position of the sediment surface varied by 19 mm during the deployment. Oxygen penetration depth covered a range of 5 to > 40 mm below the sediment surface and appeared to be correlated to the sediment surface position. Particularly deep oxygen penetration took place when the surface position was low and vice versa. Profiles a and c in the lowermost panel of fig. 12 show the large differences in penetration depth. A sigmoid shape with the steepest gradient well below the surface, as it was generally observed in the profiles, is considered an indication of advection (Revsbech et al. 1980; Lohse et al. 1996). Further indications of advective transport are observed in profiles b and d: De-oxygenation seems initially most pronounced in the top 10 mm of the sediment, i.e., in close proximity of oxygen-rich bottom water (b). The subsequent increase in penetration depth, on the other hand, seems to start well below the surface with an inflow of oxygenated pore-water (d).

The changing vertical position of the sediment surface indicates the presence of an elevated structure migrating below the profiler. Around 760 min the elevation starts to disappear. As the current direction reversed around ~ 720 min the roughness element probably moved away in the direction where it initially came from. The migrating roughness element proved to be relatively large (e.g., a ripple) as a similar elevation was concurrently detected below a second sensor mounted at a horizontal distance of approximately 120 mm (data not shown).

A low pressure region is expected to be present close to the upper part of the elevation (Huettel and Gust 1992). The resulting upwelling of reduced pore-water explains the simultaneous reduction in oxygen penetration depth (lowermost panel of fig. 12). At the time the elevation started to disappear, oxygenation resumed indicating the reestablishment of a high pressure area. Particularly fast and pronounced oxygenation and de-oxygenation at ~ 120, ~ 500, and ~ 860 min was probably supported by peak current velocities taking place around the same periods in time. Similar changes in oxygen distribution were observed in flume experiments below moving ripples under oscillating bottom flows (Precht et al. 2004) and around stationary mounds after reestablishment of unidirectional flow (Ziebis et al. 1996b).

If advection accounted for the observed oxygen dynamics, they should be reduced at the less permeable fine sand station. A similar time series of oxygen microprofiles

obtained at that station did indeed depict much less variability (data not shown). Despite a similar change in the sediment surface position (17 mm total range) oxygen penetration depth changed by only 13 mm throughout the deployment. In addition, oxygen penetration in the time series was generally shallower (on average 9.1 mm as compared to > 26 mm in the medium sand). Theoretically, the reduction in depth and variability of oxygen penetration could also be attributed to an intensified biogeochemical sediment activity that keeps the penetration depth shallower even in presence of significant pore-water advection. This is, however, contradictory to results from chamber flux studies at the same stations indicating similar activities but higher advective exchange and deeper oxygen penetration at the medium as compared to the fine sand station (Janssen et al. 2005).

Pressure gradients across roughness elements at the medium sand station can thus be expected to result in a significant advective supply of oxygen to the sediment. An estimate of this supply due to the observed ripples can also be inferred from the above model. At the given permeability, pressure head, and ripple length, advection is expected to result in pore-water exchange at a rate of 45.4 L m^{-2} d^{-1} (eq. 15 in Rutherford et al. 1995). Assuming that the bottom water was oxygen saturated ([O_2] (T ~ 15° C, S ~ 33 p.s.u.) = 257 µmol L^{-1}) this would result in an oxygen supply of 11.7 mmol m^{-2} d^{-1}. Based on a literature compilation the median of the total oxygen consumption of shelf sediments was estimated to be 13.7 mmol m^{-2} d^{-1} (Canfield and Teske 1996). The advective oxygen supply at the medium sand station, that does not include any transport by diffusion or bioirrigation, would thus already be sufficient to maintain what is considered to be a typical benthic oxygen demand in shelf areas.

As advective pore-water exchange rates scale linearly with the sediment permeability within the range of permeabilities investigated in this study (Darcy 1856), the potential of advection to supply oxygen to the sediment community would be much higher at the coarse sand station. The measurements in September confirmed that ripples are at least sometimes present at that station, too. Ripples similar to those observed at the medium sand station would lead to exchange rates of 129 L m^{-2} d^{-1} which would supply oxygen to the coarse sand at a rate of 33 mmol m^{-2} d^{-1}. The sediment at the coarse sand station thus has the potential for aerobic mineralization at

high rates in periods of high organic matter availability (e.g., during phytoplankton blooms), at least in the presence of ripples. The low permeability of the fine sand results in expected rates of pore-water exchange and oxygen supply of 5.2 L m^{-2} d^{-1} and 1.3 mmol m^{-2} d^{-1} indicating a minute contribution of advection to the total oxygen supply even in the presence of high ripples. This corresponds to results of Janssen et al. (2005), who measured similar oxygen fluxes in the presence and absence of pressure gradients at that station.

For a quantitative utilization of the supplied oxygen it is required that oxygen is entirely removed from the pore-water during sediment passage. This is likely to be the case at the medium sand station. The time for passage will strongly depend on the respective location of inflow relative to the pressure gradient (Rutherford et al. 1995). Pore-water circulation induced by the observed ripples will result in residence times in the range of hours with a median of 2.7 h for water entering the medium sand within the high pressure region at the upstream slope (at a pressure of p_0 ; $0 < p_0 < p_{max}$). Assuming that oxygen removal rates were equal to rates estimated from oxygen profiles for organically poor sands of the central North Sea, approximately 2.5 h would be needed to quantitatively remove oxygen from the pore-waters (Lohse et al. (1996); ~ 110 µmol L^{-1} h^{-1} at stations # 6 and 7; T ~ 11° C). Oxygen removal in the medium sand probably took place faster as chamber-derived oxygen fluxes were more than 2 times the estimated fluxes at the above stations # 6 and 7 (Janssen et al. 2005). Compared to the medium sand station the 2.8 times higher permeability at the coarse stand station reduces the pore-water residence times by the same factor. If the passage takes place too fast to entirely remove the oxygen this would result in a release of pore-water that is still oxygenated which could set a limit to the actual contribution of advection to sediment oxygen consumption at that site. Rutherford et al. (1995) hypothesized that there is a critical grain size where the contribution of advection to oxygen uptake of the sediments reaches a maximum. This maximum, however, will depend on a variety of factors and their connection to the sediment grain size including the availability of organic matter, the prevailing topographies, and the volumetric oxygen removal rates and oxygen uptake kinetics. However, as the residence times scale reciprocally with permeability, oxygen removal efficiency may be lower at that station,

which could set a limit to the actual contribution of advection to sediment oxygen consumption.

So far, only the steady flow has been considered which is either east- or westwards directed but unidirectional during most of the tidal cycle (upper graph of fig. 12). Recordings of near-bottom flow, however, indicate also a presence of wave-driven, oscillating currents in most occasions. This is in agreement with Antia (1993) who estimated that waves with significant heights of 1 - 2 m, as they prevail under relatively calm conditions in the area (Dette 1977; Niemeyer 1979), result in maximum oscillating current velocities of ~ 55 and ~ 18 cm s^{-1} at water depths of 10 and 20 m, respectively. Such oscillating currents are known to also result in pore-water exchange and solute transport (Oldham 1999; Precht and Huettel 2003; Precht et al. 2004).

Apart from the advection of pore-waters transport of the sediment as a whole is potentially adding to pore-water and solute exchange at all stations. Sediment movement may take place by means of bioturbation (e.g., Clifton and Hunter 1973; Smith et al. 1986; Ziebis et al. 1996a) as well as by physical transport of sediment particles (“saltation”), resulting in the migration of roughness elements (Langhorne 1982; Amos et al. 1999). Indications for a presence of biogenic and physical sediment movement has been found in the vanishing of ripples at the coarse sand between September and October, in the alignment of ripple asymmetry to the main bottom flow and in the changes in surface elevation observed in microprofile time series. Especially in the case of physical sediment reworking, the pore-water enclosed in the moving roughness elements will be quantitatively replaced by bottom water. The contribution of this process to the total solute exchange may be significant (Rutherford et al. 1993) and is dependent on the rate of sediment transport that was not resolved in this study. Relative to advection the process is considered to be most important when ripple movement is fast relative to the velocity of the pore-water (Precht et al. 2004), which might be the case at the fine sand. It is clear that advection due to unidirectional flow represents only a part of the exchange processes that are connected to the interaction of flow and topography on sands. Hence, all above calculations of exchange are most likely conservative representations of natural processes.

Conclusions

Estimates of pressure gradients and rates of advective exchange based on the observed topographies and currents allow a rough evaluation of the role of advection at the selected sites. At the medium and coarse sand station, pore-water advection is found to be an important solute carrier with large potential implications for biogeochemical processes at these sites. A time series of oxygen penetration depth in the medium sand confirmed this potential with respect to advective oxygen supply of the sediment.

Further insight into the significance of pore-water advection for larger regions of the continental shelf requires more data on topographies, currents, and permeabilities as well as refined modeling approaches. Topographies in the working area proved to be highly variable (biological vs. physical origin, > 6-fold range in average roughness element height). Future surveys should cover both the spatial and temporal variability of the surface topography to improve the site characterization and to include the contribution of sediment transport to solute exchange. In order to allow an improved assessment of the role of advection from topography and current data we suggest the following targets for future modeling: (1) identification of the horizontal length scales of roughness that have to be considered with respect to advection, (2) search for appropriate descriptors of topographies and currents that are meaningful for advective processes, (3) introduction of modeling approaches for irregular topographies that include aspect ratios and spacing of roughness elements, (4) addition of the third dimension to the models to allow for temporal changes in current direction and for different alignments of currents and ripples, (5) introduction of oscillating currents on the time scale of waves and tides, (6) consideration of changes in topographies and the consequences for solute exchange, and (7) integration of reaction terms that include the effect of changing biogeochemical zonations.

References

Amos, C. L., A. J. Bowen, D. A. Huntley, J. T. Judge, and M. Z. Li. 1999. Ripple migration and sand transport under quasi-orthogonal combined flows on the Scotian Shelf. J. Coast. Res. **15**: 1-14.

Amos, C. L., A. J. Bowen, D. A. Huntley, and C. F. M. Lewis. 1988. Ripple generation under the combined influences of waves and currents on the Canadian continental shelf. Cont. Shelf Res. **8**: 1129-1153.

Antia, E.E. 1993. Sedimentology, morphodynamics and facies association of a mesotidal barrier island shoreface (Spiekeroog, southern North Sea). In *Berichte aus dem Fachbereich Geowissenschaften*. Bremen: Univ. Bremen, Geowissenschaften.

Antia, E.E. 1994. The ebb-tidal delta model of shoreface ridge origin and evolution: appraisal and applicability along the southern North Sea barrier island coast - a discussion. Geo-Mar. Lett. **14**: 59-64.

Antia, E.E., B.W. Flemming, and G. Wefer. 1995. Calm-weather spring and neap tidal current characteristics at a shoreface connected ridge complex in the German Bight (southern North-Sea). Geo-Mar. Lett. **15**: 30-36.

Arnott, R. W., and J. B. Southard. 1990. Exploratory flow-duct experiments on combined-flow bed configurations, and some implications for interpreting storm-event stratification. J. Sediment. Petrol. **60**: 211-219.

Boudreau, B.P., M. Huettel, S. Forster, R.A. Jahnke, A. McLachlan, J.J. Middelburg, P. Nielsen, F. Sansone, G. Taghon, W.R. Van Raaphorst, I. Webster, J.M. Weslawski, P. Wiberg, and B. Sundby. 2001. Permeable marine sediments: overturning an old paradigm. EOS Trans. Am. Geophys. Union **82**: 133-136.

Briggs, K.B. 1989. Microtopographical roughness of shallow-water continental shelves. IEEE Journal of Oceanic Engineering **14**: 360-367.

Cadée, G.C. 1976. Sediment reworking by *Arenicola marina* on tidal flats in the Dutch Wadden Sea. Neth. J. Sea Res. **10**: 440-460.

Canfield, D.E., and A. Teske. 1996. Late Proterozoic rise in atmospheric oxygen concentration inferred from phylogenetic and sulphur-isotope studies. Nature **382**: 127-132.

Clifton, H.E., and R.E. Hunter. 1973. Bioturbational rates and effects in carbonate sand, St. John, U.S. Virgin Islands. J. Geol. **81**: 253-268.

Dade, W. B. 1993. Near-bed turbulence and hydrodynamic control of diffusional mass transfer at the sea floor. Limnol. Oceanogr. **38**: 52-69.

Darcy, H. 1856. Les fontaines publiques de la ville de Dijon. Victor Dalmont.

Dette, H.H. 1977. Ein Vorschlag zur Analyse eines Wellenklimas. Die Küste **31**: 166-180.

Ehrenhauss, S., U. Witte, F. Janssen, and M. Huettel. 2004. Decomposition of diatoms and nutrient dynamics in permeable North Sea sediments. Cont. Shelf Res. **24**: 721-737.

Emery, K.O. 1968. Relict sediments on continental shelves of the world. Am. Assoc. Pet. Geol. Bull. **52**: 445-464.

Fehlman, M. H. 1985. Resistence components and velocity distributions of open channel flows over bedforms. MSc. thesis thesis, Colorado State University.

Forster, S., M. Huettel, and W. Ziebis. 1996. Impact of boundary layer flow velocity on oxygen utilization in coastal sediments. Mar. Ecol. Prog. Ser. **143**: 173-185.

Fries, J.S., C.A. Butman, and R.A. Wheatcroft. 1999. Ripple formation induced by biogenic mounds. Mar. Geol. **159**: 287-302.

Fries, J.S., and J.H. Trowbridge. 2003. Flume observations of enhanced fine-particle deposition to permeable sediment beds. Limnol. Oceanogr. **48**: 802-812.

Glud, R. N., J. K. Gundersen, H. Røy, and B. B. Jørgensen. 2003. Seasonal dynamics of benthic O_2 uptake in a semienclosed bay: Importance of diffusion and faunal activity. Limnol. Oceanogr. **48**: 1265-1276.

Grant, J. 1983. The relative magnitude of biological and physical sediment reworking in an intertidal community. J. Mar. Res. **41**: 673-689.

Gundersen, J.K., and B.B. Jørgensen. 1990. Microstructure of diffusive boundary layers and the oxygen uptake of the sea floor. Nature **345**: 604-607.

Heezen, B.C., and C.D. Hollister. 1971. The face of the deep. Oxford University Press.

Huettel, M. 1990. Influence of the lugworm *Arenicola marina* on pore-water nutrient profiles of sand flat sediments. Mar. Ecol. Prog. Ser. **62**: 241-248.

Huettel, M., and G. Gust. 1992. Impact of bioroughness on interfacial solute exchange in permeable sediments. Mar. Ecol. Prog. Ser. **89**: 253-267.

Huettel, M., and A. Rusch. 2000. Transport and degradation of phytoplankton in permeable sediment. Limnol. Oceanogr. **45**: 534-549.

Huettel, M., W. Ziebis, and S. Forster. 1996. Flow-induced uptake of particulate matter in permeable sediments. Limnol. Oceanogr. **41**: 309-322.

Huettel, M., W. Ziebis, S. Forster, and G. W. Luther, III. 1998. Advective transport affecting metal and nutrient distribution and interfacial fluxes in permeable sediments. Geochim. Cosmochim. Acta **62**: 613-631.

Janssen, F., M. Huettel, and U. Witte. 2005. Pore-water advection and solute fluxes in permeable marine sediments (II): Benthic respiration at three sandy sites with different permeabilities (German Bight, North Sea). Limnol. Oceanogr. **50**: 779-792.

Jørgensen, B.B., and D.J. Des Marais. 1990. The diffusive boundary layer of sediments: oxygen microgradients over a microbial mat. Limnol. Oceanogr. **35**: 1343-1355.

Kim, S.C., C.T. Friedrichs, J.P.Y. Maa, and L.D. Wright. 2000. Estimating bottom stress in tidal boundary layer from Acoustic Doppler Velocimeter data. J. Hydraul. Eng.-ASCE **126**: 399-406.

Langhorne, D. N. 1982. A study of the dynamics of a marine sandwave. Sedimentology **29**: 571-594.

Li, M.Z., and C.L. Amos. 1999. Field observations of bedforms and sediment transport thresholds of fine sand under combined waves and currents. Mar. Geol. **158**: 147-160.

Lohse, L., E.H.G. Epping, W. Helder, and W.R. Van Raaphorst. 1996. Oxygen pore water profiles in continental shelf sediments of the North Sea: Turbulent versus molecular diffusion. Mar. Ecol. Prog. Ser. **145**: 63-75.

Marinelli, R.L., R.A. Jahnke, D.B. Craven, J.R. Nelson, and J.E. Eckman. 1998. Sediment nutrient dynamics on the South Atlantic Bight continental shelf. Limnol. Oceanogr. **43**: 1305-1320.

Miller, M.C., I.N. McCave, and P.D. Komar. 1977. Threshold of sediment motion under unidirectional currents. Sedimentology **24**: 507-527.

Monin, A.S., and A.M. Yaglom. 1971. Statistical fluid mechanics : mechanics of turbulence. 4 ed. 2 vols. Vol. 1. MIT Press.

Niemeyer, H.D. 1979. Untersuchungen zum Seegangsklima im Bereich der Ostfriesischen Inseln und Küste. Die Küste **34**: 53-70.

Nowell, A. R. M., and M. Church. 1979. Turbulent flow in a depth-limited boundary layer. J. Geophys. Res. **84**: 4816-4824.

Oldham, C. E. 1999. Porewater nutrient fluxes in a shallow fetch-limited estuary. Mar. Ecol. Prog. Ser. **183**: 39-47.

Paterson, D.M. 2001. The fine structure and properties of the sediment surface, p. 144-179. *In* B. P. Boudreau and B. B. Jørgensen, [eds.]. The benthic boundary layer: transport processes and biogeochemistry. Oxford Univ. Press.

Pilditch, C.A., C.W. Emerson, and J. Grant. 1998. Effect of scallop shells and sediment grain size on phytoplankton flux to the bed. Cont. Shelf Res. **17**: 1869-1885.

Postma, H., ed. 1982. *Hydrography of the Wadden Sea: movements and properties of water and particulate matter*. Vol. 2, *Report of the Wadden Sea Working Group*. Rotterdam: A. A. Balkema.

Precht, E., and M. Huettel. 2003. Advective pore-water exchange driven by surface gravity waves and its ecological implications. Limnol. Oceanogr. **48**: 1674-1684.

Precht, E., U. Franke, L. Polerecky, and M. Huettel. 2004. Oxygen dynamics in permeable sediments with wave-driven pore water exchange. Limnol. Oceanogr. **49**: 693-705.

Raffel, M., C. Willert, and J. Kompenhans. 1998. Particle image velocimetry. Springer.

Reimers, C. E. 1987. An in situ microprofiling instrument for measuring interfacial pore water gradients: methods and oxygen profiles from the North Pacific Ocean. Deep-Sea Research Part A: Oceanographic Research Papers **34**.

Revsbech, N. P., B. B. Jørgensen, and T. H. Blackburn. 1980. Oxygen in the sea bottom measured with a microelectrode. Science **207**: 1355-1356.

Røy, H., M. Huettel, and B. B. Jørgensen. 2005. The influence of topography on the functional exchange-surface of soft sediments, assessed from *in situ* measured sediment topography. Limnol. Oceanogr. **50**: 106-112.

Røy, H., M. Huettel, and B.B. Jørgensen. 2002. The role of small-scale sediment topography for oxygen flux across the diffusive boundary layer. Limnol. Oceanogr. **47**: 837-847.

Rutgers van der Loeff, M.M. 1981. Wave effects on sediment water exchange in a submerged sand bed. Neth. J. Sea Res. **15**: 100-112.

Rutherford, J. C., G. J. Latimer, and R. K. Smith. 1993. Bedform mobility and benthic oxygen uptake. Water Res. **27**: 1545-1558.

Rutherford, J.C., J.D. Boyle, A.H. Elliott, T.V.J. Hatherell, and T.W. Chiu. 1995. Modeling benthic oxygen uptake by pumping. J. Environ. Eng. **121**: 84-95.

Savant, S.A., D.D. Reible, and L.J. Thibodeaux. 1987. Convective transport within stable river sediments. Water Resour. Res. **23**: 1763-1768.

Smith, C.R., P.A. Jumars, and D.J. DeMaster. 1986. *In situ* studies of megafaunal mounds indicate rapid sediment turnover and community response at the deep-sea floor. Nature **323**: 251-253.

Swift, S.A., C.D. Hollister, and R.S. Chandler. 1985. Close-up stereo photographs of abyssal bedforms on the Nova Scotian continental rise. Mar. Geol. **66**: 303-322.

Tanner, W.F. 1967. Ripple mark indices and their uses. Sedimentology **9**: 89-104.

Thomas, T.R. 1982. Rough surfaces. Longman.

Wentworth, C.K. 1922. A scale of grade and class terms for clastic sediments. J. Geol. **30**: 377-392.

Wenzhöfer, F., O. Holby, and O. Kohls. 2001. Deep penetrating benthic oxygen profiles measured in situ by oxygen optodes. Deep-Sea Res. Part I **48**: 1741-1755.

Wheatcroft, R.A. 1994. Temporal variation in bed configuration and one-dimensional bottom roughness at the mid shelf STRESS site. Cont. Shelf Res. **14**: 1167-1190.

Yager, P.L., A.R.M. Nowell, and P.A. Jumars. 1993. Enhanced deposition to pits: a local food source for benthos. J. Mar. Res. **51**: 209-236.

Ziebis, W., S. Forster, M. Huettel, and B.B. Jørgensen. 1996a. Complex burrows of the mud shrimp *Calianassa truncata* and their geochemical impact in the sea bed. Nature **382**: 619-622.

Ziebis, W., M. Huettel, and S. Forster. 1996b. Impact of biogenic sediment topography on oxygen fluxes in permeable seabeds. Mar. Ecol. Prog. Ser. **140**: 227-237.

Oxygen uptake by aquatic sediments measured with a novel non-invasive eddy-correlation technique

Peter Berg [1,4], Hans Røy [2], Felix Janssen [2], Volker Meyer [2], Bo Barker Jørgensen [2], Markus Huettel [2,3] & Dirk de Beer [2]

[1] Department of Environmental Sciences, University of Virginia, 291 McCormick Road, Charlottesville, Virginia 22904-4123, USA

[2] Max Planck Institute for Marine Microbiology, Celsiusstrasse 1, D-28359 Bremen, Germany

[3] Present address: Florida State University, Department of Oceanography, 0517 OSB, West Call Street, Tallahassee, Florida 32306-4320, USA

[4] corresponding author. E-mail: pb8n@virginia.edu

This Manuscript is published in Marine Ecology Progress Series (**262**: 75-83)

Acknowledgements

This study was cosponsored by the National Science Foundation (OCE-0221259) and the Max Planck Society. The skipper at Genetica II, Verner Dam, is thanked for his help during our visit to the marine sites.

Abstract

This paper presents a new non-invasive technique for measuring sediment O_2 uptake, which in its concept differs fundamentally from other methods used today. In almost all natural aquatic environments, the vertical transport of O_2 through the water column towards the sediment surface is facilitated by turbulent mixing. The new technique relies on measuring two turbulent quantities simultaneously and at the same point in the water above the sediment: the fluctuating vertical velocity using an Acoustic Doppler Velocimeter and the fluctuating O_2 concentration using an O_2 microelectrode. From these two quantities, which typically are measured 10-50 cm above the sediment surface for a period of 10-20 min and at a frequency of 15-25 Hz, the vertical flux of O_2 towards the sediment surface is derived. Based on measurements performed under realistic field conditions and comparisons with in situ flux chamber measurements, we believe that the new technique is the optimal approach for determining O_2 uptake by sediments. The technique is superior to conventional methods as measurements are done under true in situ conditions without any disturbance of the sediment. Furthermore, the technique can be used for bio-irrigated or highly porous sediments, such as sands, where traditional methods often fail. While this paper only focuses on O_2 uptake by sediments, the technique can also be applied to other solutes that can be measured at sufficiently high temporal resolution.

Introduction

Consumption of O_2 in aquatic sediments is attributed to two types of reactions: aerobic decomposition of organic matter and oxidation of reduced products of anaerobic decay, including NH_4^+, Mn^{2+}, Fe^{2+}, H_2S, FeS, and FeS_2. Sediment O_2 uptake provides valuable information on these reactions and is a frequently measured parameter in biogeochemical studies of aquatic sediments. At the same time, it is a parameter that is often difficult to measure accurately with the methods available today.

Oxygen uptake by sediments is affected strongly by the transport processes responsible for the movement of O_2 from the overlying water down through the sediment. These transport processes include molecular diffusion, bioturbation (the diffusion-like transport caused by movements of fauna), bio-irrigation (the pumping activity of tube-dwelling animals) and current- or wave-driven advection. Recent studies have shown that bioturbation is often a significant transport process comparable in strength to molecular diffusion (Aller and Aller 1992; Forster et al. 1995; Berg et al. 2001). Likewise, bio-irrigation can be a dominant transport process in sediments densely populated by tube-dwelling animals (Aller 1983; Pelegri et al. 1994; Wang and Van Cappellen, 1996). Other transport processes also can stimulate O_2 uptake by sediments. Currents over an uneven bottom or wave action on more shallow sites can induce a significant advective transport, either through the interstitial pores in more permeable sediments such as sand, or through tubes and borrows created by fauna (Rutgers van der Loeff 1981; Savant et al. 1987; Thibodeaux and Boyle 1987; Shum 1992; Webster 1992; Webster and Taylor 1992). In some sediments, this advection is the dominant transport process and enhances O_2 uptake many-fold relative to uptake dominated by molecular diffusion (Forster et al. 1996; Lohse et al. 1996).

The two commonly used methods for determining O_2 uptake by sediments are laboratory measurements in recovered sediment cores kept in a controlled environment as close to the in situ conditions as possible (e.g., Rasmussen and Jørgensen 1992) and measurements with in situ chambers which isolate a fraction of the sediment surface and bottom water from the surroundings (e.g., Jahnke and Christiansen 1989). In both cases, the sediment O_2 uptake is determined by measuring O_2 depletion in the overlying water over time. Typically, sediment cores have a diameter of 5-10 cm while chambers cover

a larger area of the sediment surface, for example 30 x 30 cm (Glud et al. 1998 and 1999).

One problem with these methods is that they may affect active transport processes that influence O_2 uptake in the undisturbed sediment. While a good representation of in situ molecular diffusion and also in situ bioturbation caused by smaller animals (meiofauna) can be obtained in sediment cores, this method tends to underestimate the effects of bioturbation and bio-irrigation caused by larger animals (macrofauna). Studies comparing O_2 uptake measured in cores and in situ chambers for the same sediment have found O_2 uptake to be several fold lower in cores. The difference was explained as a result of more realistic representation of irrigating macrofauna in the larger chambers (Glud et al. 1998, 1999 and 2003). When measurements are made in both sediment cores and in situ chambers the overlying water is kept fully mixed by stirring. This induced rotational flow differs from naturally occurring flow patterns over the sediment surface and represents another problem of these conventional methods. For example, representative O_2 uptake generally can not be measured in cores or in in situ chambers where advective transport processes within the sediment are created by current or wave action (Huettel and Webster 2001; Reimers et al. 2001). In addition to these shortcomings, sediment core and in situ chamber measurements are difficult to perform when objects such as rocks, mussels, epifauna, and macroalgae are abundant either on the sediment surface or in the upper sediment layer. Under such circumstances it is difficult not to disturb the sediment considerably when cores are collected or when the in situ chambers are deployed.

In this paper we present a new non-invasive technique for measuring O_2 uptake by aquatic sediments. In almost all natural environments, O_2 taken up such sediments is transported down through the water column by turbulent motions. The technique relies on measuring the turbulent fluctuations of the vertical velocity and the corresponding O_2 concentration, simultaneously and at the same point above the sediment surface. If such measurements are done with an adequate temporal resolution to capture these fluctuations and for a period long enough to obtain a statistically sound representation of their variations, then the vertical flux of O_2 can be derived. If possible to perform from a technical point of view, such measurements obviously do not suffer from the same shortcomings as sediment core and in situ chamber measurements because O_2

uptake is determined under true in situ conditions and without any disturbance of the sediment. This technique has been used for several decades to determine land-atmosphere exchanges of CO_2, moisture, and energy in the atmospheric boundary layer (e.g., Wyngaard 1989) and is commonly referred to as flux determination or measurement by eddy correlation. The latter term is adopted here. Despite the clear advantages of the technique, it has only been used a few times in aquatic environments to determine fluxes of energy, for example between water and sea ice (Fukuchi et al. 1997, Shirasawa et al. 1997). The obvious reason is that other than for temperature, it is difficult to construct a sensor that can measure scalar properties such as O_2 concentration in water at a well-defined point and with a sufficiently fast response to capture all turbulent fluctuations. However, as documented below, we have been able to make these measurements with O_2 microelectrodes specially constructed to have a fast response. The fluctuating vertical velocity is measured using a standard instrument, an Acoustic Doppler Velocimeter, referred to as the ADV below, which is commercially available. The ADV gives the full 3D turbulent velocity field, and is widely used in aquatic environments to study processes such as the transport of particles in the shear layer over sediment surfaces. While this paper only focuses on O_2 uptake by sediments, the technique can also be applied to other solutes that can be measured at sufficiently high temporal resolution.

Theory

Fig. 1 shows an example of a depth profile of the O_2 concentration in a marine muddy sediment and the overlying water, measured in situ with a microelectrode. The O_2 is consumed in the upper 1.5 mm of the sediment and the smoothness of the profile suggests that the important mechanisms for the vertical transport of O_2 in the sediment are molecular diffusion and possibly bioturbation caused by meiofauna. In the water column, where the two possible transport mechanisms are molecular diffusion and advection, no concentration gradients are visible 0.7 mm, or more, above the sediment surface. This reflects a shift in the dominant transport process from molecular diffusion within the diffusive boundary layer to advection above the layer. It is also evident that this advective transport of O_2 results exclusively from turbulent motions since there was no continuous flow pointing toward the sediment at this site. The characteristic variation of the turbulence is that the O_2 concentration is higher when the vertical velocity is pointing toward the sediment and lower when the velocity is pointing upward. Over

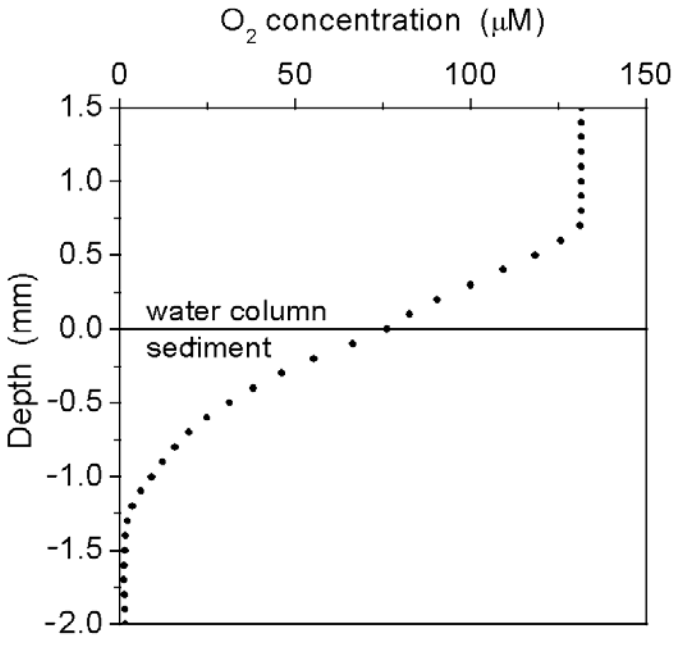

Fig. 1. Depth profile of the O_2 concentration measured in situ with a microelectrode in a marine muddy sediment and the overlying water.

time this gives rise to a net transport of O_2 toward the sediment. An example of this pattern is shown in fig. 2 from some of our measurements with high temporal resolution of the vertical velocity and the connected O_2 concentration.

The mathematical expression for the vertical O_2 flux in any position in the water column, at any point in time and as the result of advection and molecular diffusion is

$$Flux = UC - D\frac{dC}{dx} \tag{1}$$

where U is the vertical velocity, C is the O_2 concentration, D is the molecular diffusivity of O_2 in water, and x is the depth coordinate (e.g., Berner 1980 or Boudreau 1997).

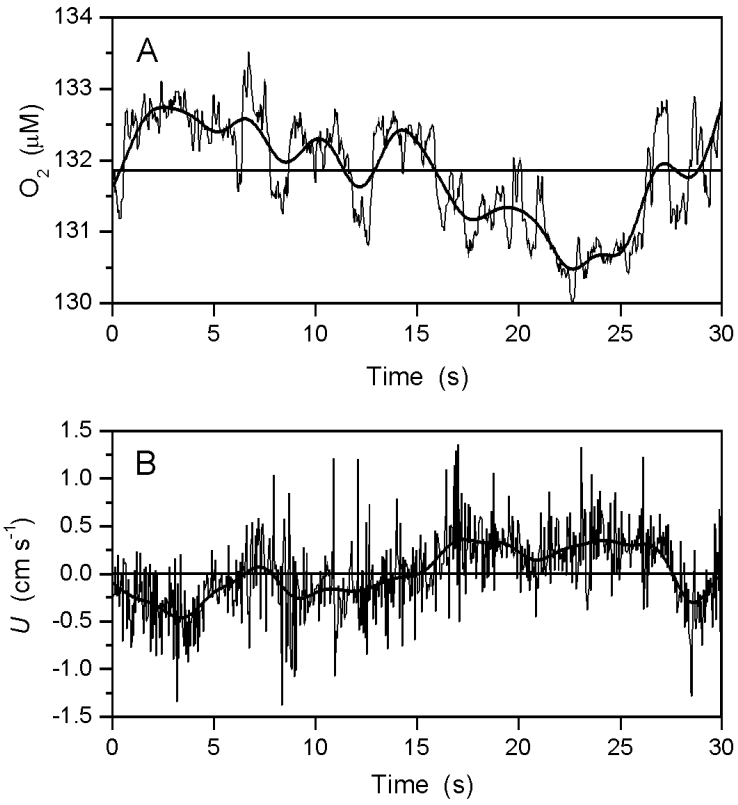

Fig. 2. A time series of the fluctuating O_2 concentration (A, thin lines) and the connected vertical velocity (B, thin lines). Negative velocity values indicate a flow towards the sediment surface. The data were measured 15 cm above a sediment surface at a frequency of 25 Hz. The mean values for the time series are also shown (horizontal lines) as are the smoothing of the O_2 concentration and vertical velocity (thick lines).

In the water column above the diffusive boundary layer, turbulent mixing is the dominant vertical transport in almost all natural aquatic environments. Even when density stratifications caused by temperature or salinity differences are present and vertical concentration gradients are evident, molecular diffusion is usually insignificant relative to turbulent mixing. For that reason, the diffusive term in Eq. (1) can be neglected. Furthermore, it is a common practice when dealing with turbulent advections to separate both instantaneous values of U and C into two components equal to $\overline{u} + u'$ and $\overline{c} + c'$ where $\overline{u}$ is the mean vertical velocity, u' is the vertical turbulent fluctuating velocity, $\overline{c}$ is the mean concentration, and c' is the turbulent fluctuating concentration (e.g., Stanišić 1985). It should be noted that there are no simplifications hidden in these separations. The separations are now substituted into Eq. (1), which is then averaged over a period of time significantly longer than the time scale of the turbulent fluctuations, in which case both averages of u' and c' becomes equal to zero. It is finally assumed that that the mean vertical velocity is equal to zero ($\overline{u} = 0$). Unless there is a continuous flow into or out of the sediment, which is a rare situation, $\overline{u}$ is by nature equal to zero. With these assumptions Eq. (1) gives the following expression for the vertical O_2 flux averaged over time

$$\overline{Flux} = \overline{u'c'} \tag{2}$$

where the bars symbolize the averaging (e.g., Stanišić 1985). Equation (2) has been used for decades to determine fluxes by eddy correlation in the atmospheric boundary layer (e.g., Wyngaard 1989). In such applications of Eq. (2), where time series of u' ($u'_1, u'_2, u'_3, \cdots u'_N$) and c' ($c'_1, c'_2, c'_3, \cdots c'_N$) are extracted from measurements, the flux is simply calculated as the average of the sum $u'_1c'_1 + u'_2c'_2 + u'_3c'_3 + \cdots + u'_Nc'_N$.

When measuring U in the water column under stationary conditions, where no changes in size or direction of the current occur, $\overline{u}$ can be defined as the mean of all U, $\overline{U}$. Since it is difficult to position the ADV so that the U is measured exactly perpendicular to the sediment surface, which in turn may not be completely even and well-defined, $\overline{U}$ is likely to have some small value and a correction must be made for Eq. (2) to be valid. The correction can be made either by rotating the measured 3D velocity field (U, V, W, where V and W are to two horizontal velocity components) so

$\overline{U}$ equals zero, or if $\overline{U}$ is only slightly off from zero, simply by subtracting $\overline{U}$ from each individual U value. In the latter case, u' becomes equal to $U - \overline{U}$ and the average of all u' will consequently always equal zero as assumed in the derivation of Eq. (1). If non-stationary conditions are present, the correction must vary in time and u' can, for example, be calculated from the running average of U. A challenging aspect of this more advanced correction, as discussed in detail below, is to determine how many adjacent data points to include in the running averaging. If too few points are included, some of the larger scale turbulent fluctuations are filtered out, and if too many points are included, non-turbulent motions may affect the flux calculation. The isolation of c' from the measured O_2 concentration, C, is done along the same lines.

Analysis of our measurements have shown that u' can often be calculated as $U - \overline{U}$, while c' in most situations technically should involve running averaging since non-turbulent variations in C occur, presumably caused by a slow drift in the O_2 microelectrode calibration. However, one can show that the running averaging can be avoided if these variations happen on a time scale significantly larger that the scale of the turbulent fluctuations. In such situations C can be used directly in the flux calculation and Eq. 2 simplifies to

$$\overline{Flux} = \overline{u'C} \tag{3}$$

Equation 3 represents the simplest way to determine sediment O_2 uptake from measured time series of U and C.

If both u' and c' are extracted from the measured data, other advantages exist. Both Eq. (2) and (3) include an integration in the time domain. This integration can also be performed in the frequency domain after Fast Fourier Transformation of the time series of u' and c'. More specifically, one can show that the vertical O_2 flux can also be expressed as the integral over the frequency of the one-sided cospectrum of $u'c'$

$$\overline{Flux} = \int_0^\infty \mathrm{Co}_{u'c'}(f)\, df \tag{4}$$

where f is the frequency (e.g., Priestley 1992). The cospectrum of $u'c'$ itself offers immediate information on the frequencies of the turbulent eddies that are responsible for

the vertical O_2 transport. As shown below, this is a valuable approach to evaluate if the O_2 microelectrode responds fast enough to capture all turbulent fluctuations facilitating the vertical transport of O_2.

Methods

Instrument

The ADV is a commercially available instrument manufactured by companies such as Nortek AS, Norway and SonTek/YSI Inc, USA. The ADV measures the 3D velocity field in a small cylindrical volume, approximately 1.5 cm long and 0.6 cm in diameter, located on the ADV's center line 10 cm from the base of the three sensors, as marked on fig. 3. The velocities are determined with a resolution in time as fine as 25 Hz and in the velocity ranges from ± 3 to ± 250 cm s^{-1}. The ADV measurements are largely unaffected by water quality (O'Riordan et al. 1996; Yang et al. 1996). However, the speed of sound in water is correlated to temperature and salinity, and these parameters must be known in order to obtain the most accurate determination of the 3D velocity field.

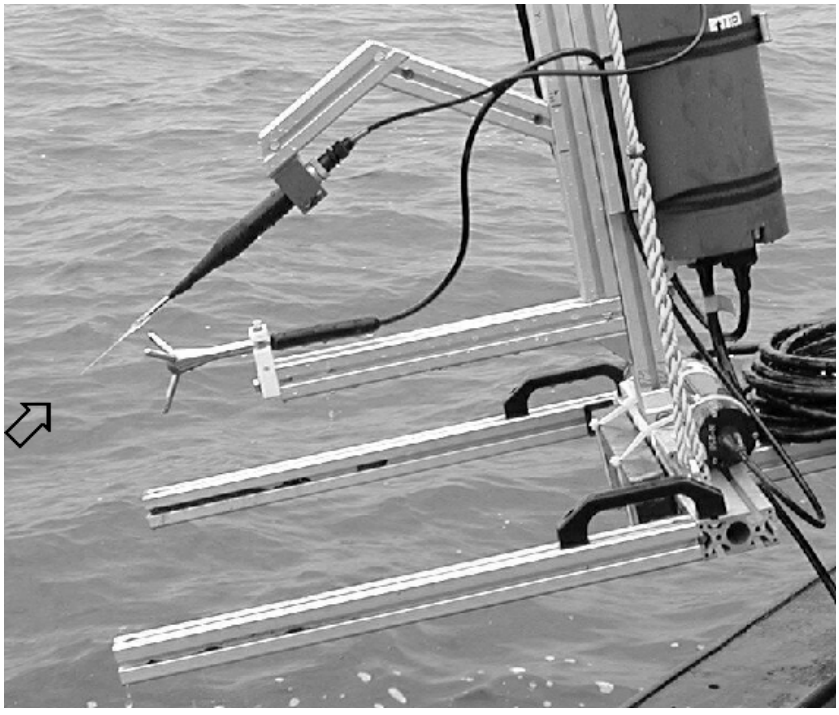

Fig. 3. The Acoustic Doppler Velocimeter and the O_2 microelectrode mounted on a rack. The position of the Acoustic Doppler Velocimeter's measuring volume and the tip of the O_2 microelectrode are marked with an arrow.

The O_2 microelectrode is of the Clark-type (Revsbech 1989) and was constructed to have a short response time by using a thin silicon membrane and a compact tip architecture. The sensor has a 10 μm tip diameter and a 0.2 s response time for a 90% response to concentration changes. To maximize signal to noise ratios, sensitivity and signal speed, the cable connections between sensor and pico-ampere meter were kept as short as possible. This was achieved by using a customized submersible pico-ampere meter where the sensor was inserted directly in the amplifier housing. Since seawater acts as shielding, this pico-ampere meter can resolve significantly smaller fluctuations in situ than under normal laboratory conditions.

Both the ADV and the O_2 microelectrode were mounted on a rack constructed for initial tests of the technique (fig. 3). The tip of the microelectrode was located immediately next to the border of the ADV's measuring volume. The rack was designed so that the position of the measuring volume and the tip of the microelectrode could be adjusted in the range of 10-55 cm above the sediment surface. Prior to measurements the rack was positioned manually on the sediment surface with the sensors facing up into the current, and the ADV and pico-ampere meter were connected to the surface through independent cables. Data acquisition was controlled above the water surface by an IBM compatible PC, which communicated digitally with the ADV and by analog with the pico-ampere meter. The PC and supporting electronics were powered by batteries and were isolated galvanically from all other electronic devices.

Both the velocity and the O_2 concentration measurements contain some high frequency noise (fig. 2). The noise from the ADV is purely random, can be assumed to follow a Gaussian distribution, and consequently converges to the value zero when averaged over multiple data points without introducing bias (SonTek/YSI Inc 2001). The electronic circuitry and components behind the O_2 concentration measurements are all well-known and well-described (Tietze and Schenk 1993), and have similar noise characteristics as the ADV. This was confirmed by measurements during which the O_2 microelectrode was replaced with a dummy electrode. These measurements led to the calculation of an O_2 uptake of zero. A similar result was also obtained in other measurements where the O_2 microelectrode and the ADV were positioned apart.

Measurements

The technique was tested under field conditions on three occasions. The first series of measurements was done in the river Wümme near Bremen, Germany, which is approximately 7 m wide, with a water depth of 1 m and a sandy bottom. This site allowed us to keep all equipment not mounted on the rack on land, and also to make easy adjustments of the orientation of the rack and the measuring height above the sediment surface. Additional measurements for comparison of the O_2 uptake in recovered sediment cores or in situ chambers were not pursued since these two methods are likely to fail in permeable sands, as described above. At the time of measurement the river current was 13 cm s^{-1}. Three time series were sampled for each of the four measuring heights, 15, 20, 40 and 55 cm, above the sediment surface. Each time series had a duration of 10 min and was sampled at a frequency of 25 Hz to ensure that all concentration changes that could be registered by the O_2 microelectrode were sampled.

The second series of measurements was done in Aarhus Bay, Denmark, a relevant marine environment with respect to future use of the new technique. The sediment was a fine-grained mud and was located at 12 m water depth. At the time of measurement, the current was 2 cm s^{-1} at 15 cm above the sediment surface. Four 10 min time series were sampled 15 cm above the sediment surface at a frequency of 25 Hz. For comparison to the eddy correlation measurements, four in situ chambers were deployed. These chambers had a 19 cm inner diameter and were 32 cm tall. The lid on each chamber had a large venting opening that was closed by a stopper after deployment, a sampling port with syringe holder for water samples and a second port for replacement of sampled water. The water inside the chambers was stirred during measurements by a flat rotating disk, 15 cm in diameter and 1 cm in height. Throughout the 3 h incubation, the disks were rotated at a speed of 20 rpm in a position approximately 7 cm above the sediment surface. Prior to measurements the chambers were pushed approximately 20 cm into the sediment enclosing a water volume of approximately 3.4 l. A more accurate estimate of this water volume was calculated from the dilution of 50 ml of a neutrally buoyant sodium bromide solution injected into each chamber. Oxygen concentrations in the chambers were monitored during the incubation with O_2 optodes (Presens) mounted in the lids. In addition, the O_2 concentration in the chambers was determined by Winkler

titration of water samples retrieved at the beginning and the end of the incubation. For additional comparison, three depth profiles of the O_2 concentration were measured with microelectrodes in sediment cores collected at the site. The deployment of the rack holding the ADV and the O_2 microelectrode, the deployment of the in situ chambers and the collection of sediment cores were done by divers.

The third and last series of measurements were done in the sound, Limfjorden, Denmark. The sediment was a fine-grained mud and was located at 8 m water depth. At the time of measurement, directional changes in the current were observed and its strength varied between 1.5-4 cm s^{-1} at 40 cm above the sediment surface. Six 10 min time series were sampled 40 cm above the sediment surface at a frequency of 25 Hz. For comparison to the eddy correlation measurements, six in situ chambers were deployed and operated as described for the Aarhus Bay site.

Results and Discussion

The results of the eddy correlation measurements in the river Wümme are shown in fig. 4. The sediment O_2 uptake was calculated from Eq. 3 where u' was determined as $U - \overline{U}$. Some aerial variation in uptake was expected since the rates represent an increasing upstream area of the sediment surface as increasing measuring heights were used. However, the mean values of the O_2 uptake were not significantly different (ANOVA, $p > 0.18$), and an overall mean of 210 ± 16 mmol m^{-2} d^{-1} was calculated from the combined data. It is expected that some advective transport in the upper sediment layer was induced at the main current of 13 cm s^{-1} during the eddy correlation measurements, which presumably explains the relatively high O_2 uptake. This high uptake, combined with the relatively small error estimates, is seen as a promising result for the new technique. All potential shortcomings and errors in the eddy correlation measurements, such as the response time of the O_2 microelectrode being too slow to capture all important turbulent fluctuations, would lead to an underestimation of the O_2 uptake.

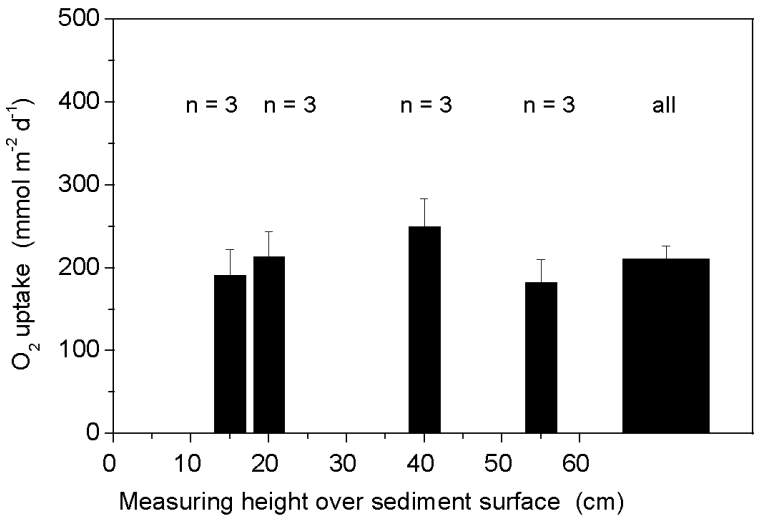

Fig. 4. The O_2 uptake by a sandy river sediment (Wümme) determined by the eddy correlation technique (Error bars represent 1 SE).

Also for the time series from Aarhus Bay, u' was determined as $U - \overline{U}$ and the sediment O_2 uptake was calculated from Eq. 3. The uptake is shown in fig. 5 as are the results from the in situ chambers and the calculated uptake from the O_2 micro-profiles using the gradients in the diffusive boundary layer. Bio-irrigation is not included in the latter calculation, which may explain the lower estimated O_2 uptake relative to the chamber measurements. The O_2 uptake determined in chambers and by the new technique are different (ANOVA, p = 0.03), and the difference is most likely explained by an underrepresentation of faunal activity, especially the irrigating macro-fauna, in the chambers. Since the current was low when the measurements were made and given the impermeable structure of the muddy sediment, it seems unlikely that advective transport, other than that induced by irrigating fauna, would influence the O_2 uptake in the sediment. The relative standard error estimate of 7% for the O_2 uptake determined by eddy correlation was of the same magnitude as the 10% and 6% standard errors found in the chamber measurements and the flux calculations from micro-profiles.

Fig. 5

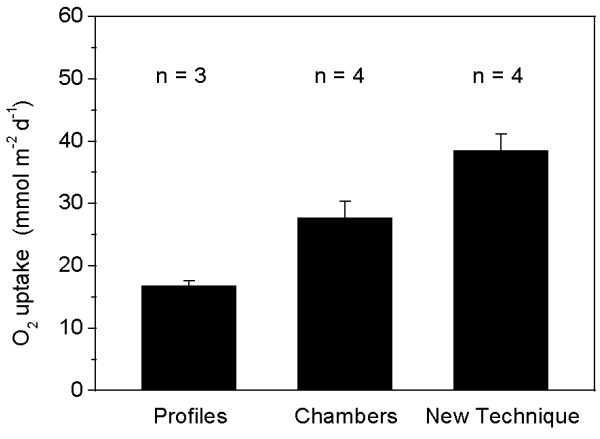

Fig. 6

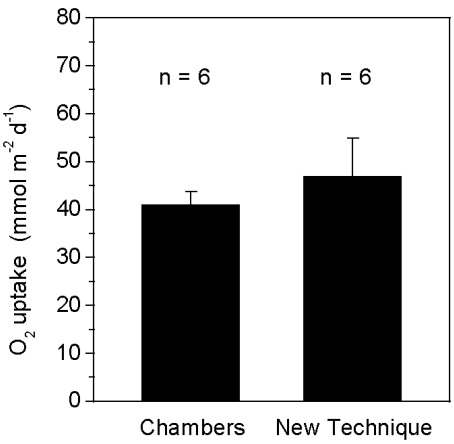

Fig. 5. The O_2 uptake by a muddy marine sediment (Aarhus Bay) determined by O_2 micro-profiles, in situ chambers and the eddy correlation technique (Error bars represent 1 SE).

Fig. 6. The O_2 uptake by a muddy marine sediment (Limfjorden) determined by in situ chambers and the eddy correlation technique (Error bars represent 1 SE).

As the result of the non-stationary current conditions observed during the measurements in Limfjorden, u' was determined from the running average of U before the sediment O_2 uptake was calculated from Eq. 3. The number of adjacent data points used in the running average was found in an analysis as described in detail below. The O_2 uptake is shown in fig. 6 as are the results from the in situ chambers. The two uptake rates are not different (ANOVA, p = 0.50), and have relative standard error estimates of 7% for chamber measurements and 17% for the new technique. The latter standard error is considerably larger than those found when using the technique for the other sites and is probably explained by several factors. First, some natural variation in the uptake was expected with the observed changes in current, both in direction and strength. Second, in order to avoid boundary errors, the first and the last data points in the 10 min time series were used only to calculate the running average of U, and not used directly in the flux calculation. The flux was for that reason calculated from connected values of u' and C only covering a time interval of less than 8 min, which obviously increased the uncertainty of the calculation. A smaller standard error would likely have been found if time series longer than 10 min had been measured at this site.

A further analysis of the eddy correlation measurements requires that the fluctuating component of the O_2 concentration, c', also is known. Data from the Aarhus Bay site were used in the example presented below. Since the measured O_2 concentration generally contained some large scale variations in time, presumably representing a slow drift in the O_2 microelectrode calibration, c' must be determined from the running average of C. The number of adjacent data points, N_r, included in the running average was found by calculating the O_2 uptake repeatedly from Eq. 2 for increasing N_r and observing how the uptake changed. An example for one time series is shown in fig. 7A. Obviously, if N_r equals 1, all fluctuations in the time series are filtered out, which means that c' equals zero and results in an O_2 uptake of zero. For increasing N_r an increasing number of turbulent fluctuations are included in the calculation, the ones with the highest frequency first. The resulting increase in O_2 uptake levels off and reaches a nearly constant value of 33 mmol m^{-2} d^{-1}. It should be noted that the same O_2 uptake also was calculated for this particular time series by using Eq. 3. The value of N_r chosen from the results shown and used in the further

calculations was 3700, which corresponds to an average over 148 s. By knowing both c' and u', the cumulative O_2 uptake for the time series can be calculated, which exhibited a relatively steady increase through time as shown in fig. 7B. In order to avoid boundary errors, the first and the last 1850 data points were used only to calculate the running average of *C*, and were not used directly in the flux calculation. This represents a disadvantage of the running averaging or other similar averaging methods.

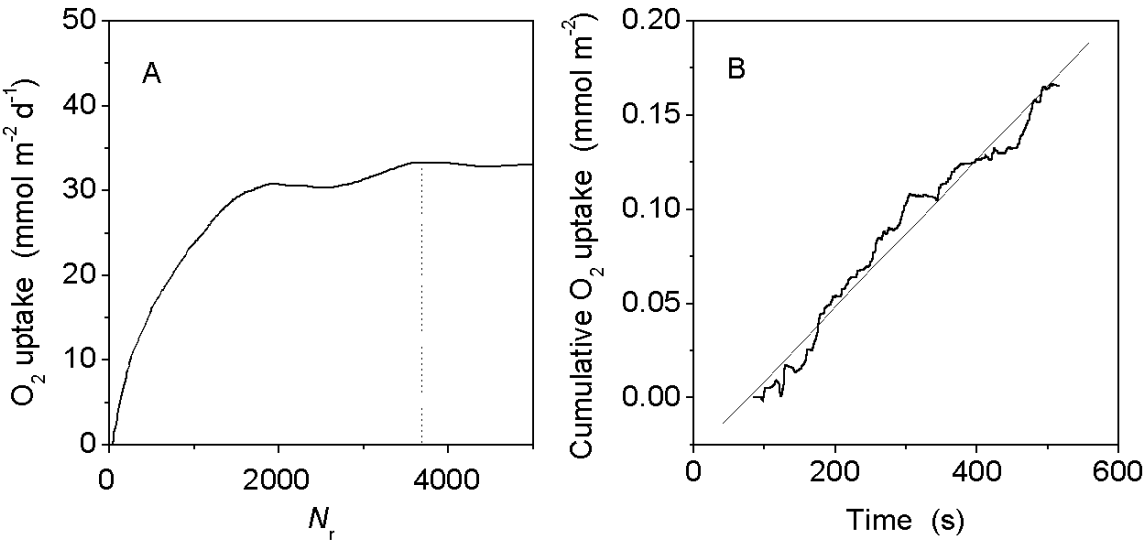

Fig. 7. (A) Determination of the number of data points, N_r, that is used in calculation of the running average of *C*. (B) The cumulative O_2 uptake over time. The thin line represents a linear fit.

One of our initial concerns in evaluating the new technique was whether the O_2 microelectrode would respond fast enough to capture all turbulent fluctuations responsible for the vertical O_2 transport towards the sediment. Although the high O_2 uptake calculated using the technique suggested that all fluctuations were probably accounted for, we investigated this question further. From fig. 8A, which shows the same data as fig. 7A but now on a logarithmic x-axis, it is evident that no contributions to O_2 uptake are calculated for N_r smaller than 40, which corresponds to average over 1.6 s. Although the running averaging is not a sharp-cutting filter, it is reasonable to assume that turbulent eddies with frequencies higher than 1 Hz would be included in the calculation at this value of N_r. It should be emphasized that all measurements were

done using O_2 microelectrodes with a 0.2 s response time for a 90% response to concentration chances. With that in mind, these results show that the turbulent transport was facilitated exclusively by fluctuations with frequencies lower than 1 Hz. In addition, this result is supported by a calculation of the one-sided cospectrum of $u'c'$, shown in fig. 8B, for the same time series. Although longer time series are required to obtain more homogeneous results, no contributions to the O_2 uptake are visible for frequencies higher than 1 Hz. Similar results were obtained in an equivalent analysis of the first series of measurements for the sandy river sediment where current velocity was more than 6 times larger.

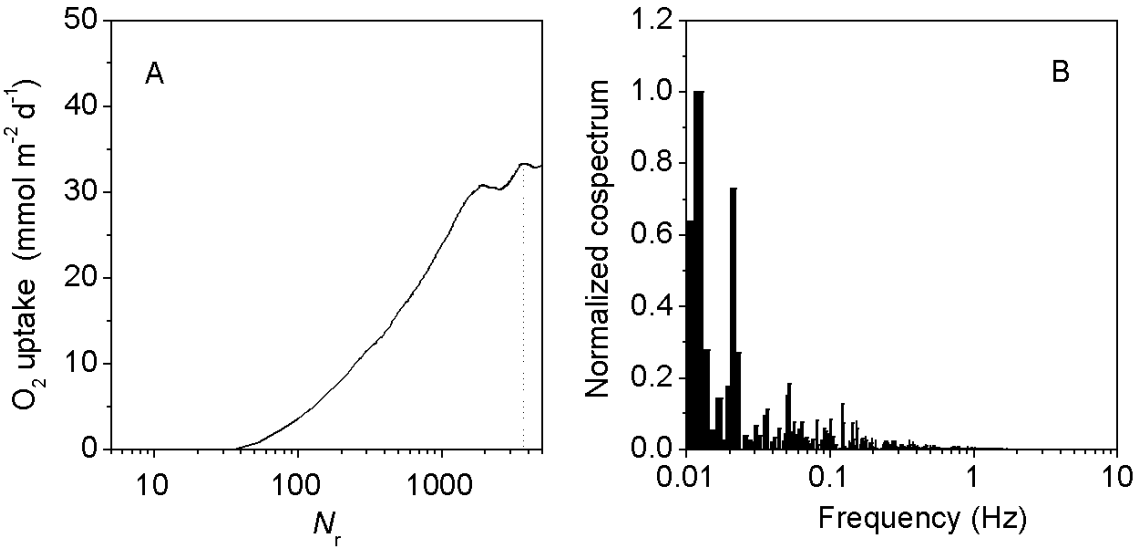

Fig. 8. (A) Same data as shown in fig. 7A, but now on a logarithmic x-axis. (B) The normalized one-sided cospectrum of showing the frequencies of the turbulent eddies that are responsible for the vertical O_2 transport.

The tests of the new technique presented here were conducted under realistic field conditions and resulted in successful determination of O_2 uptake (fig. 4, 5 and 6). An analysis of the turbulent fluctuations showed that the O_2 microelectrodes responded sufficiently fast to capture all turbulent eddies contributing to the vertical transport of O_2 towards the sediment (fig. 7 and 8). Based on these results, we conclude that O_2 uptake by aquatic sediments can be determined by the new eddy correlation technique and we believe that the technique may become a standard approach for determining O_2

uptake by sediments in the future. The technique is superior to conventional methods as measurements are done under true in situ conditions and without any disturbance of the sediment. In addition, the technique can be used for highly porous sediments, such as sands, where conventional methods often fail. While this paper only focuses on O_2 uptake by sediments, the technique can also be applied to other solutes that can be measured at sufficiently high temporal resolution.

We are currently constructing a new device that can position the ADV and the O_2 microelectrode at a defined height above the sediment surface, turn these instruments in the horizontal plane, lock them into a position facing the current, and perform measurements, all without support from divers. All electronic equipment will be mounted on the device and we anticipate that sampling can be done under most weather conditions down to a water depth of 200 m. The new device will be used to collect data for various sediments and field conditions including different current velocities and in the presence of density gradients which have the potential for dampening the vertical turbulence.

References

Aller R.C. 1983. The importance of the diffusive permeability of animal burrow linings in determining marine sediment chemistry. J. Marine Res. **41**: 299-322.

Aller R.C., and J.Y. Aller. 1992. Meiofauna and solute transport in marine muds. Limnol. Oceanogr. **37**: 1018-1033.

Berg P, S. Rysgaard, P. Funch, and M.K. Sejr. 2001. Effects of bioturbation on solutes and solids in marine sediments. Aquat. Microb. Ecol. **26**: 81-94.

Berner R.A. 1980. Early diagenesis. A theoretical approach. Princeton University Press.

Boudreau B.P. 1997. Diagenetic models and their implementation. Springer.

Forster S., G. Graf, J. Kitlar, and M. Powilleit. 1995. Effects of bioturbation in oxic and hypoxic conditions: a microcosm experiment with a North Sea sediment community. Mar. Ecol. Prog. Ser. **116**: 153-161.

Forster S., M. Huettel, and W. Ziebis. 1996. Impact of boundary layer flow velocity on oxygen utilization in coastal sediments. Mar. Ecol. Prog. Ser. **143**: 173-185.

Fukuchi M., L. Legendre, and T. Hoshiai. 1997. The Canada-Japan SARES project on the first-year ice of Saroma-ko Lagoon (northern Hokkaido Japan) and Resolute Passage (Canada High Arctic). J. Mar. Sys. **11**: 1-8.

Glud R.N., J.K. Gunnersen, and O. Holby. 1999. Benthic *in situ* respiration in the upwelling area off central Chile. Mar. Ecol. Prog. Ser. **186**: 9-18.

Glud R.N., J.K. Gunnersen, H. Røy, B.B. Jørgensen. 2003. Seasonal dynamics of benthic O2 uptake in a semi enclosed bay: Importance of diffusion and fauna activity. Limnol. Oceanogr. **48**: 1265-1276.

Glud R.N., O. Holby, F. Hoffmann, and D.E. Canfield. 1998. Benthic mineralization and exchange in Arctic sediments (Svalbard, Norway). Mar. Ecol. Prog. Ser. **173**: 237-251.

Huettel M., and I.T. Webster. 2001. Porewater flow in permeable sediments. *In* B.P. Boudreau and B.B. Jørgensen [eds.]. The benthic boundary layer: transport processes and biogeochemistry Oxford Univ. Press.

Jahnke R.A., and M.B. Christiansen. 1989. A free-vehicle benthic chamber instrument for sea floor studies. Deep-Sea Res. **36**: 625-637.

Lohse L., E.H.G. Epping, W.Helder, W.Van Raaphorst. 1996. Oxygen pore water profiles in continental shelf sediments of the North Sea – turbulent versus molecular diffusion. Mar. Ecol. Prog. Ser. **145**: 63-75.

O'Riordan C.A., M.A. Maldiney, J.M. Mouchel, and M. Poulin. 1996. A new exploration module for the study of particulate matter transport in rivers. Comptes Rendus Acad. Sci. **322**: 285-292.

Pelegri S.P., L.P. Nielsen, T.H. Blackburn. 1994. Denitrification in estuarine sediment stimulated by the irrigation activity of the amphipod *Corophium volutator*. Mar. Ecol. Prog. Ser. **105**: 285-290.

Priestley M.B. 1992. Spectral analysis and time series. Academic Press.

Rasmussen H., and B.B. Jørgensen. 1992. Microelectrode studies of seasonal oxygen uptake in a coastal sediment: role of molecular diffusion. Mar. Ecol. Prog. Ser. **81**: 289-303.

Revsbech N.P. 1989. An oxygen microelectrode with a guard cathode. Limnol. Oceanogr. **34**: 474-478.

Reimers C.E., R.A. Jahnke, and L. Thomsen. 2001. *In situ* sampling in the benthic boundary layer. *In* B.P. Boudreau and B.B. Jørgensen [eds.]. The benthic boundary layer: transport processes and biogeochemistry Oxford Univ. Press.

Rutgers van der Loeff M.M. 1981. Wave effects on sediment water exchange in a submerged sand bed. Neth. J. Sea Res. **15**: 100-112.

Savant S.A., D.D. Reible, and L.J. Thibodeaux. 1987. Convective transport within stable river sediments. Water Resour. Res. **23**: 1763-1768.

Shirasawa K., R.G. Ingram, E.J.J. Hudier. 1997. Oceanic heat fluxes under thin sea ice in Saroma-ko Lagoon, Hokkaido Japan. J. Mar. Sys. **11**: 9-19.

Shum K.T. 1992. Wave-induced advective transport below a rippled water-sediment interface. J. Geophys. Res. **97**: 789-808.

Stanišić M.M. 1985. The mathematical theory of turbulence. Springer.

SonTek/YSI Inc. 2001. Acoustic doppler velocimeter principles of operation. Technical note, September 1.

Thibodeaux L.J., and Boyle J.D. 1987. Bedform-generated convective transport in bottom sediments. Nature **325**: 341-343.

Tietze U., Schenk U.C. 1993. Halbleiter-Schaltungstechnik, Springer

Wang Y, and P. van Cappellen. 1996. A multicomponent reactive transport model of early diagenesis: Application to redox cycling in coastal marine sediments. Geochim. Cosmochim. Acta **60**: 2993-3014.

Webster I.T. 1992. Wave enhancement of solute exchange within empty burrows. Limnol. Oceanogr. **37**: 630-643.

Webster I.T., and J.H. Taylor. 1992. Rotational dispersion in porous media due to fluctuating flows. Water Resour. Res. **28**: 109-119.

Wyngaard J.C. 1989. Scalar fluxes in the planetary boundary layer – Theory, modeling, and measurement. Boundary-Layer Meteorol. **50**: 49-75.

Yang Y, M. Hirano, D. Kimoto. 1996. Experimental studies on turbulent structure of solid-liquid upflow by using ADV. Jpn. Soc. Civil Eng. **40**: 819-824.

Thesis summary and outlook

Thesis summary and outlook

Within the last decades a number of laboratory studies revealed that pore-water advection in permeable sands can lead to intense exchange of solutes and particles between the bottom water and the sediment. An intensified exchange is believed to enhance the metabolic activity of these sediments. This led to the hypothesis that pore-water advection boosts organic matter mineralization in shelf sands, and that sandy shelf areas contribute much more to carbon and nutrient cycling than previously assumed. Despite the ecological significance, in situ quantifications of advective exchange and mineralization rates in the presence of advection are still largely missing. This thesis evaluated the prevailing physical preconditions for advection and the effect of pore-water advection on sediment metabolism at fine- medium- and coarse-grained North Sea sands to improve our understanding of the role of advection in the natural environment.

Natural pressure gradients that potentially drive advection at the study site were assessed based on concurrent measurements of sediment surface topography and bottom flow. This was done with a combined surface scanning and current meter device that was developed as part of this work. For the first time, topographies of permeable sands were measured at a resolution close to the size of the individual sand grains, i.e., down to the smallest roughness elements that may result in pressure gradients and advective pore-water exchange.

In situ flux measurements were obtained with a new autonomous benthic chamber system that was also developed within the thesis work. Stirrer-induced pressure gradients at the surface of the enclosed sediment proved to be similar to those developing when bottom flow passes over ripples or mounds. As the pressure gradients, and hence, the rates of advective exchange are easily adjusted by the applied stirring rate, the new instrument is perfectly suited to investigate the effect of advection on benthic fluxes of oxygen and other solutes.

The measured topographies and currents indicated the presence of advection at the study site. At the medium-grained site, the current-induced pressure gradients along the roughness elements at the sediment surface are expected to result in interfacial pore-

water exchange rates of up to 45 L m^{-2} d^{-1}. At that exchange rate the inflow of oxygenated bottom water provides an oxygen supply of ~ 12 mmol m^{-2} d^{-1} to the sediment community. Time series of in situ oxygen microprofiles confirmed the presence of advective oxygen supply by inflowing bottom water, resulting in an enhanced oxygen penetration depth. Shallow oxygen penetration in outflow areas, on the other hand, indicated that the supplied oxygen was efficiently consumed during the sediment passage of the pore-water.

The chamber flux measurements confirm an efficient consumption of oxygen that is supplied to the sands by advection. Stirrer induced advection at rates corresponding to natural conditions enhanced the total oxygen uptake of the medium and coarse sands by ~ 11 mmol m^{-2} d^{-1}. This corresponded to an increase by a factor of 1.4 to 1.9 as compared to uptake rates in the absence of advection. These measurements represent the first direct field evidence for an enhanced oxygen uptake of sandy shelf deposits in the presence of advection. This provides strong evidence for a potential of advection to favor metabolic activity and organic matter mineralization in these organically poor sands.

Advective exchange and its potential to enhance sediment metabolism proved to largely depend on sediment permeability. Even in the presence of the highest observed roughness elements the relatively low permeability at the fine sand station (0.3 $\times$ 10^{-11} m^2) would restrict advective exchange rates to ~ 5 L m^{-2} d^{-1}. Uniform and shallow oxygen penetration in profile time series and the absence of any effect of stirrer induced pressure gradients on oxygen consumption similarly suggested that advective flushing was irrelevant at that site. The prevailing permeabilities will thus determine the relevance of advection-related processes in the natural environment. Reported grain size data for the German Bight indicate that 40 % of the area is covered with sediments that are equally or less permeable than the sediment at the fine sand site. Thus, based on the findings of this study, advection cannot be expected to significantly affect sediment processes in these areas. In the remaining 60 % of the German Bight permeabilities are expected to range between those of the fine and the medium sand station (0.3 and 2.6 $\times$ 10^{-11} m^2) and significant pore-water advection may take place and promote both sediment oxygenation and metabolic activity.

The topographies at the study area differed substantially between sites and also between the different cruises. In some cases, topographies were strongly affected by bioroughness while on other occasions rippled surfaces prevailed. The roughness element height also differed strongly with average values between 3 and 20 mm with strong implications for the rates of advection. This clearly shows that the driving forces of advection may be highly variable on small temporal and spatial scales and that a detailed knowledge of the specific conditions in a given area is needed to appropriately evaluate the significance of advection.

This work has to be considered as a case study that was carried out to exemplary investigate the major aspects that determine the role of advection for organic matter turnover in the natural environment. The new methodology that was developed will facilitate forthcoming studies that would have to extend investigations to a larger spatial scale. The in situ chambers allow experimentation under well defined conditions which makes them most suitable for future investigations on the potential of advection for pathways and rates of sediment metabolic processes. Investigations should include the addition of organic matter pulses in order to evaluate maximum mineralization rates in times of high organic matter availability. Topography and permeability measurements have to be extended to identify the prevailing physical preconditions of advection. Furthermore, new models that account for irregular topographies and changes in current direction and velocity are needed to integrate results on advection-related metabolic rates and on the prevailing physical conditions. Important future task are also the development of new methods that allow direct benthic flux measurements without changing the hydrodynamic conditions above the sand. The eddy correlation technique that allows a non-invasive quantification of benthic oxygen fluxes (see fourth manuscript) represents such a new approach with a large potential for future studies in sandy environments.

Manuscripts not included in this thesis

Decomposition of diatoms and nutrient dynamics in permeable North Sea sediments

Sandra Ehrenhauss [1,4], Ursula Witte [1,3] Felix Janssen [1] & Markus Huettel [1,2]

[1] Max Planck Institute for Marine Microbiology, Celsiusstrasse 1, D-28359 Bremen, Germany

[2] Present address: Florida State University, Department of Oceanography, 0517 OSB, West Call Street, Tallahassee, Florida 32306-4320, USA

[3] Present address: University of Aberdeen, Oceanlab, Newburgh, Aberdeen AB41 6AA, Scotland, UK

[4] corresponding author. E-mail: sehrenha@gmx.de

At the time the thesis was handed in, the manuscript was accepted for publication in Continental Shelf Research, where it is published by now (**24**: 721-737).

The manuscript has not been included in this thesis as F. Janssen supplied only a part of the data on sediment characteristics. F. Janssen aided in carrying out the experiments on board F.S. HEINCKE, and provided editorial help upon writing of the manuscript. Reprints can be made available upon request.

Abstract

This study addresses the decomposition of sedimented diatoms in different permeable North Sea sand beds. During 3 cruises in 2001 to the southern German Bight, the regeneration of nutrients was assessed after the experimental deposition of organic matter corresponding to a typical spring diatom bloom in in situ and on-board chamber experiments. The diatom pulse was followed by a rapid and high regeneration of nutrients during the first day: 5 to 10% d^{-1} of the added nitrogen was converted to NH_4^+ and up to 0.67% d^{-1} of the added biogenic silica was dissolved to $Si(OH)_4$. These results are used to interpret the response of pore water nutrient concentrations in permeable North Sea sands to seasonal nutrient and phytoplankton dynamics in the water column. The rapid advective solute exchange in these permeable sediments reduces the accumulation of regenerated nutrients, and, thus pore water concentrations of $Si(OH)_4$, PO_4^{3-} and NH_4^+ decreased with increasing permeability. All sands were characterized by relatively high NO_3^- concentrations down to 10 cm sediment depth, indicating that the upper sediment layers are oxidized by advective flushing of the bed. Our results demonstrate that biogenic silica and organic matter are rapidly degraded in permeable coastal sands, revealing that these sediments are very active sites of nutrient recycling.

Near-bottom performance of the Acoustic Doppler Velocimeter (ADV) - a comparative study

Elimar Precht[1,3], Felix Janssen [1] & Markus Huettel [1,2]

[1] Max Planck Institute for Marine Microbiology, Celsiusstrasse 1, D-28359 Bremen, Germany

[2] Present address: Florida State University, Department of Oceanography, 0517 OSB, West Call Street, Tallahassee, Florida 32306-4320, USA

[3] corresponding author. E-mail: eprecht@mpi-bremen.de

At the time the thesis was handed in, the manuscript was submitted to Aquatic Ecology and is in press by now.

The manuscript has not been included in this thesis, as it focuses on technical aspects that are only loosely connected to the rest of the work presented here. F. Janssen did the measurements as well as part of the data evaluation. The knowledge of the ADV-performance near boundaries was used to optimize the sensor configuration for the measurements of near-bottom flow and the eddy-correlation technique (see manuscripts three and four). The manuscript can be made available upon request.

Abstract

In a laboratory flume, a comparative study on the near-bottom performance of the Acoustic Doppler Velocimeter (ADV) was conducted. We tested two different ADV systems at different configurations and two flow velocities (9 cm s^{-1}, 18 cm s^{-1}). The results were compared with synchronous measurements with a Laser Doppler Anemometer (LDA). Near-bottom velocity measurements with the ADV have to be interpreted carefully as the ADV technique underestimates flow velocities in a zone close to the sediment. The height of this zone above the sediment varies with different ADV systems and configurations. The values for nominal sampling volume heights (SVH) given by the software often underestimate the true, effective sampling volume heights. Smaller nominal SVH improve the ADV near-bottom performance, but the vertical extent of the zone in which the ADV underestimates flow by > 20 % may be larger than true SVH/2 by a factor of 2 (= true SVH). When the measurement volume approaches the bottom, ADV data quality parameters (signal-to-noise-ratio (SNR) and signal amplitude) exceeding the average "open water" level, are clear indicators that the ADV has begun to underestimate the flow velocity. Unfortunately, this is not a safe indicator for the range of reliable measurements as the ADV may begin to underestimate velocities even with unchanged "open water" data quality parameters. Thus, we can only recommend avoiding measurements below a distance from the bottom that we defined empirically comparing the ADV and the LDA velocity profiles. This distance is 2.5 × nominal sampling volume height for the tested ADV systems and experimental settings.

Benthic biogeochemistry: state of the art technologies and guidelines for the future of in situ survey

E. Viollier [1,14], C. Rabouille [2], S. E. Apitz [3], E. Breuer [4], G. Chaillou [5], K. Dedieu [2], Y. Furakawa [6], C. Grenz [7], P. Hall [8], F. Janssen [9], J. L. Morford [10], J.-C. Poggiale [7], S. Roberts [11], T. Shimmield [4], M. Taillefert [12], A. Tengberg [13], F. Wenzhöfer [13] & U. Witte [9]

[1] Laboratoire de Géochimie des Eaux, Université Paris cedex, France
[2] Laboratoire des Sciences du Climat et de l'Environnement, Gif/Yvette, France
[3] Sediment Management Laboratory, Environmental Sci. Div., San Diego, CA, USA
[4] SAMS, Dunstaffnage Marine Laboratory, Oban, UK
[5] Université Bordeaux 1, Talence cedex, France
[6] Naval Research Laboratory, Seafloor Sciences Branch, MS, USA
[7] Laboratoire d'Océanologie et de Biogéochimie, Marseille, France
[8] Department of Analytical and Marine Chemistry, Goteborg University, Sweden
[9] Max Planck Institut for Marine Microbiology, Bremen, Germany
[10] Woods Hole Oceanographic Inst., Dep. Mar. Chem. Geochem., Woods Hole, MA, USA
[11] School of biological Sciences, Monash University, Clayton, Victoria, Australia
[12] Georgia Institute of Technology, School of Earth and Atmosph. Sci., Atlanta, GA, USA
[13] Marine Biological Laboratory, University of Copenhagen, Helsingør, Denmark

[14] corresponding author. E-mail: viollier@ipgp.jussieu.fr

The manuscript has been published in Journal of Experimental Marine Biology and Ecology (**285-286**: 5-31)

This manuscript was not included in this thesis, as it is a review paper on in situ techniques that are mostly beyond the scope of this thesis. F. Janssen wrote a part of the manuscript with respect to benthic chambers and future work to be carried out in sandy shelf areas. Reprints can be made available upon request.

Abstract

Sediment and water can potentially be altered, chemically, physically and biologically as they are sampled at the seafloor, brought to the surface, processed and analysed. As a result, in situ observations of relatively undisturbed systems have become the goal of a growing body of scientists. Our understanding of sediment biogeochemistry and exchange fluxes was revolutionized by the introduction of benthic chambers and in situ micro-electrode profilers that allow for the direct measurement of chemical fluxes between sediment and water at the sea floor and for porewater composition. Since then, rapid progress in the technology of in situ sensors and benthic chambers (such as the introduction of gel probes, voltammetric electrodes or one- and two-dimensional optodes) have yielded major breakthroughs in the scientific understanding of benthic biogeochemistry. This paper is a synthesis of discussions held during the workshop on sediment biogeochemistry at the "Benthic Dynamics: in situ surveillance of the sediment-water interface" international conference (Aberdeen, UK, March 25 - 29, 2002). We present a review of existing in situ technologies for the study of benthic biogeochemistry dynamics and related scientific applications. Limitations and possible improvement (e.g., technology coupling) of these technologies and future development of new sensors are discussed. There are countless important scientific and technical issues that lend themselves to investigation using in situ benthic biogeochemical assessment. While the increasing availability of these tools will lead research in yet unanticipated directions, a few emerging issues include greater insight into the controls on organic matter (OM) mineralization, better models for the understanding of benthic fluxes to reconcile microelectrode and larger-scale chamber measurements, insight into the impacts of redox changes on trace metal behavior, new insights into geochemical reaction pathways in surface sediments, and a better understanding of contaminant fate in nearshore sediments.